

**WORLD METEOROLOGICAL ORGANIZATION**

**GLOBAL ATMOSPHERE WATCH**

**WORLD DATA CENTRE FOR GREENHOUSE GASES**



**GLOBAL  
ATMOSPHERE  
WATCH**

**WMO WDCGG DATA SUMMARY**

**WDCGG No. 46**

**GAW DATA**  
**Volume IV-Greenhouse and Related Gases**

**PUBLISHED BY**  
**JAPAN METEOROLOGICAL AGENCY**  
**IN CO-OPERATION WITH**  
**WORLD METEOROLOGICAL ORGANIZATION**

**AUGUST 2022**



## CONTENTS

	Page
<b>PREFACE</b>	1
<b>1. CARBON DIOXIDE</b>	3
<b>2. METHANE</b>	9
<b>3. NITROUS OXIDE</b>	15
<b>4. HALOCARBONS AND OTHER HALOGENATED SPECIES</b>	21
<b>5. CARBON MONOXIDE</b>	29
<b>APPENDICES</b>	35
<b>A ANALYSIS</b>	36
<b>B CALIBRATION AND STANDARD SCALES</b>	38
<b>C LIST OF OBSERVATIONAL STATIONS</b>	60
<b>D LIST OF CONTRIBUTORS</b>	72
<b>E LIST OF ABBREVIATIONS</b>	95
<b>F LIST OF WMO/WDCGG PUBLICATIONS</b>	99
<b>REFERENCES</b>	101

## PREFACE

Global observations of greenhouse gases are essential for understanding of the global carbon cycle and the role these gases play in driving climate change. The results of observations demonstrate accelerating increase of levels of various greenhouse gases in the atmosphere which is a result of the increased emissions of greenhouse gases to the atmosphere from anthropogenic activity (such as fossil fuel combustion and deforestation) since the beginning of the industrial era in around 1750. The increasing greenhouse gas concentrations are driving detectable tropospheric warming. To avoid negative consequences of climate change, urgent action should be taken towards the reduction of greenhouse gas emissions based on scientifically robust information. Against this background, there is an increased demand for available and reliable greenhouse gas data to meet needs of scientific research and provide information for use by policy makers.

The World Data Centre for Greenhouse Gases (WDCGG) has been operated by the Japan Meteorological Agency (JMA) since 1990 in response to a request from the World Meteorological Organization (WMO). It holds the status of a World Data Centre (WDC) under the WMO Global Atmosphere Watch (GAW) programme and provides critical services to the community through data collection, archiving and distribution of data on greenhouse and related gases (such as CO) in the atmosphere and oceans from surface stations, mobile platforms and satellites worldwide. WDCGG plays a critical role in the data management system of GAW. The data are provided online free of charge with a requirement for acknowledgment or co-authorship accreditation when used in publications (see the WDCGG website for details). WDCGG has an open data policy that is compliant with the WMO Unified Data Policy adopted in 2021.

Information on the global state of major greenhouse gases in the atmosphere is regularly published in the WMO Greenhouse Gas Bulletin, to which WDCGG contributes via the calculation of globally averaged mole fractions, long-term trends and growth rates. The WMO WDCGG Data Summary in addition to reports on global averages covered in bulletins, also provides latitudinal or hemispheric averages and individual observational data used in global analysis. The Data Summary contains information on CO and certain halogenated species, which are not covered by the bulletins.

This issue of the Data Summary covers observational data collected at surface stations and on certain ships for the period from 1968 to 2020 based on monthly mean data submitted to WDCGG by September 2021. Observational data and the results of related analysis indicate that mole fractions of major greenhouse gases (CO<sub>2</sub>, CH<sub>4</sub>, N<sub>2</sub>O, SF<sub>6</sub> and certain HCFCs and HFCs) are increasing, while those of certain ozone-depleting substances (e.g., CFCs) are not. The globally averaged mole fractions of CO<sub>2</sub>, CH<sub>4</sub> and N<sub>2</sub>O reached new highs of 413.2±0.2 ppm, 1,889±2 ppb and 333.2±0.1 ppb in 2020, corresponding to 149, 262 and 123% of pre-industrial levels, respectively. More detailed information is provided in the main text of this publication. The value-added analytical information presented in this Data Summary is expected to support scientific research, assessments and policy-making in relation to environmental issues.

WDCGG thanks all data contributors worldwide for their efforts in maintaining accurate long-term observations and for their ongoing data submissions. Contributors include the National Oceanic and Atmospheric Administration (NOAA) Global Monitoring Laboratory (GML) and its cooperative air-sampling network, the Advanced Global Atmospheric Gases Experiment (AGAGE), and a variety of other observational stations operating under the framework of GAW and other programmes as listed in Appendix D. All organizations submitting data to WDCGG are acknowledged as invaluable contributors to the Data Summary.

Mailing address:

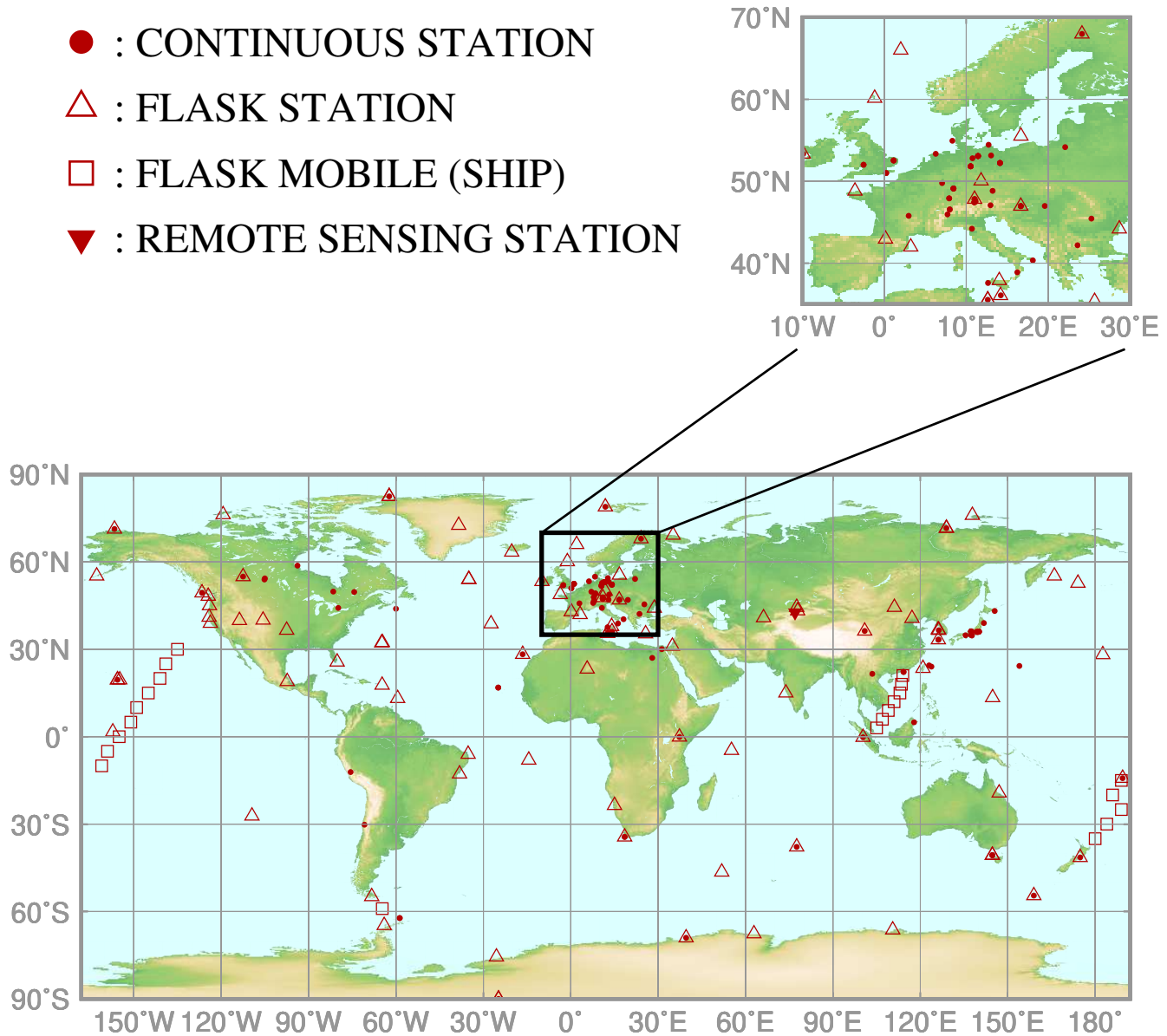
WMO World Data Centre for Greenhouse Gases (WDCGG)  
c/o Japan Meteorological Agency  
3-6-9, Toranomon, Minato City, Tokyo 105-8431, Japan  
E-mail: wdcgg@met.kishou.go.jp  
Telephone: +81-3-3434-9127  
Website: <https://gaw.kishou.go.jp/>



# 1.

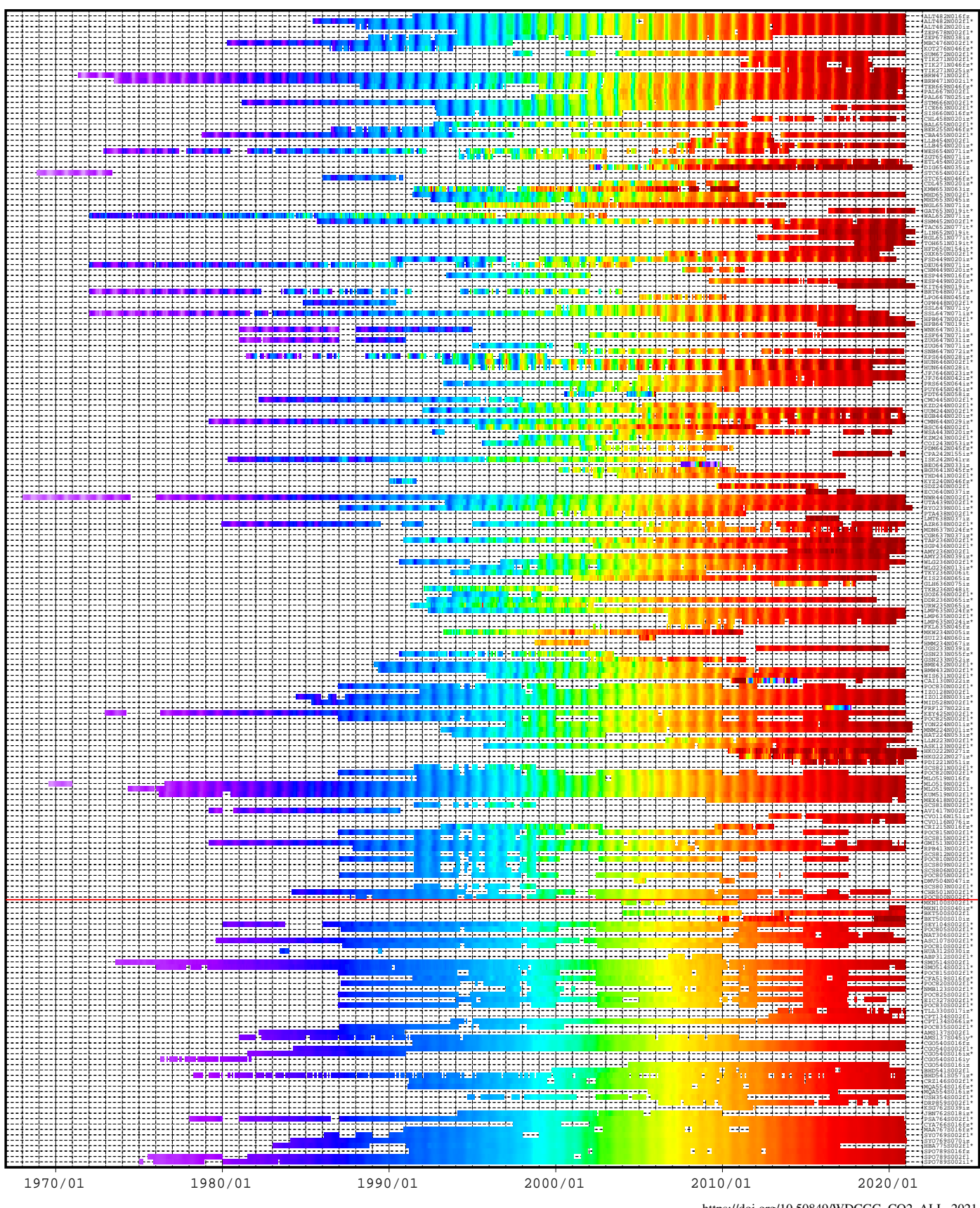
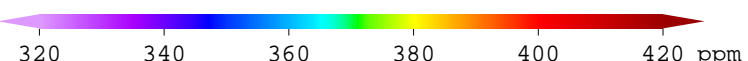
## CARBON DIOXIDE (CO<sub>2</sub>)

- : CONTINUOUS STATION
- △ : FLASK STATION
- : FLASK MOBILE (SHIP)
- ▼ : REMOTE SENSING STATION



This map shows locations of the stations that have submitted data for monthly mean mole fractions.

# CO<sub>2</sub> Monthly Data

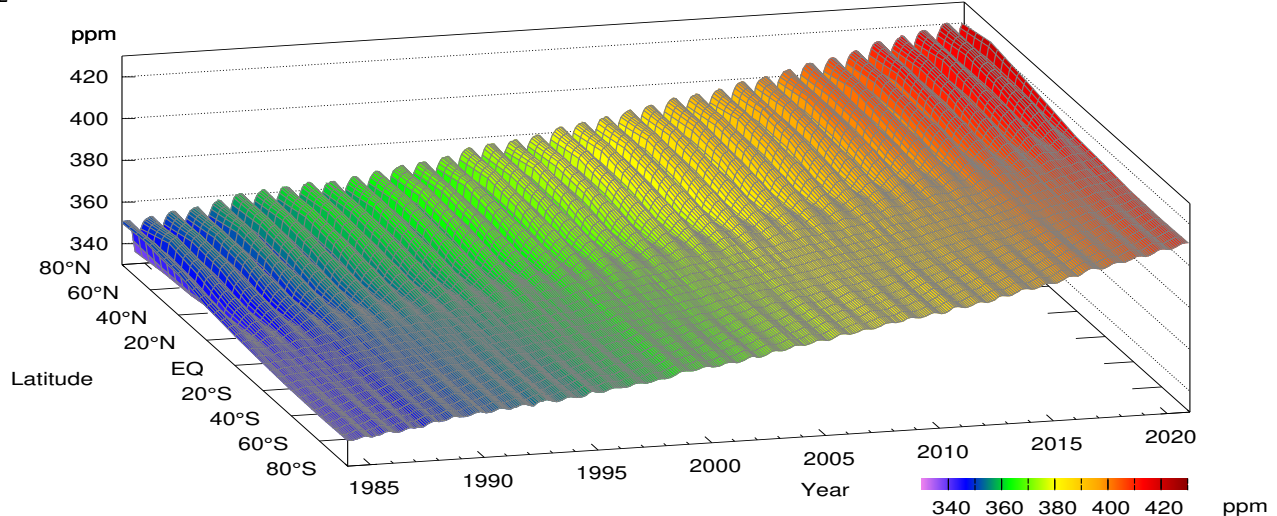


[https://doi.org/10.50849/WDCGG\\_CO2\\_ALL\\_2021](https://doi.org/10.50849/WDCGG_CO2_ALL_2021)

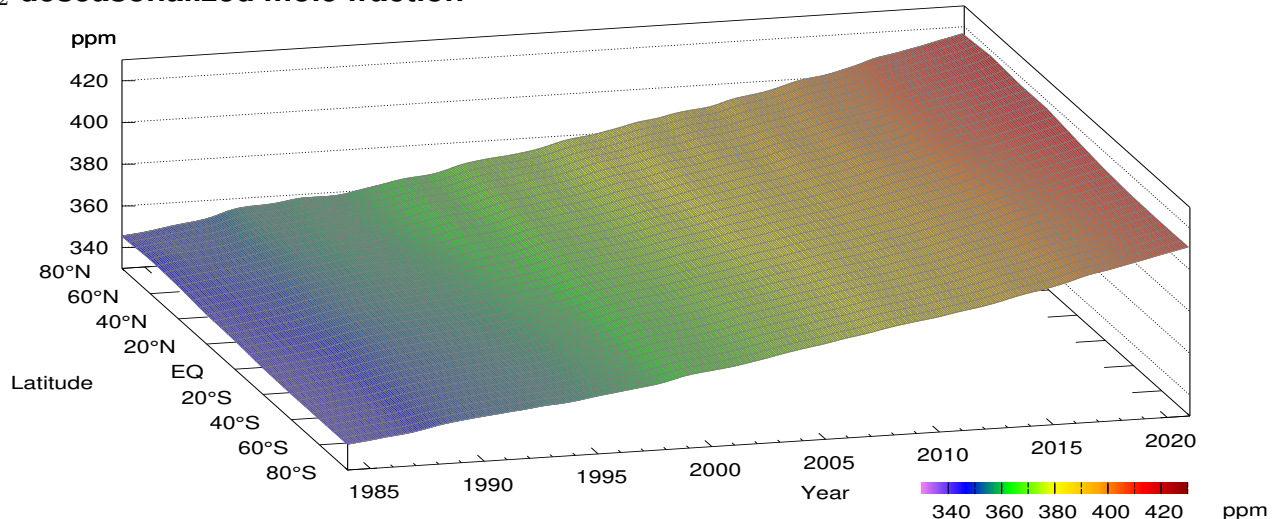
**Plate 1.1** Monthly mean CO<sub>2</sub> mole fractions that have been reported to the WDCGG. The mole fractions are illustrated in different colors.

The sites are listed in order from north to south. The red line indicates the equator. In cases where data are reported for two or three different altitudes, only the data at the highest altitudes are illustrated. In cases where monthly means are not reported, the WDCGG calculates them from hourly or other mole fractions reported to the WDCGG by simple arithmetic mean. The data from the sites with an asterisk at the end of the station index were used for the analyses shown in Plate 1.2 (see Appendix A).

## CO<sub>2</sub> mole fraction



## CO<sub>2</sub> deseasonalized mole fraction



## CO<sub>2</sub> growth rate

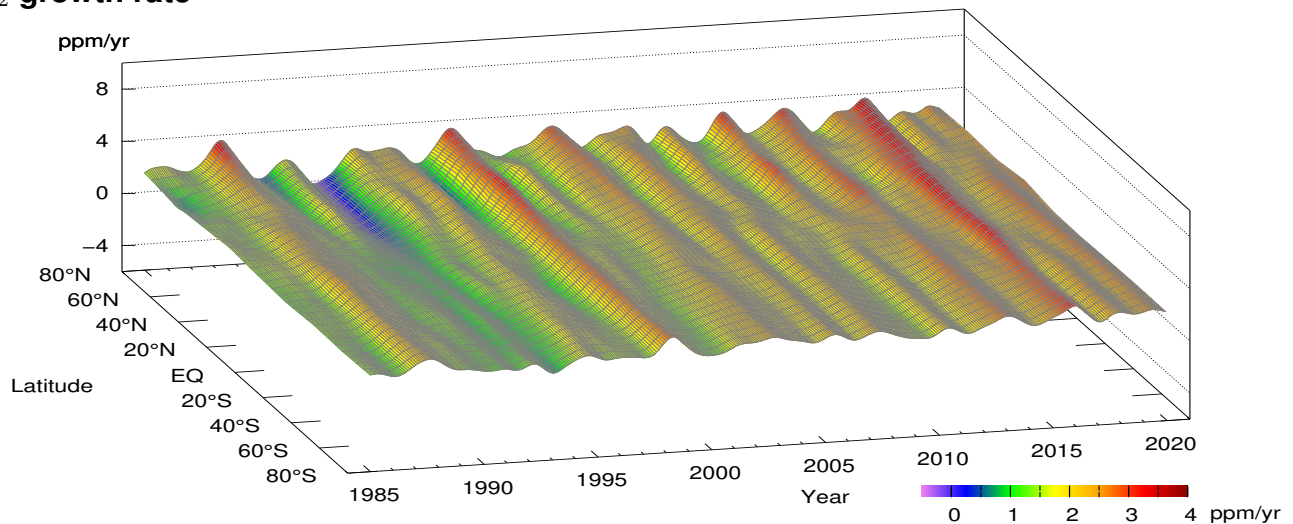


**Plate 1.2** Variation of zonally averaged monthly mean CO<sub>2</sub> mole fractions (top), deseasonalized long-term trends (middle), and growth rates (bottom). The zonally averaged mole fractions were calculated for each 20° zone. The deseasonalized trends and growth rates were derived as described in Appendix A.

# 1. CARBON DIOXIDE (CO<sub>2</sub>)

Atmospheric mole fractions of carbon dioxide (CO<sub>2</sub>) – the most significant long-lived greenhouse gas related to anthropogenic activities – have been increasing since the beginning of the industrial era in around 1750. The globally averaged mole fraction of CO<sub>2</sub> reached a new high of 413.2±0.2 ppm in 2020, representing an increase of 2.5 ppm from the previous year. This mole fraction constitutes 149% of the pre-industrial level of 278 ppm as inferred from ice-core studies. CO<sub>2</sub> is responsible for around 66% of radiative forcing (relative to the pre-industrial era) caused by all long-lived greenhouse gases (WMO, 2021a).

The increase in CO<sub>2</sub> mole fractions is primarily attributable to human activity, particularly fossil fuel combustion, cement production and deforestation. Around half of anthropogenic CO<sub>2</sub> emissions are removed by the biosphere and oceans, and the rest remains in the atmosphere. The fraction of CO<sub>2</sub> that stays in the atmosphere has been on average stable within past 60 years (WMO, 2021a), but it experiences substantial interannual variations. This determines the annual CO<sub>2</sub> increment in the atmosphere. The red columns in Fig. 1.1 show the observed growth rate for atmospheric CO<sub>2</sub> dry mole fractions, and the green line shows theoretical growth rates for CO<sub>2</sub> based on the assumption that all annual fossil fuel CO<sub>2</sub> emissions remain in the atmosphere. Despite a drop of around 5.4% in fossil fuel CO<sub>2</sub> emissions in 2020 due to COVID-19 confinement measures (Friedlingstein *et al.*, 2021), the observed growth rate was slightly higher than the average growth rate for the past decade. The lack of correlation between these time-series suggests that variations of the CO<sub>2</sub>

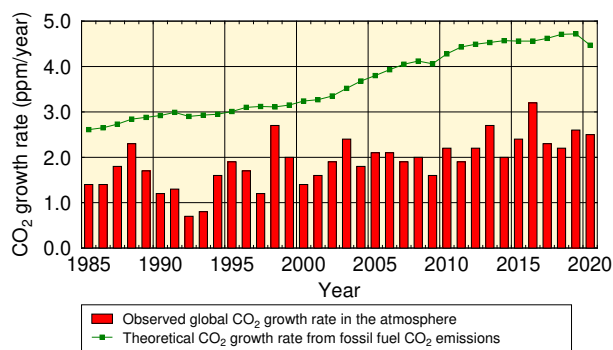


Fig. 1.1 Annual growth rates for CO<sub>2</sub> in the atmosphere calculated from observational data (red columns), and theoretical rates driven by fossil fuel emissions (green curve). The theoretical data were calculated taking CO<sub>2</sub> emissions as a proxy (from the Global Carbon Project (Friedlingstein *et al.*, 2021)), converted to mole fractions based on the conversion factor (2.124 PgC/ppm) (Ballantyne *et al.*, 2012). The observed growth rates were calculated by WDCGG.

growth rate are driven by the variability of the land and/or ocean sources and sinks. A comprehensive understanding of the mechanisms that control various CO<sub>2</sub> sources/sinks and their current states is of key importance in providing a scientific foundation for strategies to mitigate climate change.

## Globally averaged mole fractions

The blue dots in Fig. 1.2 show globally averaged CO<sub>2</sub> monthly mean mole fractions (top) and related growth rates (bottom). The red line in the top panel shows the long-term trend after removal of seasonal cycles from the monthly means shown by the blue dots. Details of the analysis are provided in Appendix A.

Throughout the period for which observational data are available, the CO<sub>2</sub> mole fraction shows a continuous increase accompanied by characteristic seasonal cycle, with higher values from boreal winter to spring and lower values in summer. The seasonal cycle of CO<sub>2</sub> mole fractions (Fig. 1.5) is mainly driven by activity of the terrestrial biosphere, where plant photosynthesis is active in summer and large amounts of CO<sub>2</sub> are consumed, while

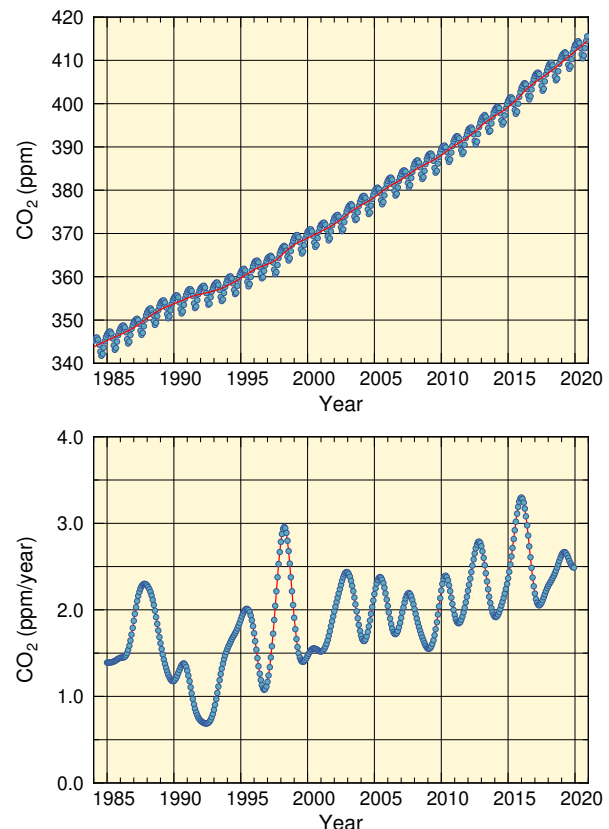


Fig. 1.2 Globally averaged monthly mean mole fraction of CO<sub>2</sub> (top) and its growth rate (bottom) from 1984 to 2020. Red line on the top panel presents the deseasonalized long-term trend.

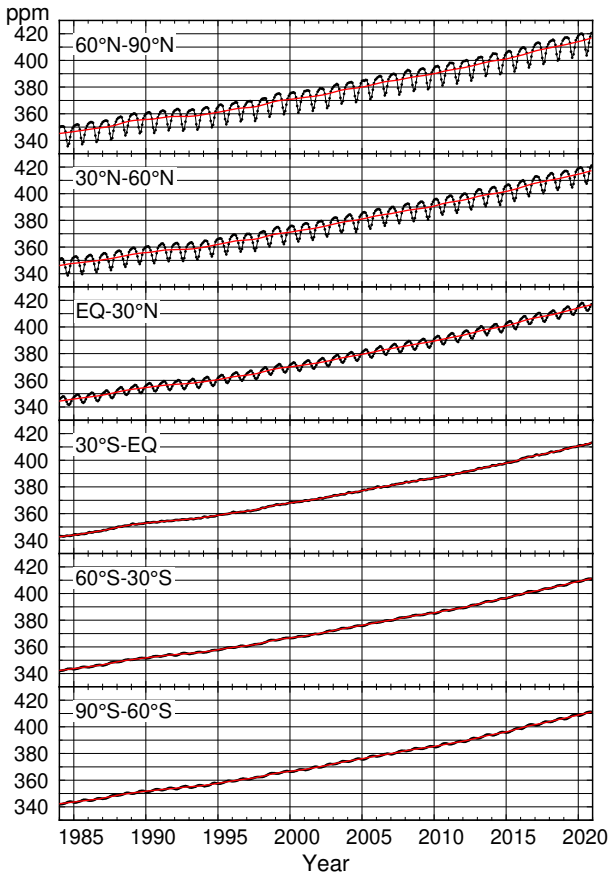


Fig. 1.3 Monthly mean mole fractions of CO<sub>2</sub> from 1984 to 2020 averaged over each 30° latitudinal zone (black) and their deseasonalized long-term trends (red).

plant respiration and organic-matter decomposition in soil become dominant in winter and emissions exceed the amount absorbed.

The activity of the terrestrial biosphere is characterized by significant interannual fluctuations, as reflected in the CO<sub>2</sub> growth rate variations shown in the bottom panel of Fig. 1.2. The growth rate has been particularly high during El Niño events, such as those of 1986 – 1988, 1997/1998, 2002/2003, 2009/2010 and 2014 – 2016. El Niño conditions are usually associated with high temperatures and droughts in tropical land areas. High temperatures enhance plant respiration and organic-matter decomposition in soil, thereby increasing CO<sub>2</sub> emissions, while droughts suppress CO<sub>2</sub> consumption via plant photosynthesis and induce forest/peat fires, which also contribute to CO<sub>2</sub> emissions. The CO<sub>2</sub> growth rate was exceptionally low during the El Niño event of 1991/1992. This is largely attributed to the eruption of Mt. Pinatubo in June 1991, which caused low-temperature anomalies on a global scale leading to a terrestrial biosphere response opposite to the one described above.

### Latitudinal dependence of mole fractions

The black lines in Fig. 1.3 show monthly mean CO<sub>2</sub>

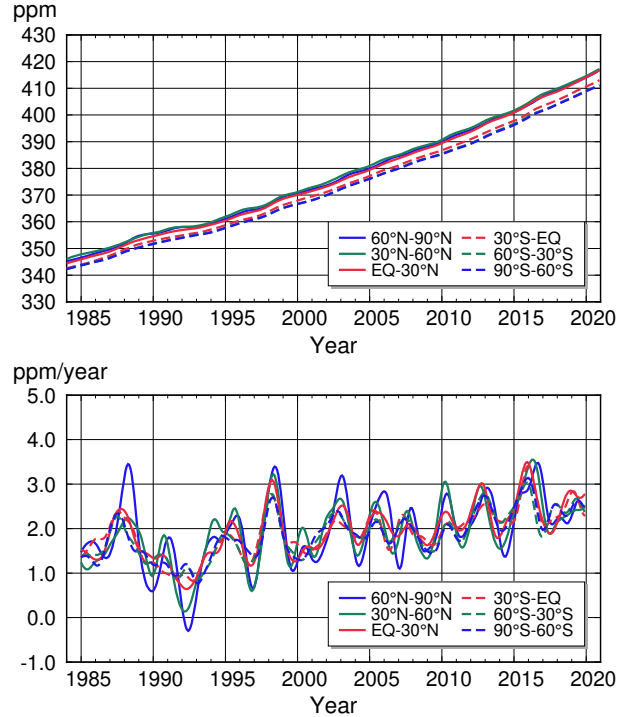


Fig. 1.4 Long-term trends of the CO<sub>2</sub> mole fractions for each 30° latitudinal zone (top) and their growth rates (bottom).

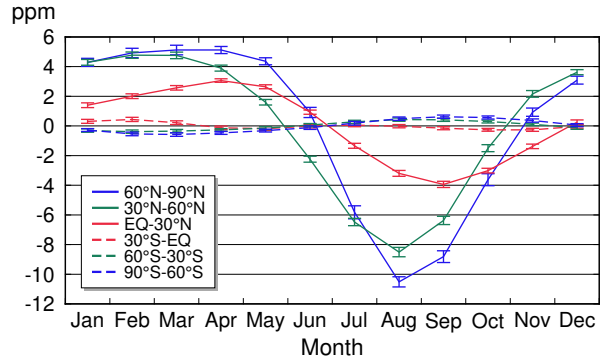


Fig. 1.5 Average seasonal cycles of the CO<sub>2</sub> mole fractions for each 30° latitudinal zone obtained by subtracting long-term trends from the zonally averaged time series. Vertical error bars represent the range of  $\pm 1\sigma$  which was calculated for each month (period 1984 to 2020).

mole fractions averaged over six 30° latitudinal bands (60°–90°N, 30°–60°N, etc.). Long-term trends are shown by red lines, and are collectively presented at the top panel of Fig. 1.4. The bottom panel of Fig. 1.4 shows CO<sub>2</sub> growth rates in each latitudinal belt, and Fig. 1.5 shows average seasonal cycles of CO<sub>2</sub> mole fractions in the relevant six bands. Figure 1.6 presents monthly mean CO<sub>2</sub> mole fractions for specific months of 2020 at individual stations, which were included in calculation of the global average mole fraction, as a function of latitude.

As shown in Fig. 1.4, CO<sub>2</sub> mole fractions are higher on average in the Northern Hemisphere, largely due to greater

concentrations of human activity and the land mass areas there. However, the long-term trends are the same in all latitudinal bands. This suggests that, although the major sources and sinks of CO<sub>2</sub> are located in the Northern Hemisphere, changes in mole fractions occur on a global scale due to atmospheric transport.

Figure 1.5 indicates that seasonal cycles of CO<sub>2</sub> mole fractions have a large amplitude in northern regions, mainly because the Northern Hemisphere has larger continental areas and an extensive terrestrial biosphere. Pronounced lagging between seasonal minima in the different latitude belts is also seen. Seasonal variations are evident at the individual sites in the Northern Hemisphere as shown in Fig. 1.6. In contrast, low seasonal variability is observed in the Southern Hemisphere. In the mid- and high southern latitudes, seasonal cycles of CO<sub>2</sub> mole fractions have an opposite phase to those of northern latitudes.

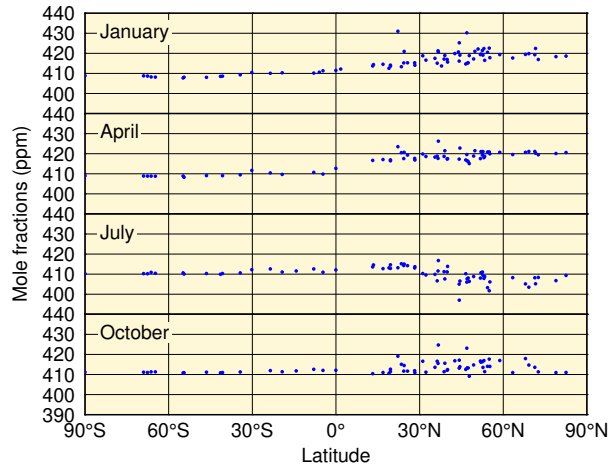


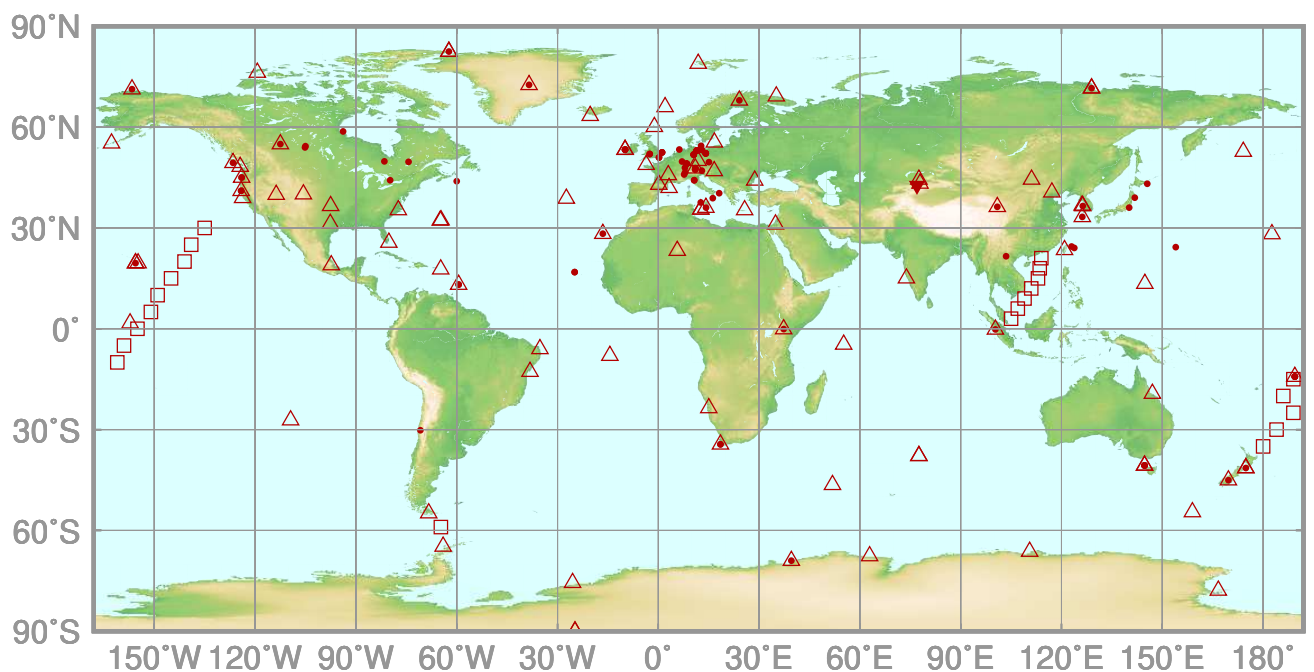
Fig. 1.6 Latitudinal distributions of the monthly mean mole fractions of CO<sub>2</sub> in January, April, July and October 2020 at individual stations.

# 2.

## METHANE

### (CH<sub>4</sub>)

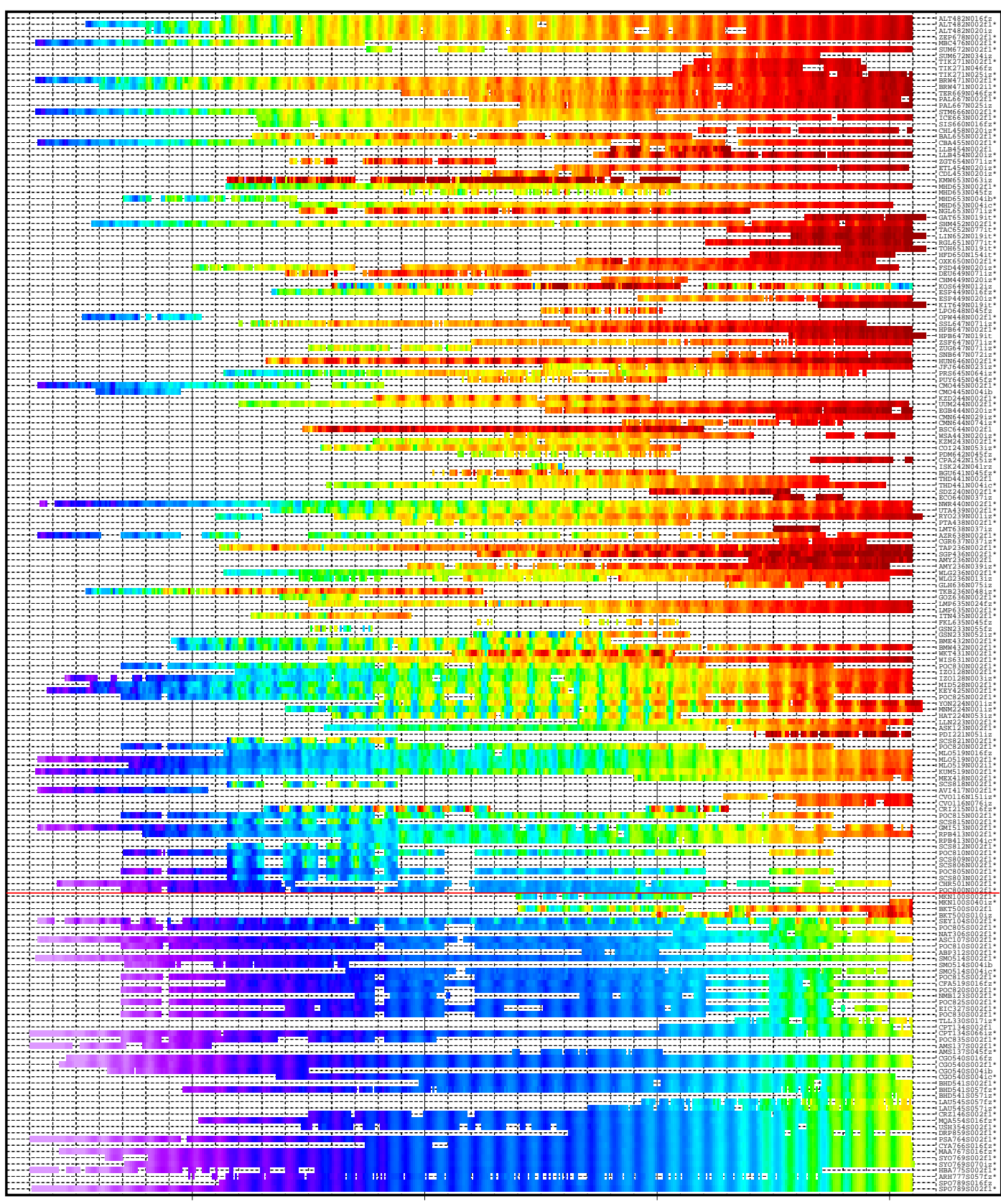
- : CONTINUOUS STATION
- △ : FLASK STATION
- : FLASK MOBILE (SHIP)
- ▼ : REMOTE SENSING STATION



This map shows locations of the stations that have submitted data for monthly mean mole fractions.

# CH<sub>4</sub> Monthly Data

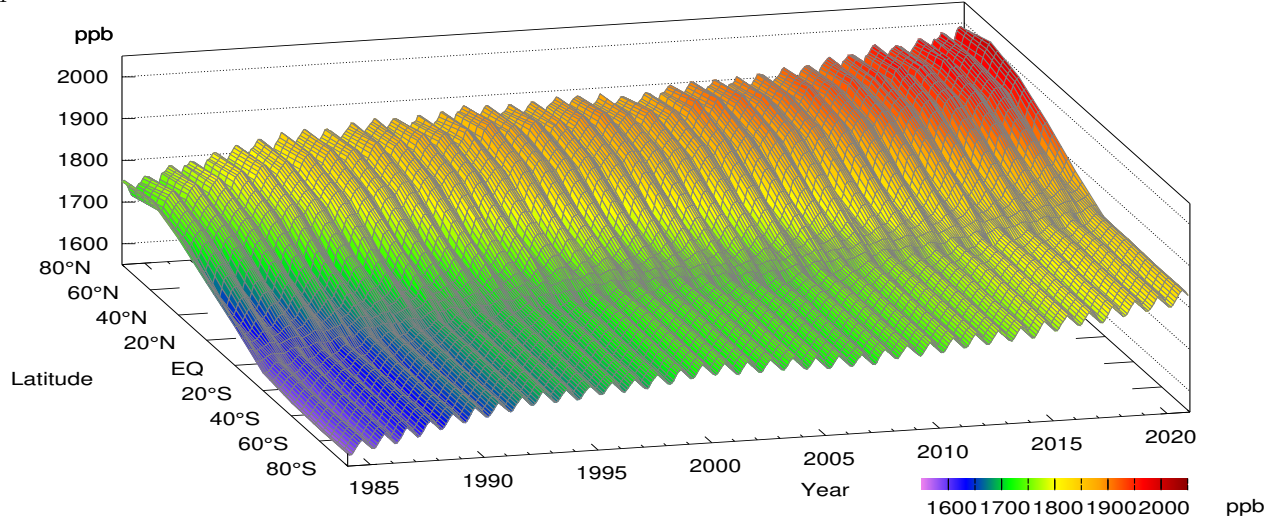
1600 1700 1800 1900 2000 ppb



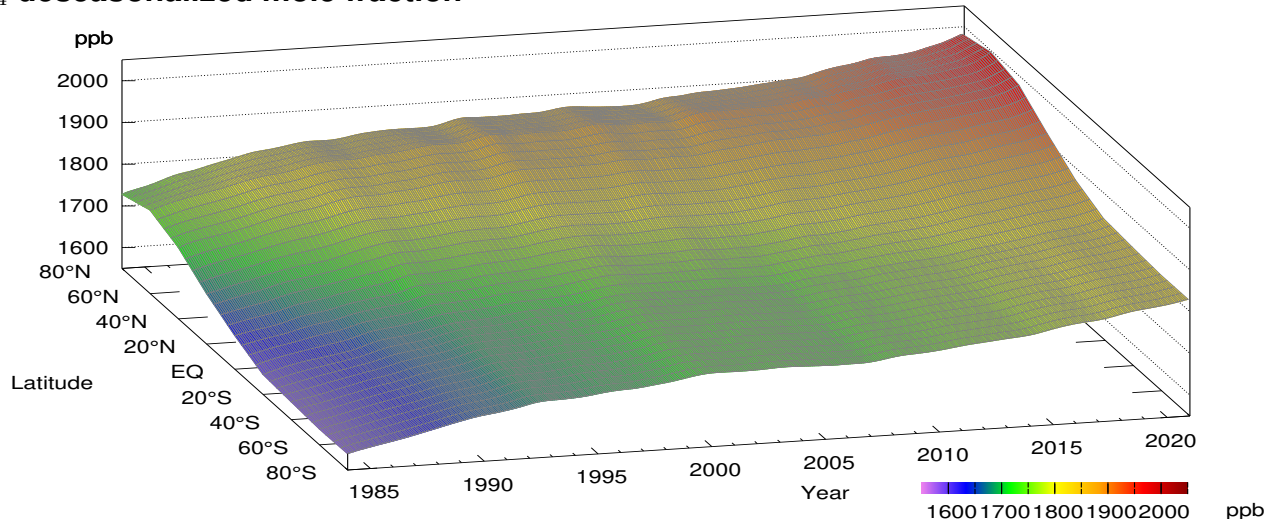
[https://doi.org/10.50849/WDCGG\\_CH4\\_ALL\\_2021](https://doi.org/10.50849/WDCGG_CH4_ALL_2021)

**Plate 2.1** Monthly mean CH<sub>4</sub> mole fractions that have been reported to the WDCGG. The mole fractions are illustrated in different colors. The sites are listed in order from north to south. The red line indicates the equator. In cases where monthly means are not reported, the WDCGG calculates them from hourly or other mole fractions reported to the WDCGG by simple arithmetic mean. The data from the sites with an asterisk at the end of the station index were used for the analyses shown in Plate 2.2 (see Appendix A).

## **CH<sub>4</sub> mole fraction**



## **CH<sub>4</sub> deseasonalized mole fraction**



## **CH<sub>4</sub> growth rate**

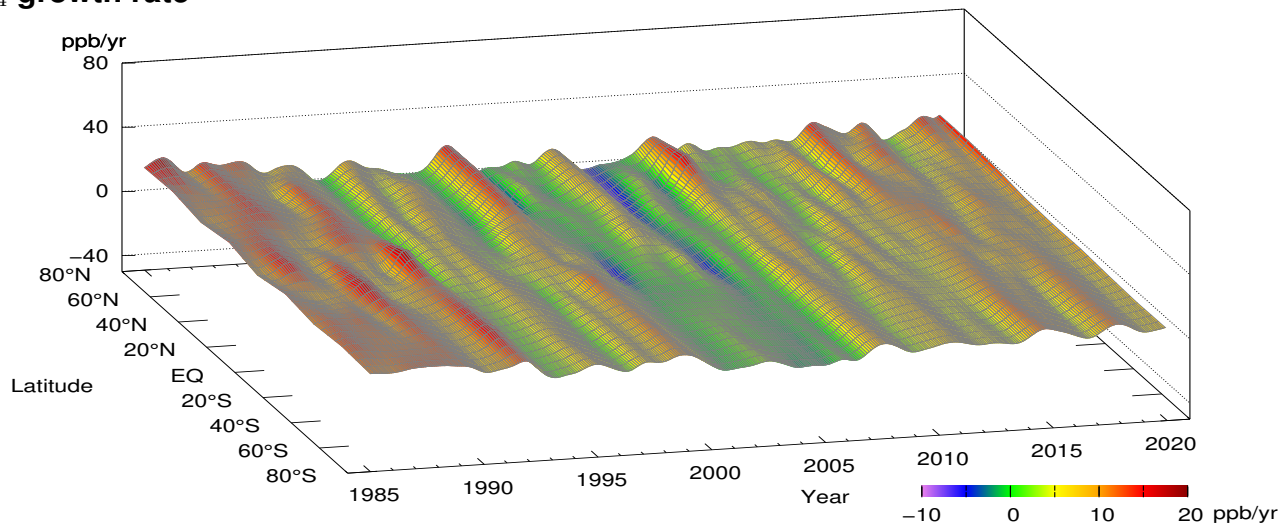


**Plate 2.2** Variation of zonally averaged monthly mean CH<sub>4</sub> mole fractions (top), deseasonalized long-term trends (middle), and growth rates (bottom). The zonally averaged mole fractions were calculated for each 20° zone. The deseasonalized trends and growth rates were derived as described in Appendix A.

## 2. METHANE ( $\text{CH}_4$ )

Atmospheric mole fractions of methane ( $\text{CH}_4$ ) – the second most significant anthropogenic greenhouse gas – have been increasing since the beginning of the industrial era (1750). The globally averaged mole fraction of  $\text{CH}_4$  was  $1,889 \pm 2$  ppb in 2020, representing an increase of 11 ppb relative to the previous year and 262% of the pre-industrial level of 722 ppb.  $\text{CH}_4$  is responsible for around 16% of radiative forcing (relative to the pre-industrial era) caused by all long-lived greenhouse gases (WMO, 2021a).

$\text{CH}_4$  has a variety of natural and anthropogenic sources. Natural ones (about 40% of emissions) are predominantly wetlands, with various other minor but significant sources including fresh water, wild animals, termites and geological sources. Emissions from ruminant livestock and rice paddies associated with agricultural activities are categorized as anthropogenic sources. Other sources are directly related to industrial activity, including gas and oil exploration, waste management and biomass burning. In contrast to the variety of sources, sinks are predominantly attributed to the destruction of  $\text{CH}_4$  via reaction with a hydroxyl (OH) radical, which is especially abundant over oceans at low latitudes since it forms from the exposure of

water vapor to ultraviolet (UV) radiation. This reaction determines  $\text{CH}_4$  lifetime in the atmosphere.

### Globally averaged mole fractions

The blue dots in Fig. 2.1 show globally averaged monthly mean  $\text{CH}_4$  mole fractions (top) and related growth rates (bottom) based on the WDCGG data analysis described in Appendix A. The red line in the top panel shows the residual component after removal of seasonal cycles from globally averaged monthly mean mole fractions (referred to here as the long-term trend).

The seasonal cycle of  $\text{CH}_4$  mole fractions depicted in Fig. 2.4 is primarily driven by the destruction of  $\text{CH}_4$  via reaction with OH radicals. More such radicals are generated in summer due to enhanced UV radiation, resulting in increased  $\text{CH}_4$  destruction. Biogenic sources such as wetlands also have individual characteristics of seasonal variability, contributing to variations in observed  $\text{CH}_4$  mole fractions.

The overall tendency of globally averaged  $\text{CH}_4$  mole fractions shows a continuous increase throughout the period for which observational data are available. The

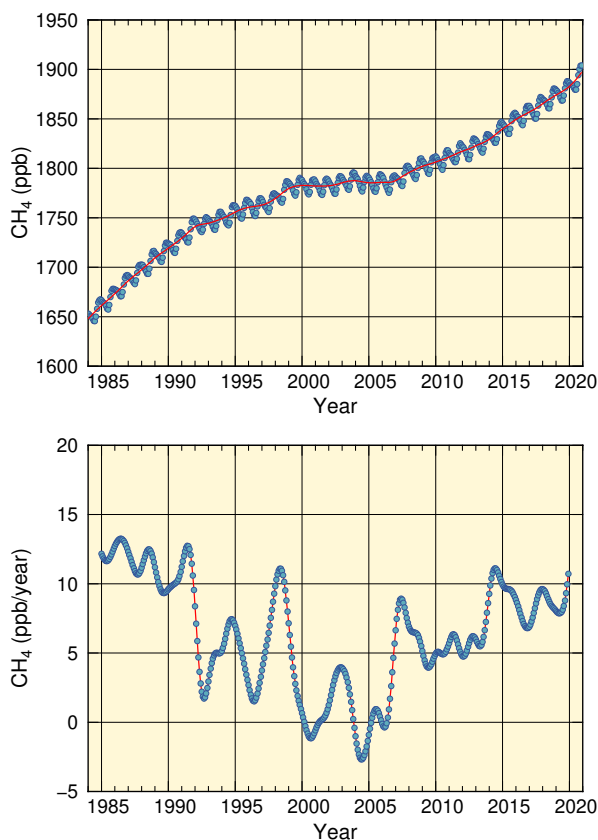


Fig. 2.1 Globally averaged monthly mean mole fraction of  $\text{CH}_4$  from 1984 to 2020 (top) and its growth rate (bottom). Red line on the top panel presents the deseasonalized long-term trend.

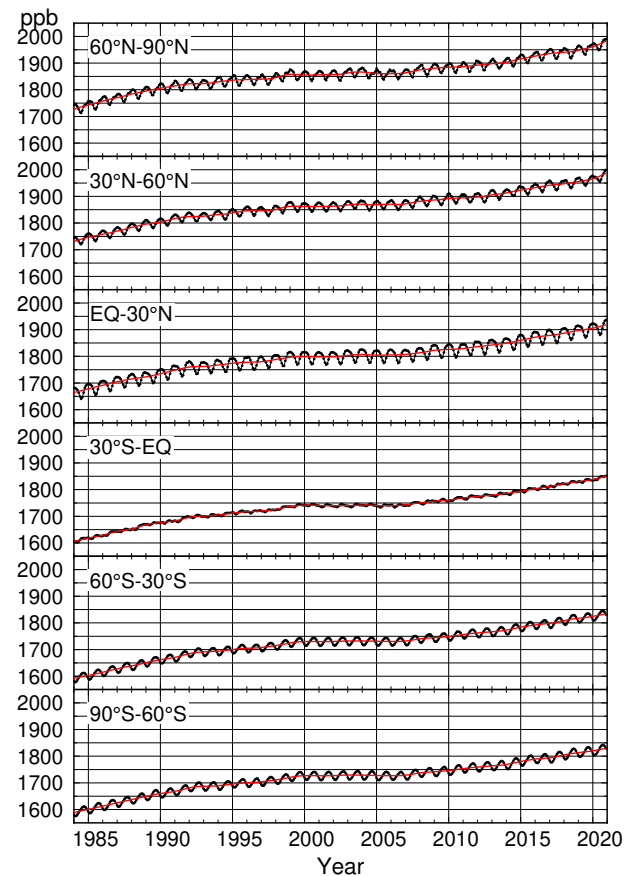


Fig. 2.2 Monthly mean mole fractions of  $\text{CH}_4$  from 1984 to 2020 for each  $30^\circ$  latitudinal zone (black) and their deseasonalized long-term trends (red).

mean annual total CH<sub>4</sub> emission for the period 2008 – 2017 is 29 TgCH<sub>4</sub>/yr larger than the estimate for 2000 – 2009 (Saunois *et al.*, 2020). Hence the increase in CH<sub>4</sub> globally averaged mole fraction is largely driven by the growing demand for energy and food (WMO, 2021a). Notably, the increase almost stagnated from 1999 to 2006. As shown in the bottom panel, the growth rate actually began to decrease in the late 1990s (in fact approaching zero during this period) for reasons that remain under discussion (IPCC (2021) and references noted therein). By way of example, anthropogenic emissions from the oil and gas sectors declined by about 10 Tg/yr through the 1990s, and atmospheric CH<sub>4</sub> loss steadily increased (Dlugokencky *et al.*, 2003; Simpson *et al.*, 2012; Crippa *et al.*, 2020; Höglund-Isaksson *et al.*, 2020; Chandra *et al.*, 2021). The situation changed in 2007 and mole fractions began increasing again. Recent studies (including work based on inverse modelling, CH<sub>4</sub> isotopic composition observation and inventory data) have suggested that concurrent emission changes from fossil fuels and agriculture have contributed to the resumed CH<sub>4</sub> growth rate observed since 2007, though there is still no consensus on this issue (Rice *et al.*, 2016; Nisbet *et al.*, 2016; Schwietzke *et al.*, 2016; Schaefer *et al.*, 2016; Worden *et al.*, 2017; Patra *et al.*, 2016; Thompson *et al.*, 2018; Lan *et al.*, 2019; Crippa *et al.*, 2020; Höglund-Isaksson *et al.*, 2020; Jackson *et al.*, 2020; Chandra *et al.*, 2021; Basu *et al.*, 2022; Oh *et al.*, 2022).

### Latitudinal dependence of mole fractions

The black lines in Fig. 2.2 show CH<sub>4</sub> mole fractions averaged over six 30° latitudinal bands. Long-term trends are shown by the red lines in each panel and summarized in the top panel of Figure 2.3. The bottom panel of this figure shows growth rates of CH<sub>4</sub> for the six latitudinal bands, and Figure 2.4 shows average seasonal cycles of CH<sub>4</sub> mole fractions for each band.

As shown in the top panel of Figure 2.3, the mole fraction gradient between the six long-term trends is the most pronounced between 30 – 60°N and EQ – 30°N and between EQ – 30°N and south hemispheric bands. These gradients are largely attributable to presence of major CH<sub>4</sub> sources in the Northern Hemisphere and to an abundance of OH radicals over oceanic regions extending southward.

The CH<sub>4</sub> growth rate exhibits similar but not identical characteristics in all latitudinal bands, as shown in the bottom panel of Figure 2.3. There are singular peaks and troughs, each of which has an individual complex origin, and collective explanation of two or more peaks is challenging. For example, the peaks observed in every band in 1998 are attributed to enhanced CH<sub>4</sub> emissions from tropical wetland areas in association with the major El Niño event observed the same year, and to forest/peat fires in Siberia and elsewhere (Dlugokencky *et al.*, 2001).

Figure 2.4 shows clear seasonal cycles of CH<sub>4</sub> mole fractions in both hemispheres, while those of CO<sub>2</sub> mole fractions are only pronounced in the Northern Hemisphere

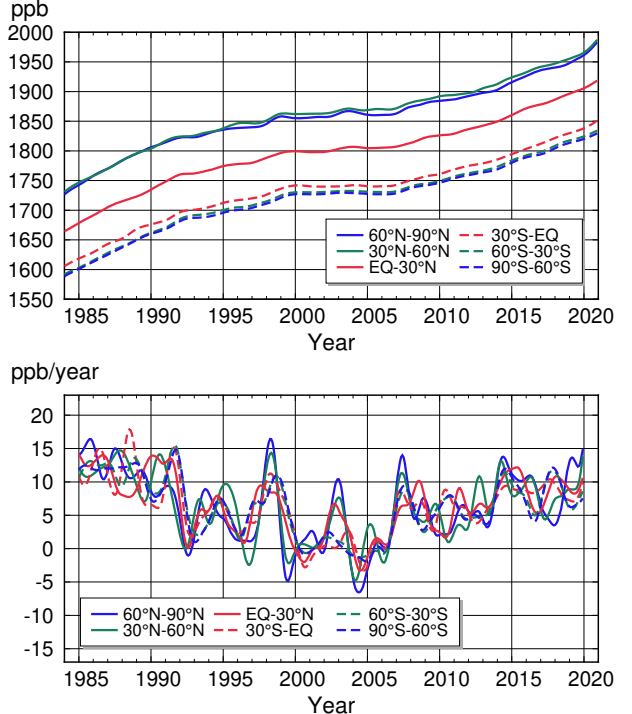


Fig. 2.3 Long-term trends of the CH<sub>4</sub> mole fractions for each 30° latitudinal zone (top) and their growth rates (bottom).

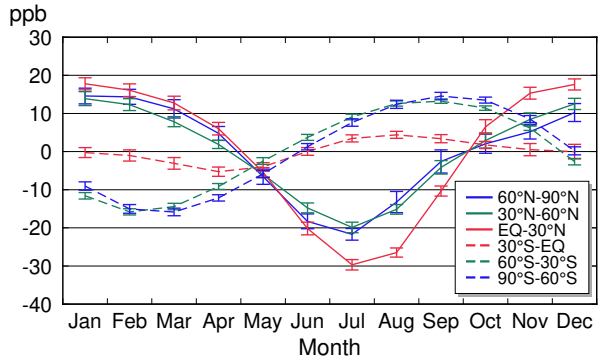


Fig. 2.4 Average seasonal cycles of CH<sub>4</sub> mole fractions for each 30° latitudinal zone obtained by subtracting long-term trends from the zonally averaged time series. Vertical error bars represent the range of  $\pm 1\sigma$  calculated for each month (period 1984 to 2020).

(Fig. 1.5). This difference is related to the differences in the processes behind the seasonal cycles of the two species. CH<sub>4</sub> sinks are mainly driven by the availability of OH radicals produced over oceans, which peak during summer in both hemispheres and at the same time. In contrast, CO<sub>2</sub> sinks in summer are mainly driven by terrestrial biosphere activity, which is limited in the ocean-rich Southern Hemisphere and has pronounced difference in the month of the maximum uptake in different latitudes. The cycles have a roughly opposite phase in each hemisphere because the seasons are opposite. The relatively low amplitude of seasonal cycles for CH<sub>4</sub> mole

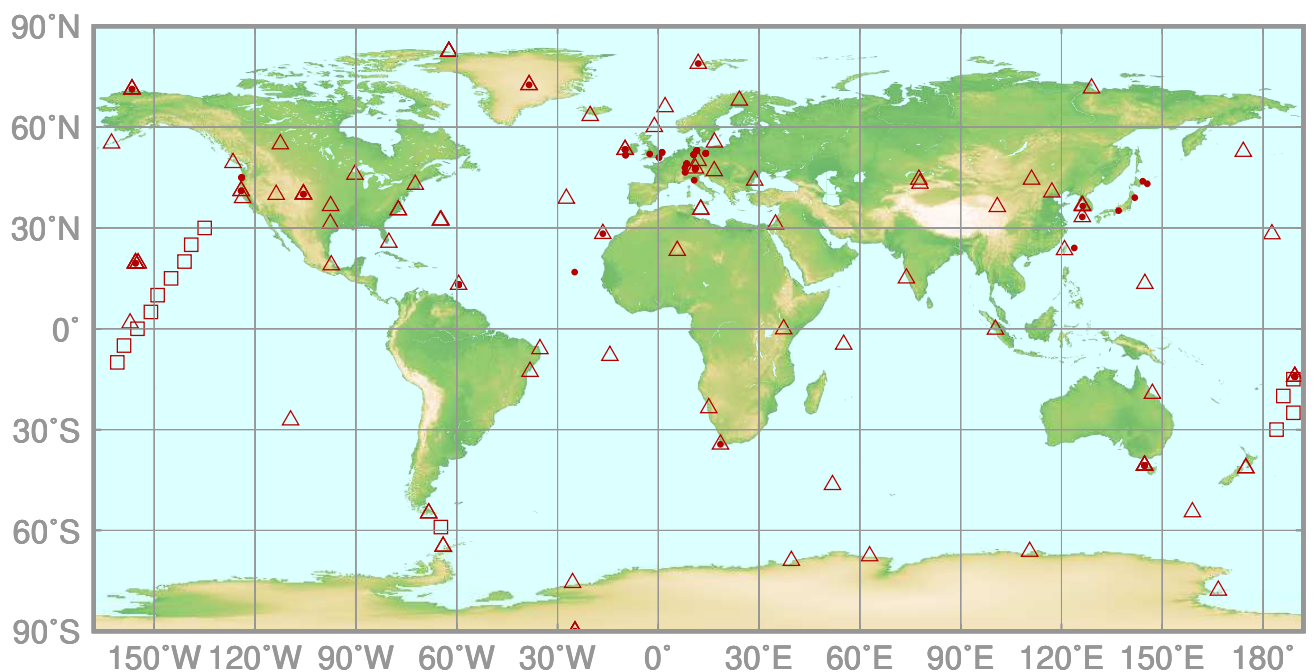
fractions in the low latitudes of the Southern Hemisphere indicates that the atmosphere in this region tends to be influenced by the mixing between the Northern Hemisphere and South Hemisphere air masses, and the cycles are partially offset. In the low latitudes of the Northern Hemisphere, mole fractions are significantly lower in summer because OH radicals are plentiful over ocean areas due to enhanced UV radiation.

# 3.

## NITROUS OXIDE

### (N<sub>2</sub>O)

- : CONTINUOUS STATION
- △ : FLASK STATION
- : FLASK MOBILE (SHIP)



This map shows locations of the stations that have submitted data for monthly mean mole fractions.

# N<sub>2</sub>O Monthly Data

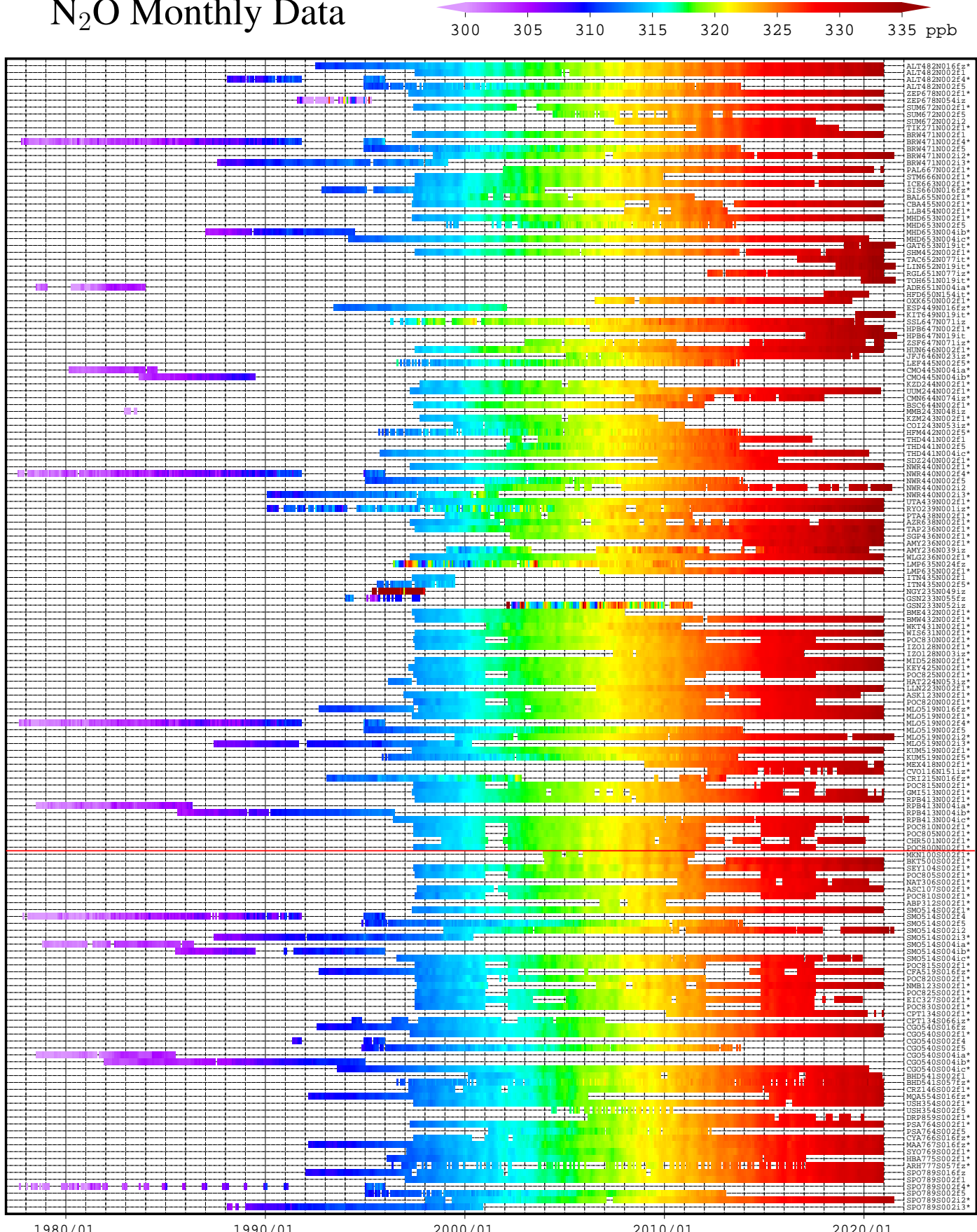
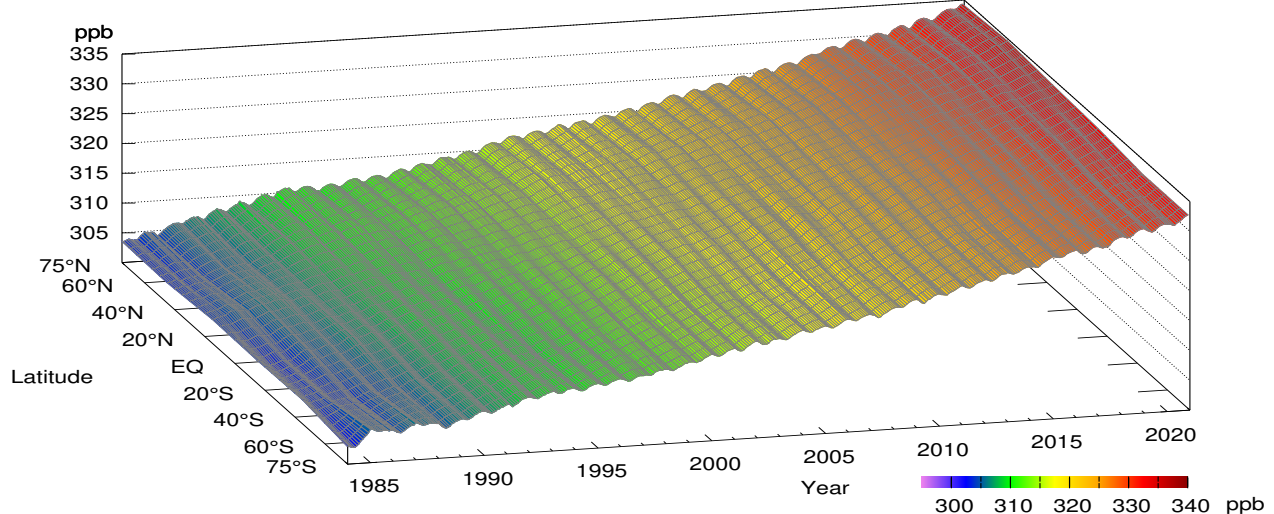
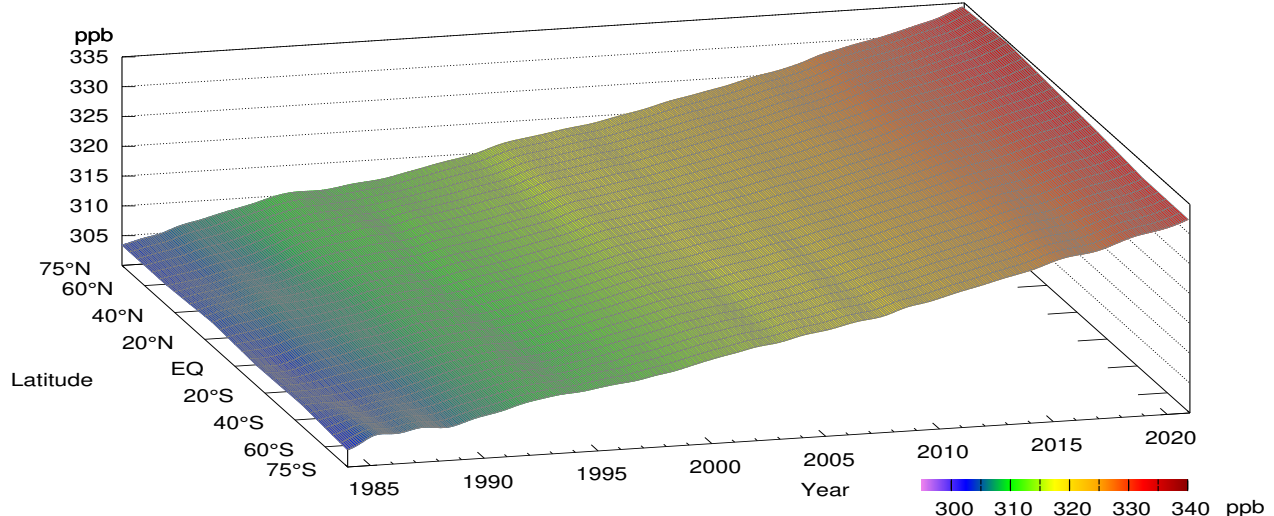


**Plate 3.1** Monthly mean  $\text{N}_2\text{O}$  mole fractions that have been reported to the WDCGG. The mole fractions are illustrated in different colors. The sites are listed in order from north to south. The red line indicates the equator. The data from the sites with an asterisk at the end of the station index are used for the analyses shown in Plate 3.2 (see Appendix A).

## N<sub>2</sub>O mole fraction



## N<sub>2</sub>O deseasonalized mole fraction



## N<sub>2</sub>O growth rate

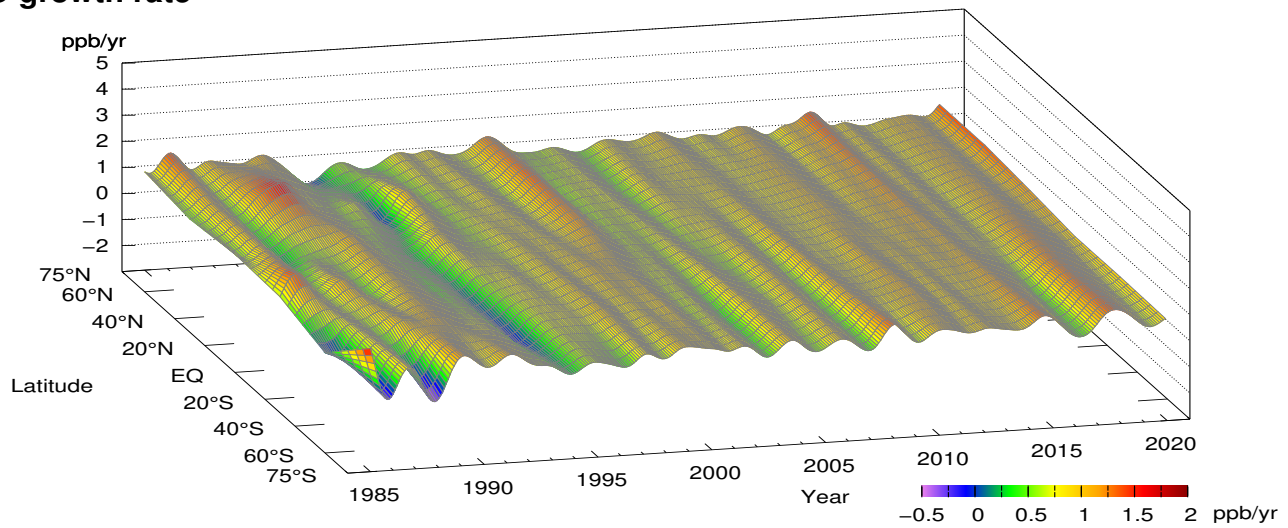


**Plate 3.2** Variation of zonally averaged monthly mean N<sub>2</sub>O mole fractions (top), deseasonalized long-term trends (middle), and growth rates (bottom). The zonally averaged mole fractions were calculated for each 30° zone. The deseasonalized trends and growth rates were derived as described in Appendix A.

### 3. NITROUS OXIDE ( $\text{N}_2\text{O}$ )

Atmospheric mole fractions of nitrous oxide ( $\text{N}_2\text{O}$ ) – a significant factor in global warming – have been increasing since the beginning of the industrial era (1750). The globally averaged mole fraction of  $\text{N}_2\text{O}$  in 2020 was  $333.2 \pm 0.1$  ppb, representing an increase of 1.2 ppb relative to the previous year and 123% of the pre-industrial level of 270 ppb.  $\text{N}_2\text{O}$  is responsible for approximately 7% of total radiative forcing (relative to the pre-industrial era) from all long-lived greenhouse gases (WMO, 2021a).

$\text{N}_2\text{O}$  sources include microbial processes (nitrification and denitrification), oceans, nitrogen fertilizers generally used in agriculture and fossil fuel/biomass combustion. Global human-induced emissions, which are dominated by nitrogen additions to croplands, increased by 30% over the past four decades and are mainly responsible for the growth in the atmospheric burden (Tian *et al.*, 2020).  $\text{N}_2\text{O}$  is relatively stable in the troposphere with a lifetime of around 121 years. Its mole fraction is relatively uniformly distributed in the troposphere and declines in the stratosphere, where it is destroyed via ultraviolet (UV) photo-decomposition.  $\text{N}_2\text{O}$  is also an important ozone-depleting substance in the atmosphere and its unmitigated

emissions will further undermine the achievements of the Montreal protocol (Solomon *et al.*, 2020).

#### Globally and hemispherically averaged mole fractions

Figure 3.1 shows globally averaged  $\text{N}_2\text{O}$  mole fraction and related growth rates. Details of the analysis are provided in Appendix A. Unlike  $\text{CO}_2$  and  $\text{CH}_4$ ,  $\text{N}_2\text{O}$  mole fractions exhibit low seasonal variability. Nevertheless, the same deseasonalization procedure was applied to  $\text{N}_2\text{O}$  datasets as to  $\text{CO}_2$  and  $\text{CH}_4$ , and the residual is shown by the red line in the top panel. The difference between original and deseasonalized time series is very small. Figure 3.2 shows  $\text{N}_2\text{O}$  mole fractions averaged over the Northern Hemisphere (dark blue) and the Southern Hemisphere (light blue) in the top panel, with corresponding growth rates in the bottom panel.

Throughout the period for which observational data are available,  $\text{N}_2\text{O}$  mole fractions have steadily increased in both hemispheres, and therefore over the whole globe. Mole fractions are higher in the Northern Hemisphere, mainly due to high concentrations of anthropogenic and

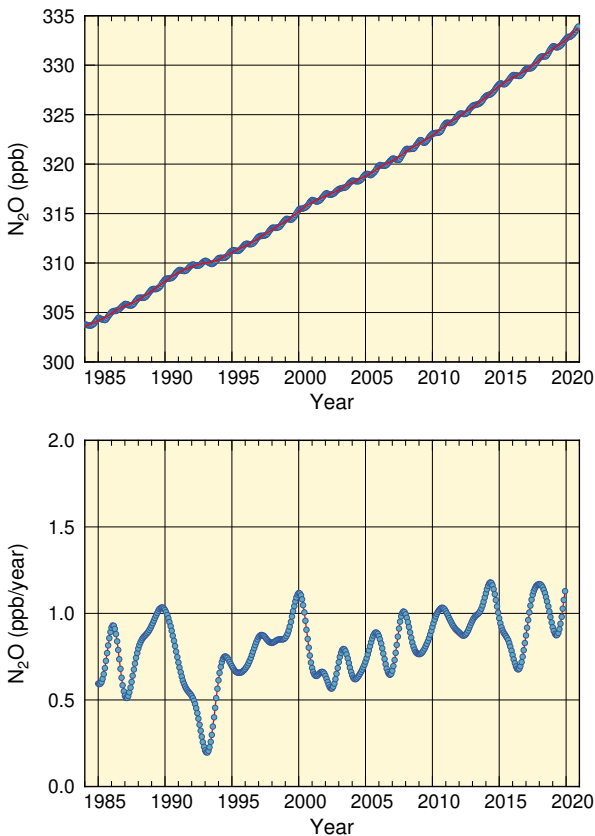


Fig. 3.1 Globally averaged monthly mean mole fraction of  $\text{N}_2\text{O}$  from 1984 to 2020 (top) and its growth rate (bottom). Red line on the top panel presents the deseasonalized long-term trend.

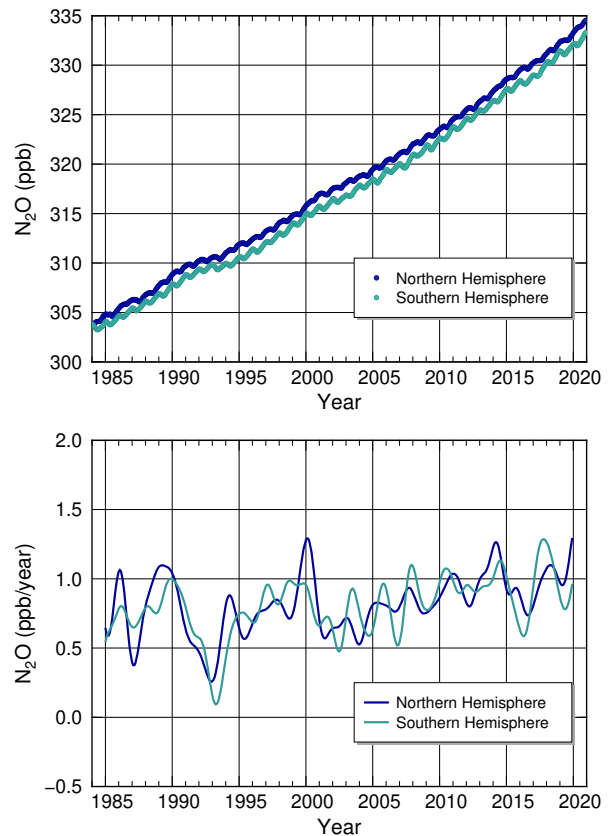


Fig. 3.2 Monthly mean mole fractions of  $\text{N}_2\text{O}$  from 1984 to 2020 (top) and their growth rates (bottom), averaged over the Northern and Southern Hemispheres.

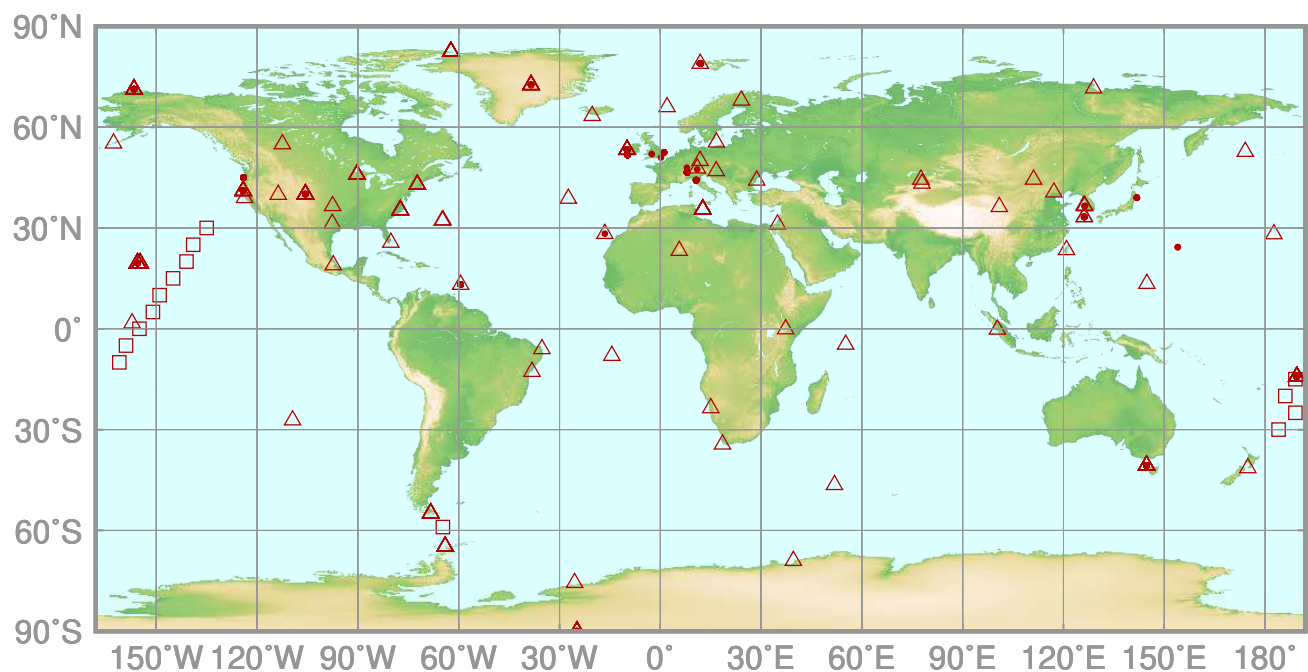
microbial sources in continental areas.

The growth rate of N<sub>2</sub>O is positive over the period 1984-2020 as a whole, although significant inter-annual variations are observed. IPCC (2021) reports that the large inter-annual variations observed in the atmospheric N<sub>2</sub>O growth rate over the tropics and sub-tropics are negatively correlated with the multivariate ENSO index (MEI) and associated anomalies in land and ocean fluxes (Ji *et al.*, 2019; Thompson *et al.*, 2019; Yang *et al.*, 2020). However, quantitative verification of specific variability patterns is challenging due to the complexity of the processes related to nitrogen cycle and uncertainty over the intensities and locations of N<sub>2</sub>O sources. Accordingly, further extension of the global observational network is needed for N<sub>2</sub>O as well as other greenhouse gases.



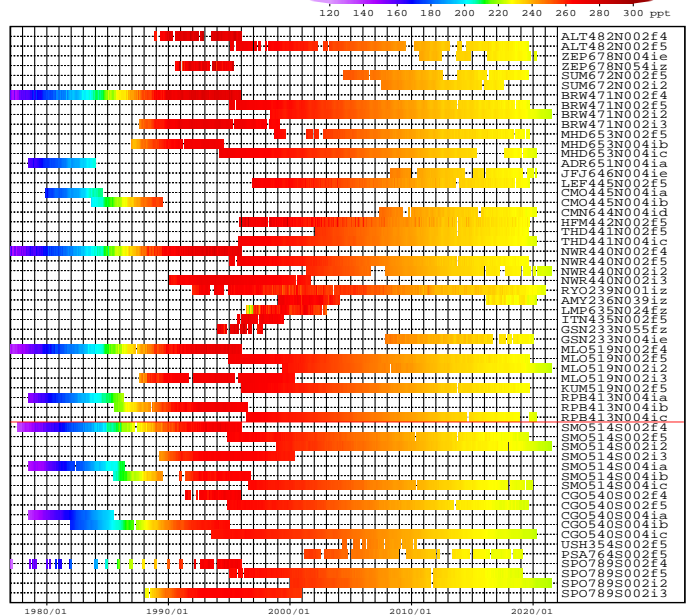
# 4. HALOCARBONS AND OTHER HALOGENATED SPECIES

- : CONTINUOUS STATION
- △ : FLASK STATION
- : FLASK MOBILE (SHIP)



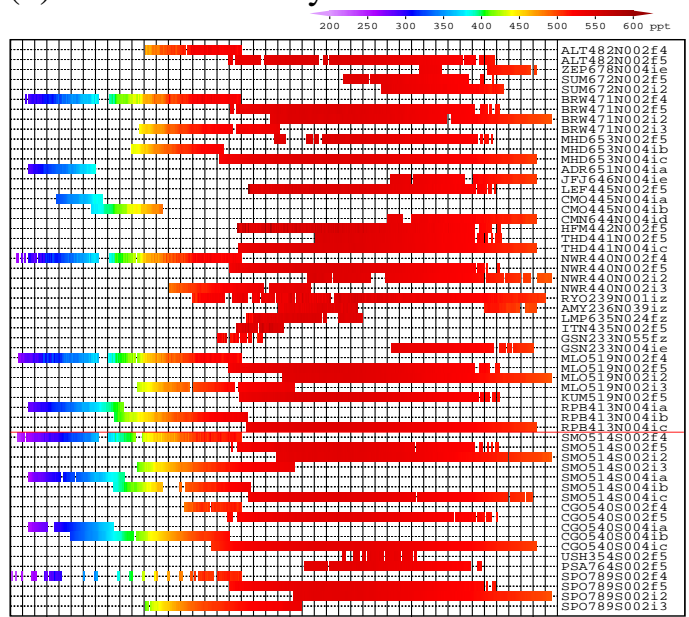
This map shows locations of the stations that have submitted data for monthly mean mole fractions.

### (a) CFC-11 Monthly Data



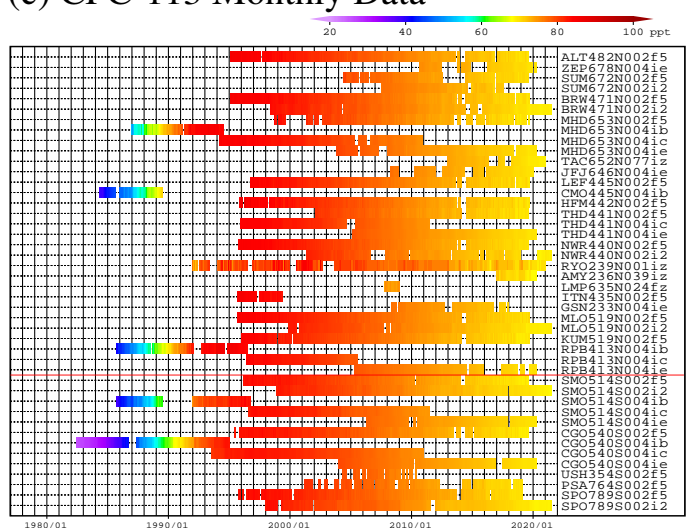
[https://doi.org/10.50849/WDCGG\\_CFC11\\_ALL\\_2021](https://doi.org/10.50849/WDCGG_CFC11_ALL_2021)

### (b) CFC-12 Monthly Data



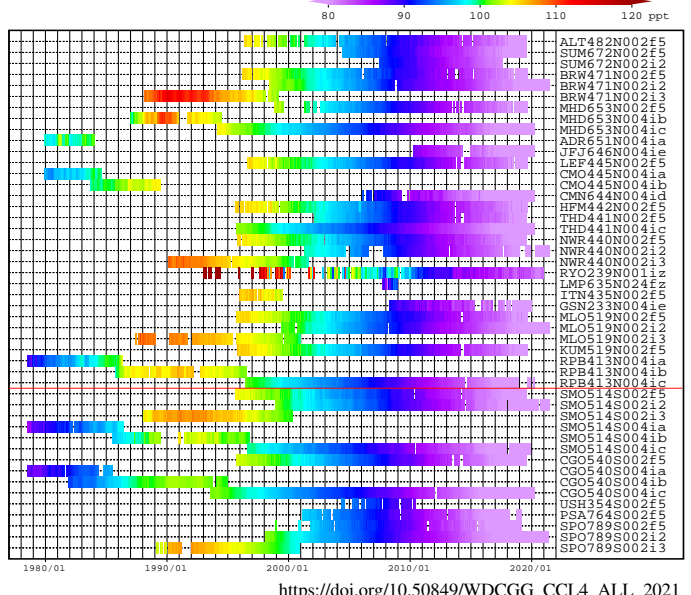
[https://doi.org/10.50849/WDCGG\\_CFC12\\_ALL\\_2021](https://doi.org/10.50849/WDCGG_CFC12_ALL_2021)

### (c) CFC-113 Monthly Data



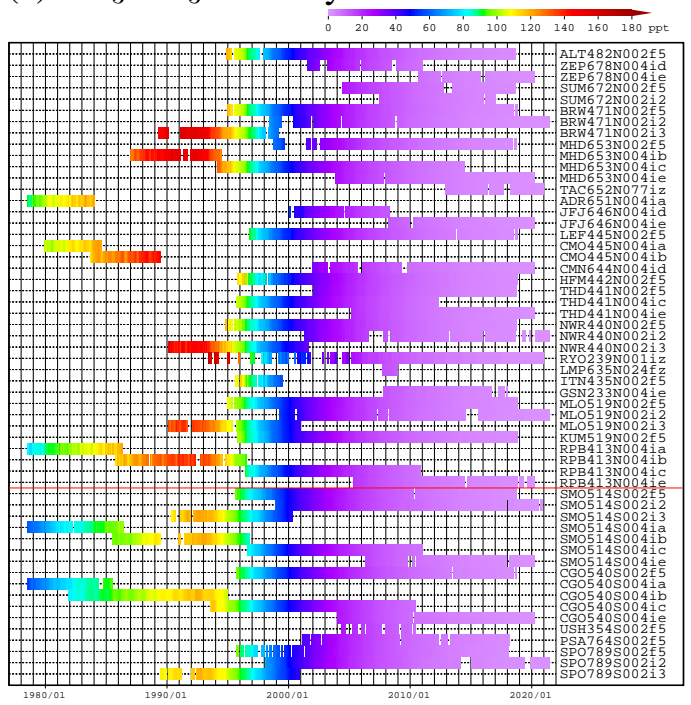
[https://doi.org/10.50849/WDCGG\\_CFC113\\_ALL\\_2021](https://doi.org/10.50849/WDCGG_CFC113_ALL_2021)

### (d) CCl<sub>4</sub> Monthly Data



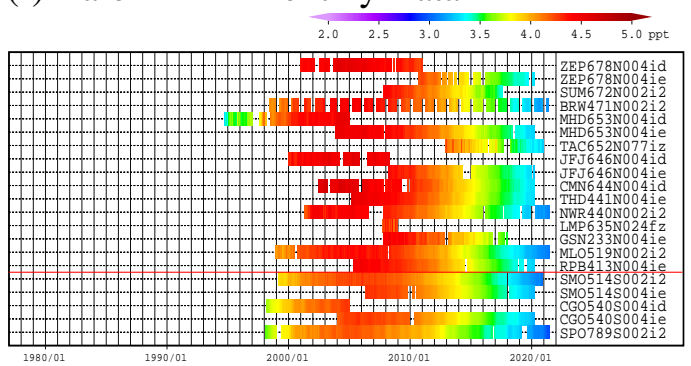
[https://doi.org/10.50849/WDCGG\\_CCL4\\_ALL\\_2021](https://doi.org/10.50849/WDCGG_CCL4_ALL_2021)

### (e) CH<sub>3</sub>CCl<sub>3</sub> Monthly Data



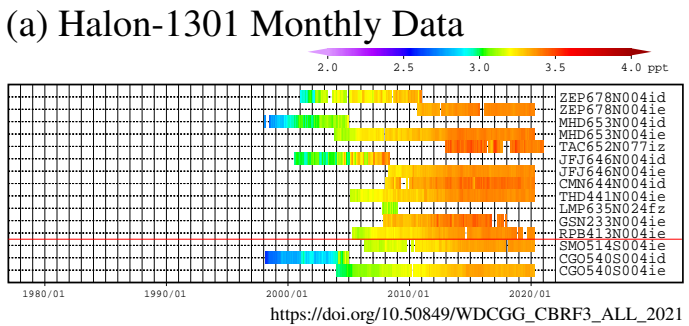
[https://doi.org/10.50849/WDCGG\\_CH3CCL3\\_ALL\\_2021](https://doi.org/10.50849/WDCGG_CH3CCL3_ALL_2021)

### (f) Halon-1211 Monthly Data

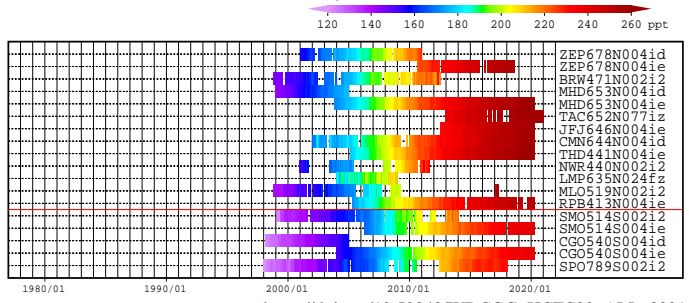


[https://doi.org/10.50849/WDCGG\\_CBRLCF2\\_ALL\\_2021](https://doi.org/10.50849/WDCGG_CBRLCF2_ALL_2021)

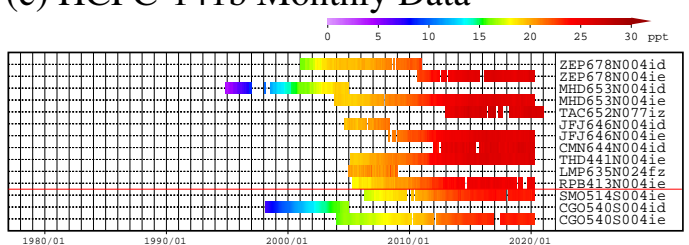
**Plate 4.1** Monthly mean (a) CFC-11, (b) CFC-12, (c) CFC-113, (d) CCl<sub>4</sub>, (e) CH<sub>3</sub>CCl<sub>3</sub>, (f) Halon-1211 mole fractions that have been reported to the WDCGG. The mole fractions are illustrated in different colors. The sites are listed in order from north to south. The red line indicates the equator.



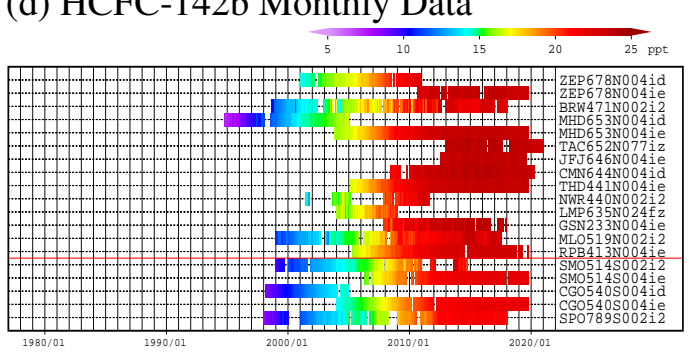
### (b) HCFC-22 Monthly Data



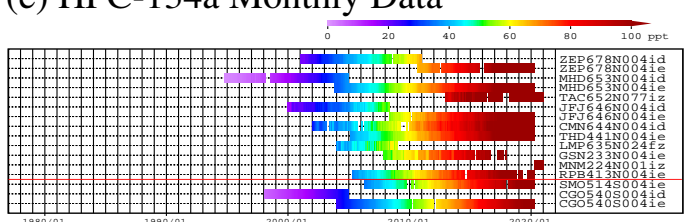
(c) HCEC-141b Monthly Data



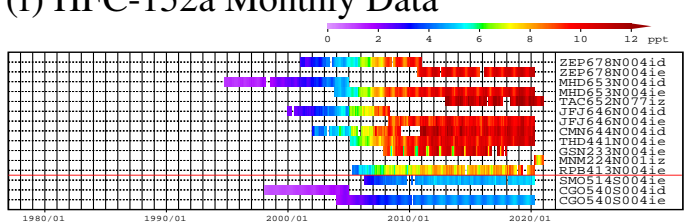
<https://doi.org/10.50849/WDCG0>



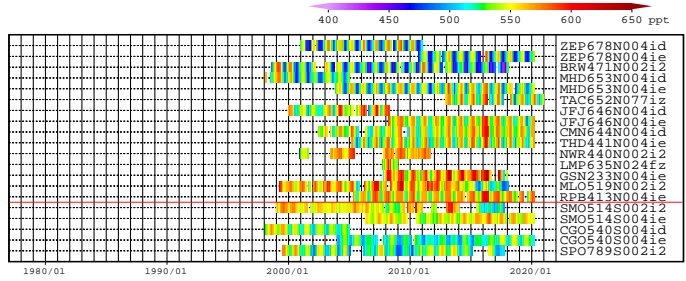
<https://doi.org/10.5084/WD>



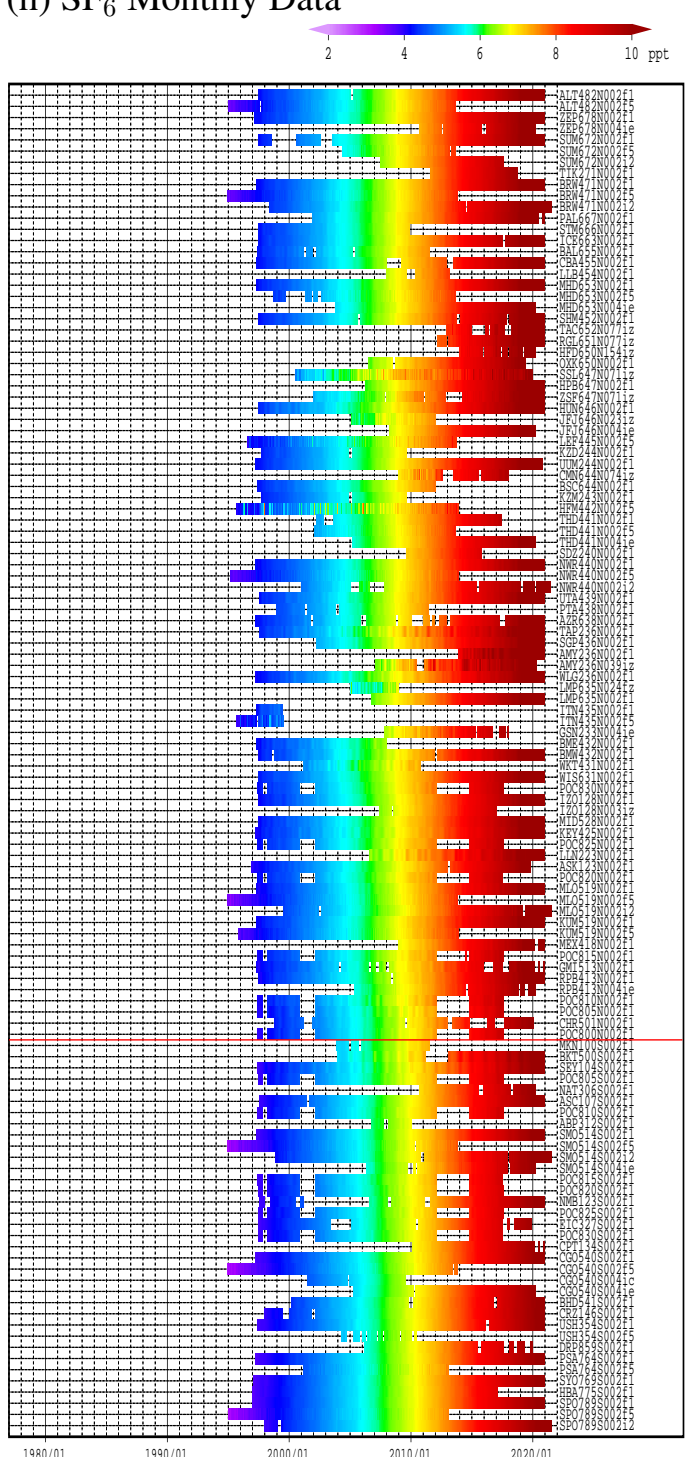
<https://doi.org/10.50849/W>



### (g) CH<sub>3</sub>Cl Monthly Data



<https://doi.org/10.5281/zenodo.4102000>



[https://doi.org/10.50849/WDCGG\\_SF6\\_ALL\\_2021](https://doi.org/10.50849/WDCGG_SF6_ALL_2021)

**Plate 4.2** Monthly mean (a) Halon-1301, (b) HCFC-22, (c) HCFC-141b, (d) HCFC-142b, (e) HFC-134a, (f) HFC-152a, (g) CH<sub>3</sub>Cl, (h) SF<sub>6</sub> mole fractions that have been reported to the WDCGG. The mole fractions are illustrated in different colors. The sites are listed in order from north to south. The red line indicates the equator.

## 4. HALOCARBONS AND OTHER HALOGENATED SPECIES

Halocarbons are generally carbon compounds containing halogens. Most are artificially generated and have much lower atmospheric mole fractions than major greenhouse gases, but they contribute significantly to global warming. These gases together are responsible for around 11% of the total increase in radiative forcing since the pre-industrial era (1750) caused by all long-lived greenhouse gases (WMO, 2021a).

Major examples include chlorofluorocarbons (CFCs; carbon compounds containing both fluorine and chlorine), with CFC-11, CFC-12 and CFC-113 having particularly significant impacts on global warming. CFCs used to be mass-produced as refrigerants, propellants, detergents and other functional substances until their connection with stratospheric ozone depletion became evident. After CFC production and consumption were internationally prohibited under the Montreal Protocol in 1989, mole

fractions of CFC-11, CFC-12 and CFC-113 decreased. However, a slowing of the decrease in CFC-11 mole fractions was observed from 2013 to 2018 (Figures 4.1, 4.2). This is considered to be associated with CFC-11 emissions from renewed production in eastern Asia (Montzka *et al.*, 2018). Since 2019, an accelerated decline in CFC-11 mole fractions has been observed (Montzka *et al.*, 2021; WMO, 2021b). Recent publications highlighted that other CFCs in the atmosphere are decreasing slower than anticipated as well as CFC-11 (Solomon *et al.*, 2020).

Carbon tetrachloride ( $\text{CCl}_4$ ), methyl chloroform (1,1,1-trichloroethane,  $\text{CH}_3\text{CCl}_3$ ), halons and hydrochlorofluorocarbons (HCFCs) are also considered ozone-depleting substances, with related production and consumption regulated under the Montreal Protocol and associated amendments made in the 1990s. Halons are carbon compounds containing bromine, with Halon-1211 and Halon-1301 as typical species. HCFCs represent carbon compounds containing hydrogen, in addition to fluorine and chlorine, with HCFC-22, HCFC-141b and HCFC-142b as major examples. Mole fractions of  $\text{CCl}_4$ ,  $\text{CH}_3\text{CCl}_3$  and Halon-1211 are decreasing. Growth rates of Halon-1301, HCFC-141b and HCFC-142b have levelled off in recent years, and mole fractions of HCFC-22 are increasing slower than in the 2000s (Figure 4.1, 4.2).

Hydrofluorocarbons (HFCs; carbon compounds containing hydrogen and fluorine but no chlorine) are not ozone depletion substances, and were developed as substitutes for CFCs and HCFCs. However, due to their significant greenhouse effects, they are regulated under the Kigali amendment to the Montreal Protocol adopted in 2016 (effective as of 2019). Typical species include HFC-134a and HFC-152a. Mole fractions of HFC-134a are rapidly increasing, while the growth rate of HFC-152a has levelled off in recent years (Figure 4.1, 4.2).

Unlike other halocarbons that have anthropogenic origin, methyl chloride (chloromethane,  $\text{CH}_3\text{Cl}$ ) comes from natural sources as well. Mole fractions of  $\text{CH}_3\text{Cl}$  show no significant long-term trend, although clear seasonal cycles are observed (see Figure 4.2).  $\text{CH}_3\text{Cl}$  is not regulated under the Montreal Protocol, but its status is monitored at many observational stations. Because  $\text{CH}_3\text{Cl}$  is one of the most abundant halocarbons in the remote atmosphere, it plays an important role as a carrier of ozone-depleting chlorine into the stratosphere (Engel *et al.*, 2018).

Although not technically a halocarbon, sulfur hexafluoride ( $\text{SF}_6$ ) is often discussed together with halocarbons and other halogenated gases.  $\text{SF}_6$  has very significant greenhouse effects despite its low abundance, and is targeted for reduction by the Kyoto Protocol. Mole fractions of  $\text{SF}_6$  show a continuous increase (see Figure 4.1, 4.2).  $\text{SF}_6$  is a substance which originates only from anthropogenic sources. It comes from the electricity and

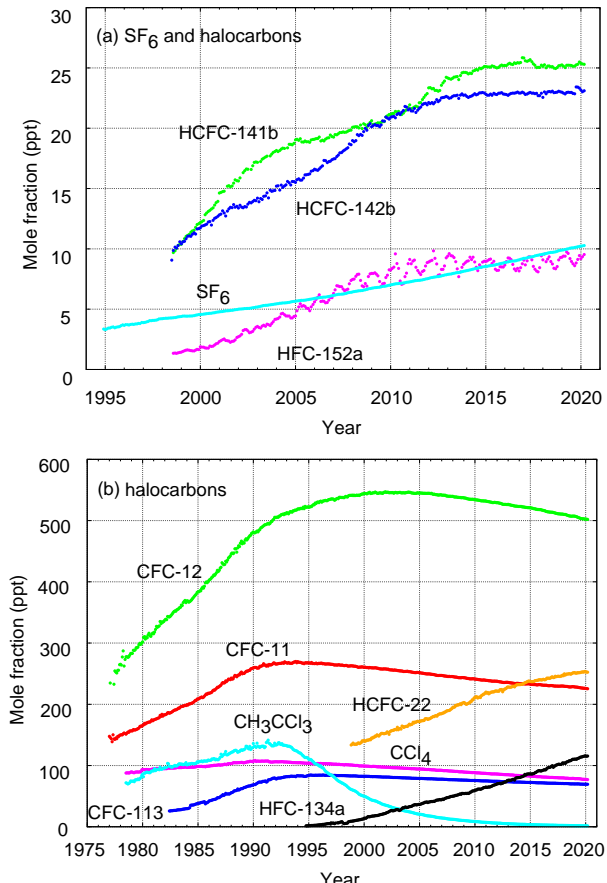


Fig. 4.1 Monthly mean mole fractions of  $\text{SF}_6$  and the most important halocarbons: (a)  $\text{SF}_6$  and lower mole fractions of halocarbons, and (b) higher halocarbon mole fractions. A number of stations are used for the analyses:  $\text{SF}_6$  (88), CFC-11 (23), CFC-12 (25), CFC-113 (22),  $\text{CCl}_4$  (22),  $\text{CH}_3\text{CCl}_3$  (25), HCFC-141b (10), HCFC-142b (15), HCFC-22 (14), HFC-134a (11), HFC-152a (10).

electronics supply industries, e.g. the semiconductor industry, where it is used as an electronic insulator due to its inertness. Increasing demand for the electricity and power networks will continue leading to SF<sub>6</sub> increases in the atmosphere.

Figure 4.2 displays mole fractions of 14 gas species, with circles representing monthly mean values at individual stations (rather than values averaged over different stations). Solid and open circles correspond to stations in the Northern Hemisphere and Southern Hemisphere, respectively. Due to more intensive production of artificial halocarbons in the Northern Hemisphere, related mole fractions tend to be higher in this region, especially in their increasing phases.

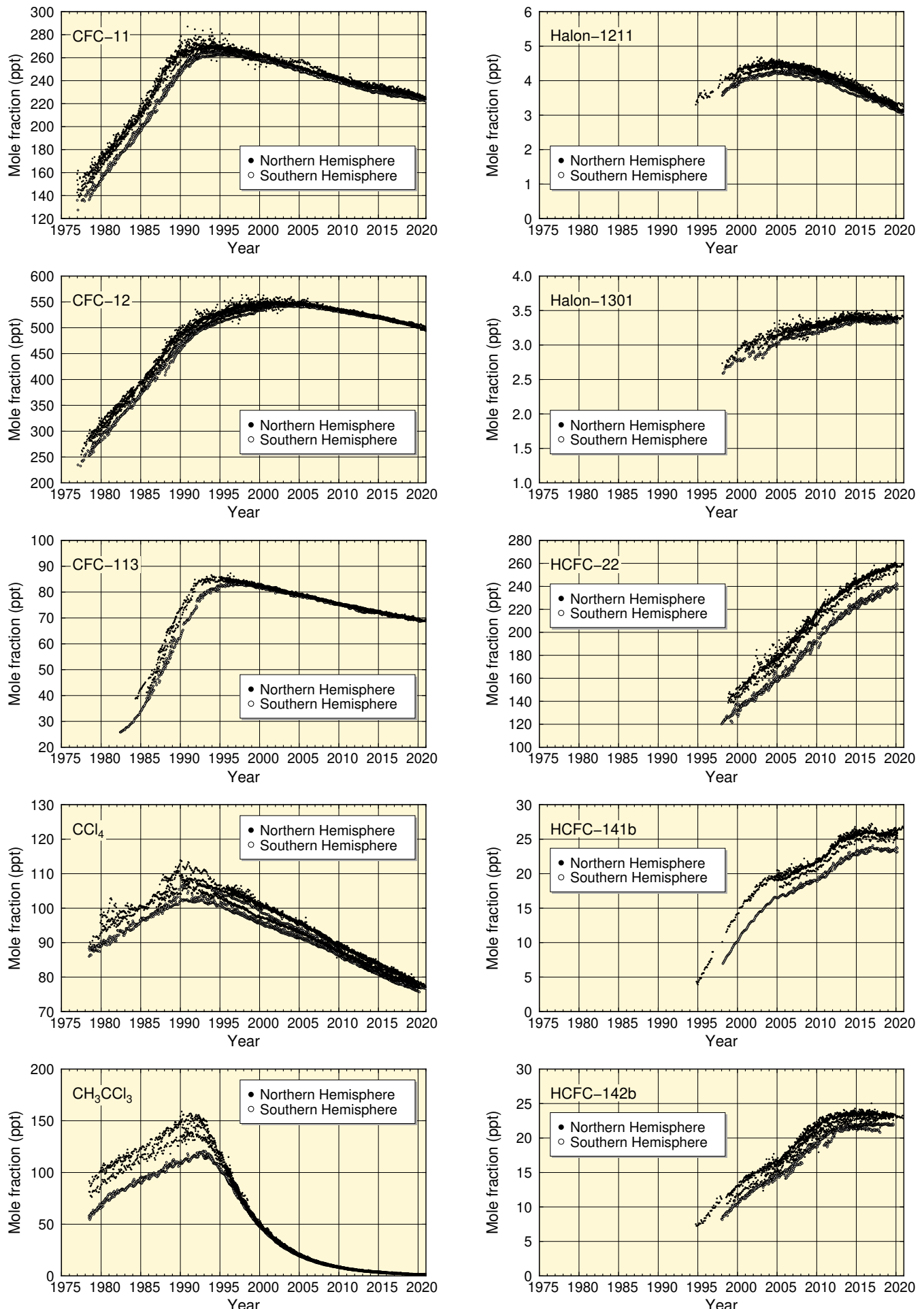


Fig. 4.2 Time series of the monthly mean mole fractions of halocarbons, other halogenated species and sulfur hexafluoride at individual stations. Solid circles show mole fractions in the Northern Hemisphere and open circles show those measured in the Southern Hemisphere.

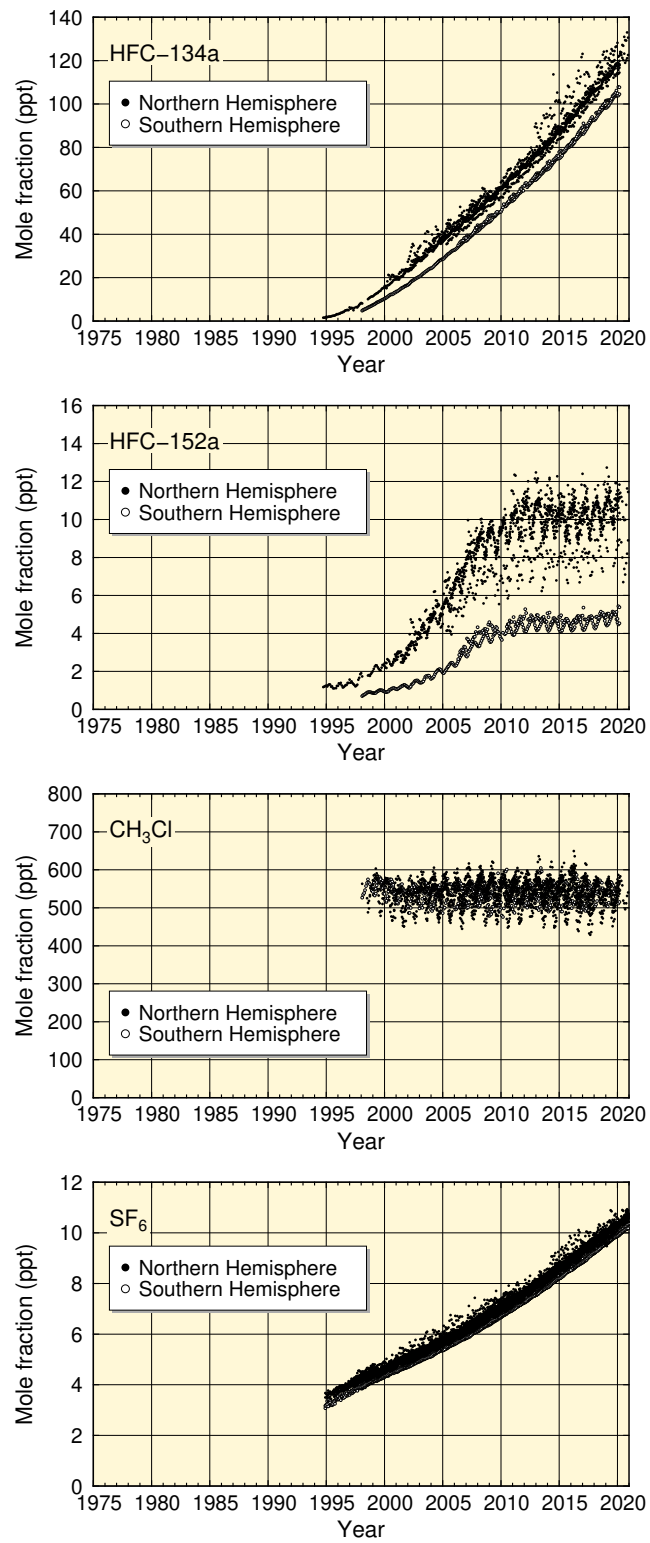


Fig. 4.2 (Continued)

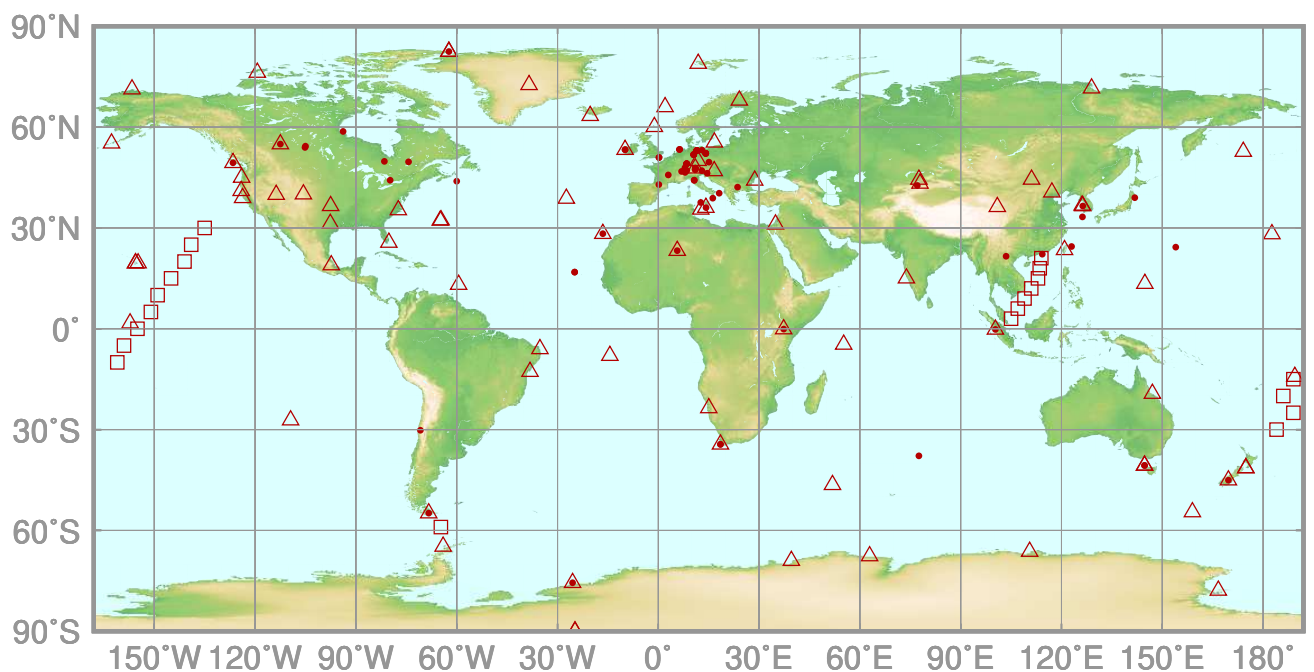


# 5.

## CARBON MONOXIDE

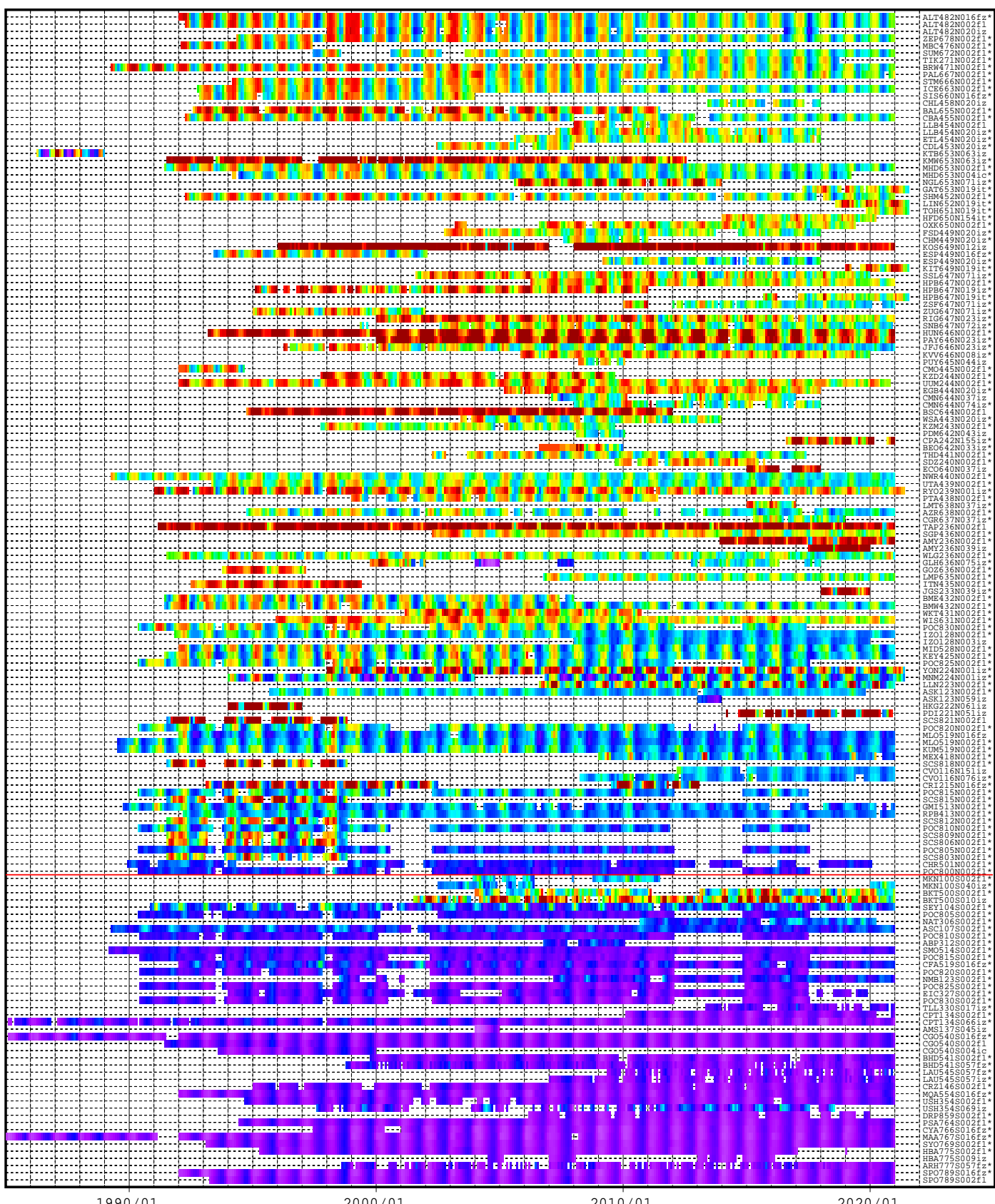
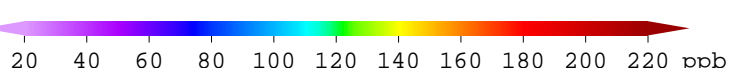
### (CO)

- : CONTINUOUS STATION
- △ : FLASK STATION
- : FLASK MOBILE (SHIP)



This map shows locations of the stations that have submitted data for monthly mean mole fractions.

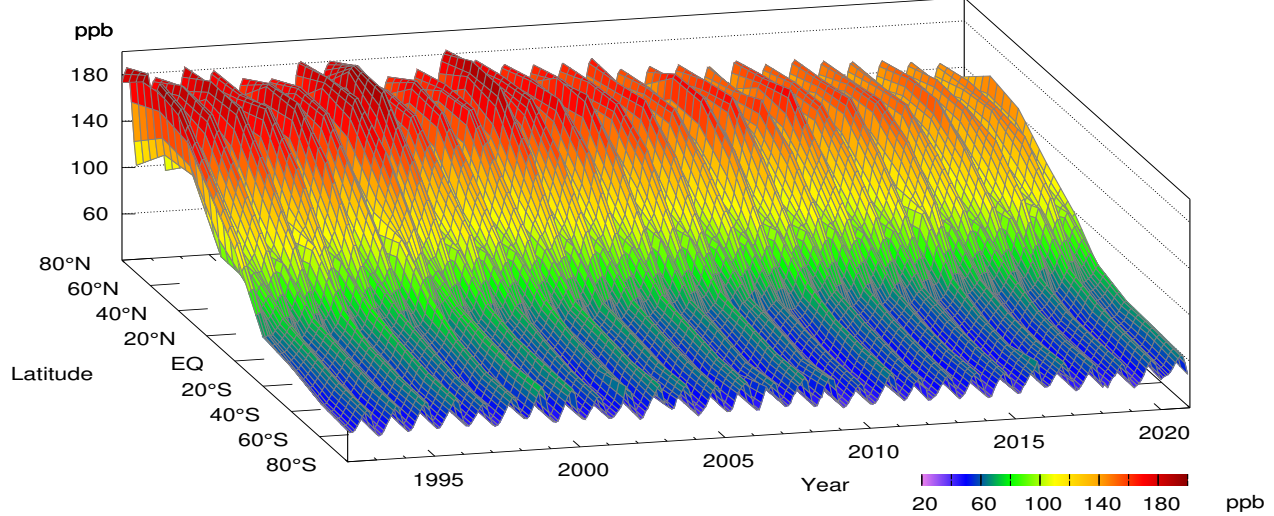
# CO Monthly Data



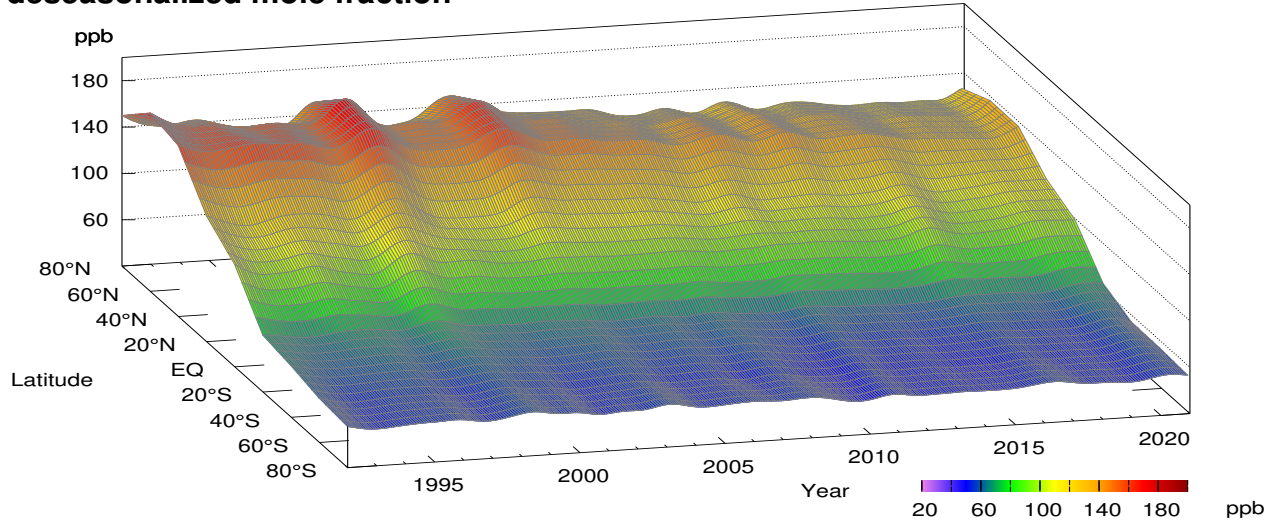
[https://doi.org/10.50849/WDCGG\\_CO\\_ALL\\_2021](https://doi.org/10.50849/WDCGG_CO_ALL_2021)

**Plate 5.1** Monthly mean CO mole fractions that have been reported to the WDCGG. The mole fractions are illustrated in different colors. The sites are listed in order from north to south. The red line indicates the equator. The data from the sites with an asterisk at the end of the station index were used for the analyses shown in Plate 5.2 (see Appendix A).

## CO mole fraction



## CO deseasonalized mole fraction



## CO growth rate

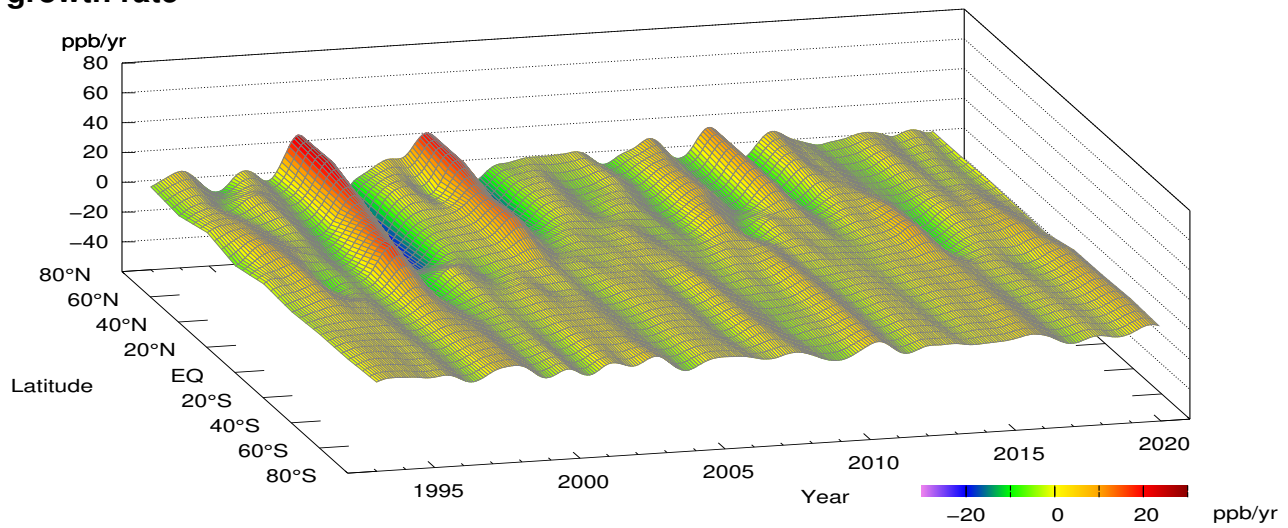


**Plate 5.2** Variation of zonally averaged monthly mean CO mole fractions (top), deseasonalized long-term trends (middle), and growth rates (bottom). The zonally averaged mole fractions were calculated for each  $20^{\circ}$  zone. The deseasonalized trends and growth rates were derived as described in Appendix A.

## 5. CARBON MONOXIDE (CO)

Carbon monoxide (CO) is not categorized as a greenhouse gas because it absorbs hardly any infrared radiation from the earth. However, it influences major greenhouse gases, particularly through reaction with hydroxyl (OH) radical, and is therefore often addressed in the context of global warming. CO is also part of the global carbon cycle.

Analysis of the global tendencies of CO is complicated by the fact that observations of CO in different part of the world are performed not in a fully consistent way. In contrast to the situation with major greenhouse gases, CO calibration scales cannot be easily interlinked (see Appendix B). Global analysis performed irrespective of scale differences showed a globally averaged CO mole fraction of  $95 \pm 3$  ppb for 2020. Similarly, the analysis results presented in this chapter are based on observations performed on different scales.

CO is emitted into the atmosphere from fossil fuel/biomass burning among other sources, and is destroyed predominantly via reaction with OH radicals. Due to its chemical reactivity, CO is characterized by a relatively short lifetime (in the range of tens of days) and

large spatial variations. Ice core measurements performed by Haan and Raynaud (1998) revealed that the CO mole fractions of approximately 90 ppb observed in Greenland around 1750 had increased to approximately 110 ppb by 1950, indicating an impact from human activity. CO mole fractions have shown a gradual decline since around the beginning of the 21st century, particularly in the Northern Hemisphere (IPCC, 2021).

### Globally averaged mole fractions

The blue dots in Fig. 5.1 show globally averaged monthly mean CO mole fractions (top) and related growth rates (bottom) based on the analysis described in Appendix A. Clear seasonal variability is observed, and the long-term trend was determined after subtraction of the seasonal component (shown by the red line in the top panel of Fig. 5.1). The globally averaged CO mole fraction exhibits a gradual but significant decrease, with the growth rate oscillating around zero. Mole fractions exhibit clear seasonal cycle, being lower in boreal summer and higher in winter. This is mainly because OH radicals, which react with and destroy CO, become more abundant

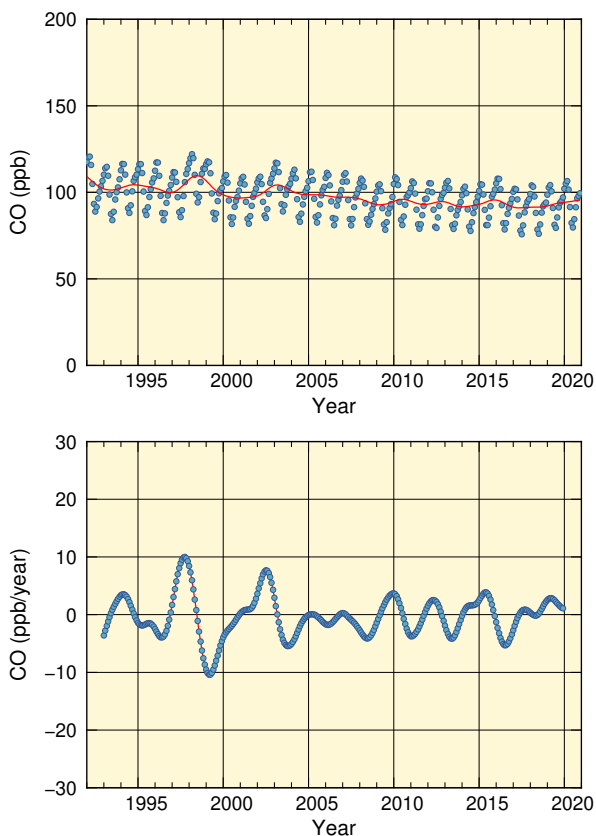


Fig. 5.1 Globally averaged monthly mean mole fraction of CO from 1992 to 2020 (top) and its growth rate (bottom). Red line on the top panel presents the deseasonalized long-term trend.

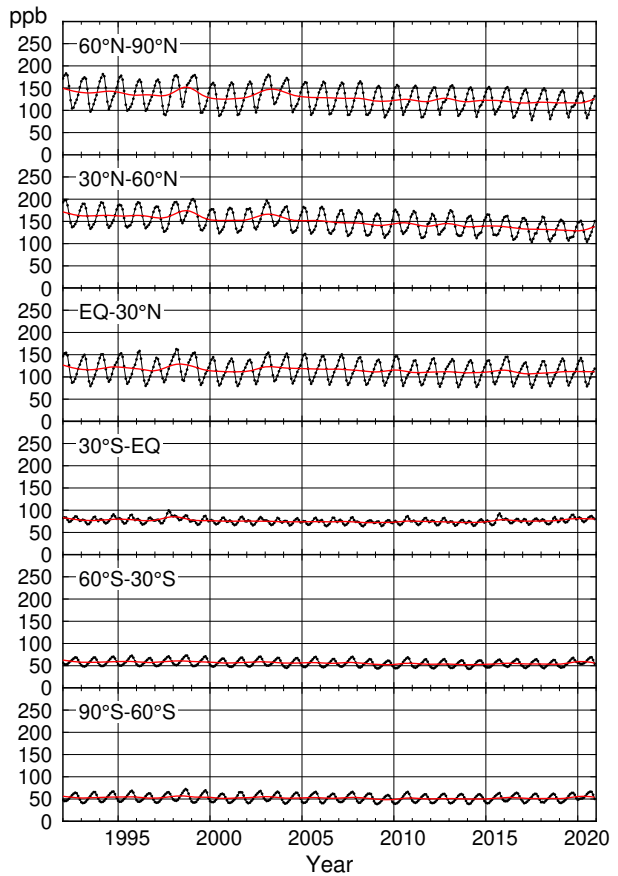


Fig. 5.2 Monthly mean mole fractions of CO from 1992 to 2020 for each  $30^\circ$  latitudinal zone (black) and their deseasonalized long-term trends (red).

in summer due to enhanced ultraviolet (UV) radiation. Seasonally varying sources such as biomass burning, domestic combustion and traffic emissions also contribute to the formation of the seasonal cycles.

### Latitudinal dependence of mole fractions

The black lines in Fig. 5.2 show CO mole fractions averaged over six  $30^{\circ}$  latitudinal bands, and the red lines show corresponding long-term trends. These trends are collectively shown in the top panel of Figure 5.3, and the corresponding growth rates are shown in the bottom panel. Average seasonal cycles of CO mole fractions for every latitudinal band are shown in Figure 5.4.

As shown in Figure 5.3, northern regions have higher mole fractions, indicating the presence of more CO sources such as fossil fuel/biomass combustion. CO mole fractions in the Northern Hemisphere have shown slight declines throughout the period for which global averaging is feasible, and have remained almost constant in the Southern Hemisphere. CO growth rates also exhibit significant spatial and temporal variability, and tend to be readily influenced by local events with limited time durations. By way of example, the large growth rate peak of 1997/1998 observed in the Northern Hemisphere and elsewhere may be considered attributable to forest fires in Siberia and tropical areas (Novelli *et al.*, 2003) during El Niño.

The amplitude of seasonal cycles for CO mole fractions is larger in northern bands than in southern bands, as shown in Figure 5.4. In the Northern Hemisphere, CO emitted from fossil fuel combustion accumulates in the mid- and high latitudes during winter and early spring under low OH radical conditions. In addition, CO emissions from biomass burning in the low latitudes peak in early spring. In summer, most of the CO accumulated during winter is destroyed by OH radicals. In the Southern Hemisphere, seasonal cycles of CO mole fractions are driven by emissions from biomass burning in the tropics and removal via reaction with OH radicals, resulting in a smaller seasonal-cycle amplitude (Novelli *et al.*, 1998). The phase of seasonal cycles for CO mole fractions in the two hemispheres is opposed due to the reversed seasons. Seasonal variability in the low latitudes of the Southern Hemisphere is slightly more complex due to impact of inter-hemispheric mixing.

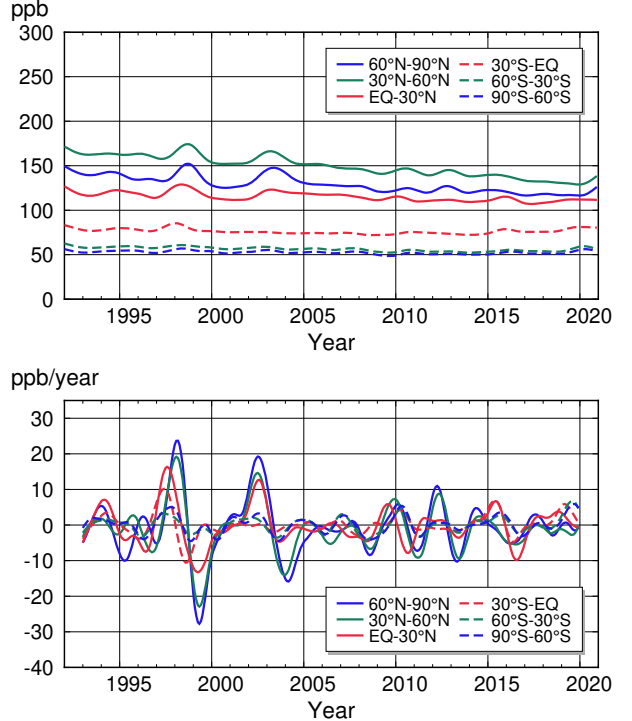


Fig. 5.3 Deseasonalized long-term trends of CO for each  $30^{\circ}$  latitudinal zone (top) and their growth rates (bottom).

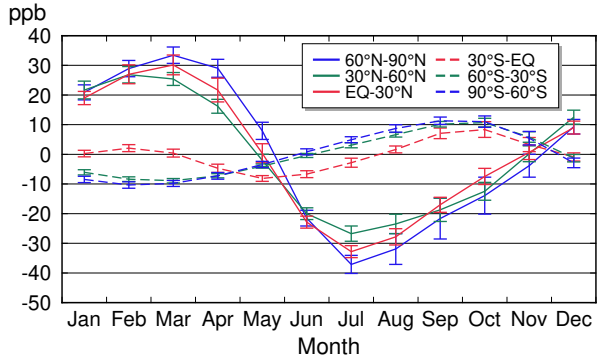


Fig. 5.4 Average seasonal cycles of CO mole fractions for each  $30^{\circ}$  latitudinal zone obtained by subtracting long-term trends from the zonally averaged time series. Error bars represent the range of  $\pm 1\sigma$  calculated for each month (period 1992 to 2020).



# **APPENDICES**

## APPENDIX A ANALYSIS

This appendix summarizes calculation of globally averaged mole fractions and related quantities of CO<sub>2</sub>, CH<sub>4</sub>, N<sub>2</sub>O and CO as described by WMO (2009).

The analysis is applied to monthly mean mole fraction data reported to WDCGG by fixed stations and ships with fixed geographic observational points. Where no monthly data are reported, values are calculated from valid daily or hourly data based on a simple arithmetic mean with the consent of data contributors. Data from mobile platforms such as ships without fixed observation points and aircraft are not used, but are considered in other analysis. Where data are reported for several different altitudes, those for the highest level are used due to their expected larger footprint.

For halocarbons, monthly mean mole fractions from observation at individual stations are presented. Scale differences are not taken into account in this analysis.

The mole fraction is defined as the number of molecules of a target gas species divided by the number of all molecules in dry air. Values are expressed as parts per million (ppm), parts per billion (ppb) and parts per trillion (ppt), corresponding to the SI units of  $\mu\text{mol/mol}$ , nmol/mol and pmol/mol, respectively.

### (1) Site selection

All observation data are objectively examined for global analysis as described here.

Data with a standard scale traceable to the WMO Mole Fraction Scale (or a compatible standard for conversion) are first selected. CO data are an exception due to the scarcity of standard scales for which accurate conversion to the WMO Scale is possible.

For individual sites, annual mean mole fractions relative to those of the South Pole (averaged over the years for which data are available) are plotted to show latitudinal distribution and fitted to the LOESS model curve (Cleveland and Devlin, 1988). Outlier sites beyond the 3 sigma (residual standard deviation) of the fitted curve are excluded from further analysis, and the process is iterated until exclusion terminates. Exclusion is not applied to N<sub>2</sub>O

due to the scarcity of annual mean data from the 1980s.

The numbers of sites that fit for global analysis (before and after this selection procedure) are shown in Table A1.

### (2) Extension of observation data to cover the entire analysis period

Time-series data from some sites may contain gaps or fail to cover the entire analysis period. To ensure the homogeneity of globally averaged values over analysis periods exceeding 30 years, shortfalls in data coverage are compensated for using interpolation and extrapolation as described below.

Gaps in time-series representations are first interpolated for each site. The longest period among continuous monthly mean mole fraction data is identified, and the seasonal cycle and long-term trend are determined as detailed in WMO (2009). In short, a time series of mole fractions is approximated based on the sum of a Fourier series up to the third harmonic of the annual cycle and a non-periodic component determined via a Lanczos filter (Duchon, 1979) with a cut-off frequency of 0.48 cycles per year; the former is a seasonal cycle, and the latter is a long-term trend. Mole fractions in gaps are then interpolated with a line connecting each end of the deseasonalized monthly values and superimposed with the seasonal cycle.

After interpolation, the data are extrapolated via a number of statistical procedures. First, a time series of mole fraction growth rates is calculated for each observation site by differentiating the long-term trend as determined from mole fractions with gaps interpolated as above. Next, for each of six 30° latitudinal bands (60 – 90°N, 30°S – EQ, etc.), an average time series of growth rates is calculated as an arithmetic mean over sites located within the band. For individual sites, the long-term trend is then extended to cover the entire analysis period based on growth rates for the latitudinal band where the site is located, and is finally superimposed with the seasonal cycle for the site determined after interpolation.

**Table A1. Numbers of sites before/after the selection procedure outlined in Section (1) for CO<sub>2</sub>, CH<sub>4</sub>, N<sub>2</sub>O and CO**

	CO <sub>2</sub>	CH <sub>4</sub>	N <sub>2</sub> O	CO
Pre-selection <sup>(a)</sup>	174	150	109	140
Post-selection <sup>(b)</sup>	139	138	105	128

(a) Figures are derived from the number of the first seven characters of the Filename Code (e.g., RYO239N) in Plate 1.1, 2.1, 3.1 and 5.1 (or Table B2 to B5), excluding duplicates.

(b) As per (a), but with Filename Codes marked with asterisks.

### **(3) Calculation of globally and hemispherically averaged mole fractions**

With the extension procedure described above, all sites selected as described in Section (1) have a time series of mole fractions covering the entire analysis period with no data gaps. From these data, latitudinally averaged mole fractions are calculated for the six bands, and globally and hemispherically averaged mole fractions are then determined by averaging the mole fractions of six and three latitudinal bands, respectively, with weighting for surface area. The seasonal cycle, long-term trend and growth rate are then determined for every averaged time series. As long-term trend calculation is less precise at either end of mole fraction time-series representations (see WMO 2009 for details), growth rates originating from the related derivative function are characterized by larger uncertainty. Accordingly, growth rates for a year each from either end of the analysis period are not shown in the figures here.

### **(4) Uncertainty estimation**

In this analysis, uncertainty in globally averaged mole fractions (at a 68% confidence level) is calculated using bootstrap analysis as described in Conway *et al.* (1994). From the dataset of mole fractions obtained after the site selection and data extension procedure described above,  $n$  sites are randomly selected, with duplication of the same sites allowed on condition that at least one site is selected from each of the six latitudinal bands, and a globally averaged mole fraction is calculated using the data from the  $n$  sites. The procedure is repeated  $m$  times to determine  $m$  different globally averaged mole fractions. Uncertainty is defined as the standard deviation of these mole fractions. In this analysis, the number of sites selected as described in Section (1) and 200 are chosen as  $n$  and  $m$ , respectively, for maximum stability in the standard deviation determination.

## APPENDIX B CALIBRATION AND STANDARD SCALES

### 1. Calibration System in the GAW Programme

Under the Global Atmosphere Watch (GAW) Programme, the Central Calibration Laboratories (CCLs) are assigned to host a Primary (Reference) Standard/scale, while the World Calibration Centres (WCCs) and Regional Calibration Centres (RCC) are responsible for the scale propagation to the stations via distribution of calibration standards for certain compounds, conducting instrument calibrations, comparison campaigns, station

audits and providing training to the station personnel. A Reference Standard/scale is designated for each variable to be used for all GAW measurements of that variable. Table B1 lists the organizations that serve as WCCs and CCLs for GAW (WMO, 2017). For CFCs, no central facilities or quality control systems have so far been established within the GAW Programme.

**Table B1. Overview of the GAW Central Calibration Laboratories (GAW-CCL, Reference Standard) and World Calibration Centres for greenhouse and other related gases. The World Calibration Centres have assumed global responsibilities, except where indicated (Am, Americas; E/A, Europe and Africa; A/O, Asia and the South-West Pacific)**

Compounds	Central Calibration Laboratory (Host of Primary Standard)	World Calibration Centre
Carbon Dioxide (CO <sub>2</sub> )	NOAA/ESRL	NOAA/ESRL (Round Robin) Empa (audits)
Carbon Dioxide (CO <sub>2</sub> ) isotopes	MPI-BGC	
Methane (CH <sub>4</sub> )	NOAA/ESRL	Empa (Am, E/A) JMA (A/O)
Nitrous Oxide (N <sub>2</sub> O)	NOAA/ESRL	KIT/IMK-IFU
Chlorofluorocarbons (CFCs)		
Sulfur Hexafluoride (SF <sub>6</sub> )	NOAA/ESRL	KMA
Molecular Hydrogen (H <sub>2</sub> )	MPI-BGC	
Carbon Monoxide (CO)	NOAA/ESRL	Empa

### 2. Carbon Dioxide (CO<sub>2</sub>)

In 1995, the National Oceanic and Atmospheric Administration's Earth System Research Laboratory (NOAA/ESRL; [https://gml.noaa.gov/ccl/co2\\_scale.html](https://gml.noaa.gov/ccl/co2_scale.html), formerly the Climate Monitoring and Diagnostics Laboratory, or CMDL) in Boulder, Colorado, took over the CCL role from the Scripps Institution of Oceanography (SIO) in San Diego, California, and has since been responsible for maintenance of the GAW Primary Standard for CO<sub>2</sub>. In this role, the laboratory maintains a high-precision manometric system for absolute calibration of CO<sub>2</sub> as reference for GAW monitoring worldwide (Zhao *et al.*, 1997), as well as carrying out round-robin operation in WCC functions. The standards of GAW monitoring laboratories should advisably be calibrated at least every three years at the CCL (WMO, 2020).

Under the WMO system there have been several calibration scales for CO<sub>2</sub>, including the SIO-based X74,

X85, X87, X93 and X2002 and the NOAA/ESRL-based WMO Mole Fraction Scale, partially based on previous SIO scales. The CCL adopted the WMO X2005 scale, reflecting historical manometric calibration of its set of cylinders and potential minor differences between SIO and NOAA/ESRL calibration. The latest WMO Mole Fraction Scale was the WMO X2019 version at the time of submission in 2021. Values on the former WMO X2007 scale can be converted to WMO X2019 values using [X2019 = 1.00079 \* X2007 - 0.142] (Hall *et al.*, 2021).

To assess differences in standard scales among monitoring laboratories, NOAA/ESRL organizes intercomparisons and round-robin experiments endorsed by WMO every three years or so. Numerous laboratories contributed to experiments conducted in 1991 – 1992, 1995 – 1997, 1999 – 2000, 2002 – 2006, 2009 – 2012 and 2014 – 2015 ([https://gml.noaa.gov/ccgg/wmorr/wmorr\\_results.php](https://gml.noaa.gov/ccgg/wmorr/wmorr_results.php)).

Table B2 lists organizations and sites contributing to the present issue of the Data Summary with standard scales of reported data and histories of contribution to

WMO intercomparison experiments. The calibration scales in the table are based on information from data contributors.

**Table B2. Status of standard scales and calibration/intercomparison for CO<sub>2</sub>.**

Organization	WDCGG Filename	Filename Code in Plate 1.1	Calibration Scale	WMO Inter-comparison
AEMET	co2_izo_surface-insitu_3_9999-9999_monthly.txt	IZO128N003iz*	WMO X1987 WMO X1993 WMO X2019	91/92, 96/97, 99/00, 09/12, 14/15
AICH	co2_mkw_surface-insitu_5_9999-9999_monthly.txt	MKW234N005iz	WMO	
AIST	co2_tky_tower-insitu_6_6028-9999_monthly.txt	TKY236N006it		96/97, 99/00, 02/06, 09/12, 14/15
BMKG	co2_bkt_surface-insitu_10_9999-9999_monthly.txt	BKT500S010iz	WMO X2007	
CMA	co2_wlg_surface-insitu_13_9999-9999_monthly.txt	WLG236N013iz*	WMO X2007	96/97, 99/00, 02/06, 09/12, 14/15
CSIRO	co2_alt_surface-flask_16_9999-9999_monthly.txt	ALT482N016fz	WMO X2019	91/92, 96/97, 99/00, 02/06, 09/12, 14/15
	co2_cfa_surface-flask_16_9999-9999_monthly.txt	CFA519S016fz*		
	co2_cgo_surface-flask_16_9999-9999_monthly.txt	CGO540S016fz		
	co2_cri_surface-flask_16_9999-9999_monthly.txt	CRI215N016fz*		
	co2_cya_surface-flask_16_9999-9999_monthly.txt	CYA766S016fz*		
	co2_esp_surface-flask_16_9999-9999_monthly.txt	ESP449N016fz*		
	co2_maa_surface-flask_16_9999-9999_monthly.txt	MAA767S016fz*		
	co2_mlo_surface-flask_16_9999-9999_monthly.txt	MLO519N016fz		
	co2_mqa_surface-flask_16_9999-9999_monthly.txt	MQA554S016fz*		
	co2_sis_surface-flask_16_9999-9999_monthly.txt	SIS660N016fz*		
	co2_spo_surface-flask_16_9999-9999_monthly.txt	SPO789S016fz		
DWD	co2_cgo_surface-insitu_16_9997-9999_monthly.txt	CGO540S016ix*	WMO X2019	
	co2_cgo_surface-insitu_16_9998-9999_monthly.txt	CGO540S016iy		
DMC	co2_cgo_surface-insitu_16_9999-9999_monthly.txt	CGO540S016iz	WMO X2007	
	co2_mqa_surface-insitu_16_9999-9999_monthly.txt	MQA554S016iz*		
ECCC	co2_tll_surface-insitu_17_9999-9999_monthly.txt	TLL330S017iz*	WMO X2019	
	co2_gat_tower-insitu_19_6342-9999_monthly.txt	GAT653N019it*	WMO X2007	
	co2_hpb_tower-insitu_19_6132-9999_monthly.txt	HPB647N019it		
	co2_kit_tower-insitu_19_6201-9999_monthly.txt	KIT649N019it		
	co2_lin_tower-insitu_19_6099-9999_monthly.txt	LIN652N019it		
ECCC	co2_toh_tower-insitu_19_6148-9999_monthly.txt	TOH651N019it*		
	co2_alt_surface-insitu_20_9999-9999_monthly.txt	ALT482N020iz	WMO X2007	91/92, 96/97, 99/00, 02/06, 09/12, 14/15
	co2_cdl_surface-insitu_20_9999-9999_monthly.txt	CDL453N020iz*		
	co2_chl_surface-insitu_20_9999-9999_monthly.txt	CHL458N020iz*		
	co2_chm_surface-insitu_20_9999-9999_monthly.txt	CHM449N020iz*		
	co2_egb_surface-insitu_20_9999-9999_monthly.txt	EGB444N020iz*		
	co2_esp_surface-insitu_20_9999-9999_monthly.txt	ESP449N020iz*		
	co2_etl_surface-insitu_20_9999-9999_monthly.txt	ETL454N020iz*		
	co2_fsd_surface-insitu_20_9999-9999_monthly.txt	FSD449N020iz*		
	co2_llb_surface-insitu_20_9999-9999_monthly.txt	LLB454N020iz*		

	co2_wsa_surface-insitu_20_9999-9999_monthly.txt	WSA443N020iz*		
EMA	co2_cai_surface-insitu_22_9999-9999_monthly.txt co2_frf_surface-insitu_22_9999-9999_monthly.txt	CAI130N022iz FRF127N022iz		
Empa	co2_jfj_surface-insitu_23_9999-9999_monthly.txt	JFJ646N023iz*	WMO X2007	09/12, 14/15
ENEA	co2_lmp_surface-flask_24_9999-9999_monthly.txt co2_lmp_surface-insitu_24_9999-9999_monthly.txt co2_mdn_surface-flask_24_9999-9999_monthly.txt	LMP635N024fz* LMP635N024iz* MDN637N024fz*	WMO X2007	91/92, 96/97, 99/00, 02/06, 09/12, 14/15
FMI	co2_pal_surface-insitu_25_9999-9999_monthly.txt co2_tik_surface-insitu_25_9999-9999_monthly.txt	PAL667N025iz* TIK271N025iz*	WMO X2019	02/06, 09/12 14/15
GERC	co2_gsn_surface-insitu_52_9999-9999_monthly.txt	GSN233N052iz	WMO X2007	
HKO	co2_hkg_surface-insitu_27_9999-9999_monthly.txt	HKG222N027iz*	WMO X2007 WMO X2019	
	co2_hko_surface-insitu_27_9999-9999_monthly.txt	HKO222N027iz	WMO X2007 WMO X2019 NIST	
HMS	co2_hun_tower-insitu_28_6116-9999_monthly.txt co2_kps_surface-insitu_28_9999-9999_monthly.txt	HUN646N028it KPS646N028iz*	WMO X2007	91/92, 96/97, 99/00, 02/06, 09/12, 14/15
IAA	co2_jbn_surface-insitu_18_9999-9999_monthly.txt	JBN762S018iz*	WMO X1993	
IAFMS	co2_cmn_surface-insitu_29_9999-9999_monthly.txt	CMN644N029iz*	WMO X1993 WMO X2007	91/92, 96/97, 02/06, 14/15
IGP	co2_hua_surface-insitu_30_9999-9999_monthly.txt	HUA312S030iz	WMO X1981	
IMKIFU	co2_wnk_surface-insitu_31_9999-9999_monthly.txt co2_zug_surface-insitu_31_9999-9999_monthly.txt	WNK647N031iz ZUG647N031iz	WMO X1974	99/00
INMH	co2_fdt_surface-insitu_58_9999-9999_monthly.txt	FDT645N058iz		
INRNE	co2_beo_surface-insitu_33_9999-9999_monthly.txt	BEO642N033iz	WMO	
IOEP	co2_dig_surface-insitu_35_9999-9999_monthly.txt	DIG654N035iz		
ISAC	co2_cgr_surface-insitu_37_9999-9999_monthly.txt co2_lmt_surface-insitu_37_9999-9999_monthly.txt	CGR637N037iz* LMT638N037iz	WMO X2007	
	co2_eco_surface-insitu_37_9999-9999_monthly.txt	ECO640N037iz		
ITM	co2_zep_surface-insitu_38_9999-9999_monthly.txt	ZEP678N038iz	WMO X2007	96/97, 99/00, 09/12
JMA	co2_mnm_surface-insitu_1_9999-9999_monthly.txt co2_ryo_surface-insitu_1_9999-9999_monthly.txt co2_yon_surface-insitu_1_9999-9999_monthly.txt	MNM224N001iz* RYO239N001iz* YON224N001iz*	WMO X2007	91/92, 96/97, 99/00, 02/06, 09/12, 14/15
KMA	co2_amy_surface-insitu_39_9999-9999_monthly.txt co2_jgs_surface-insitu_39_9999-9999_monthly.txt	AMY236N039iz* JGS233N039iz	WMO X2007	02/06, 09/12 14/15
	co2_ksg_surface-insitu_39_9999-9999_monthly.txt	KSG762S039iz	KRISS	
KMD	co2_mkn_surface-insitu_40_9999-9999_monthly.txt	MKN100S040iz*	WMO X2019	
KSNU	co2_isk_surface-remote_41_9999-9999_monthly.txt	ISK242N041rz		

KUP	co2_jfj_surface-insitu_42_9999-9999_monthly.txt	JFJ646N042iz*	WMO X2019	09/12
Kyrgyzh ydromet	co2_cpa_surface-insitu_155_9999-9999_monthly.txt	CPA242N155iz*	WMO X2019	
LSCE	co2_ams_surface-insitu_45_9998-9999_monthly.txt	AMS137S045iy*	WMO X1993 WMO X2002	91/92, 96/97, 99/00, 02/06, 09/12, 14/15
	co2_bgu_surface-flask_45_9999-9999_monthly.txt co2_lpo_surface-flask_45_9999-9999_monthly.txt co2_pdm_surface-flask_45_9999-9999_monthly.txt	BGU641N045fz* LPO648N045fz PDM642N045fz*	WMO X2001	
	co2_mhd_surface-insitu_45_9999-9999_monthly.txt	MHD653N045iz	WMO X1993	
	co2_puy_surface-insitu_45_9999-9999_monthly.txt	PUY645N045iz*	WMO X2001 WMO X2007	
	co2_fkl_surface-flask_45_9999-9999_monthly.txt	FKL635N045fz		
METRI	co2_gsn_surface-flask_55_9999-9999_monthly.txt	GSN233N055fz*	WMO X1997	96/97
MGO	co2_ber_surface-flask_46_9999-9999_monthly.txt co2_kot_surface-flask_46_9999-9999_monthly.txt co2_kyz_surface-flask_46_9999-9999_monthly.txt co2_stc_surface-flask_46_9999-9999_monthly.txt	BER255N046fz* KOT276N046fz* KYZ240N046fz* STC654N046fz*	WMO X1987	14/15
	co2_ter_surface-flask_46_9999-9999_monthly.txt	TER669N046fz*	WMO X2019	
	co2_tik_surface-flask_46_9999-9999_monthly.txt	TIK271N046fz*	WMO X2007	
MMD	co2_dmv_surface-insitu_47_9999-9999_monthly.txt	DMV504N047iz	WMO	
MRI	co2_tkb_tower-insitu_48_6201-9999_monthly.txt	TKB236N048it	MRI-87	91/92, 96/97, 99/00, 02/06, 09/12, 14/15
NIES	co2_coi_surface-insitu_53_9999-9999_monthly.txt co2_hat_surface-insitu_53_9999-9999_monthly.txt	COI243N053iz* HAT224N053iz*	NIES 95**	96/97, 99/00, 02/06, 09/12, 14/15
NIWA	co2_bhd_surface-insitu_57_9999-9999_monthly.txt	BHD541S057iz*	WMO X2007	91/92, 96/97, 99/00, 02/06, 09/12, 14/15
NOAA	co2_abp_surface-flask_2_3001-9999_monthly.txt co2_alt_surface-flask_2_3001-9999_monthly.txt co2_ams_surface-flask_2_3001-9999_monthly.txt co2_amy_surface-flask_2_3001-9999_monthly.txt co2_asc_surface-flask_2_3001-9999_monthly.txt co2_ask_surface-flask_2_3001-9999_monthly.txt co2_avi_surface-flask_2_3001-9999_monthly.txt co2_azr_surface-flask_2_3001-9999_monthly.txt co2_bal_surface-flask_2_3001-9999_monthly.txt co2_bhd_surface-flask_2_3001-9999_monthly.txt co2_bkt_surface-flask_2_3001-9999_monthly.txt co2_bme_surface-flask_2_3001-9999_monthly.txt co2_bmw_surface-flask_2_3001-9999_monthly.txt co2_brw_surface-flask_2_3001-9999_monthly.txt co2_brw_surface-insitu_2_3001-9999_monthly.txt co2_bsc_surface-flask_2_3001-9999_monthly.txt	ABP312S002f1* ALT482N002f1* AMS137S002f1 AMY236N002f1 ASC107S002f1* ASK123N002f1* AVI417N002f1* AZR638N002f1* BAL655N002f1* BHD541S002f1 BKT500S002f1 BME432N002f1* BMW432N002f1* BRW471N002f1 BRW471N002i1* BSC644N002f1	WMO X2019	91/92, 96/97, 99/00, 02/06, 09/12, 14/15

co2_cba_surface-flask_2_3001-9999_monthly.txt	CBA455N002f1*
co2_cgo_surface-flask_2_3001-9999_monthly.txt	CGO540S002f1*
co2_chr_surface-flask_2_3001-9999_monthly.txt	CHR501N002f1*
co2_cmo_surface-flask_2_3001-9999_monthly.txt	CMO445N002f1*
co2_cpt_surface-flask_2_3001-9999_monthly.txt	CPT134S002f1
co2_crz_surface-flask_2_3001-9999_monthly.txt	CRZ146S002f1*
co2_drp_ship-flask_2_3001-9999_monthly.txt	DRP859S002f1*
co2_eic_surface-flask_2_3001-9999_monthly.txt	EIC327S002f1*
co2_gmi_surface-flask_2_3001-9999_monthly.txt	GMI513N002f1*
co2_goz_surface-flask_2_3001-9999_monthly.txt	GOZ636N002f1*
co2_hba_surface-flask_2_3001-9999_monthly.txt	HBA775S002f1*
co2_hpb_surface-flask_2_3001-9999_monthly.txt	HPB647N002f1*
co2_hun_surface-flask_2_3001-9999_monthly.txt	HUN646N002f1*
co2_ice_surface-flask_2_3001-9999_monthly.txt	ICE663N002f1*
co2_izo_surface-flask_2_3001-9999_monthly.txt	IZO128N002f1
co2_key_surface-flask_2_3001-9999_monthly.txt	KEY425N002f1*
co2_kum_surface-flask_2_3001-9999_monthly.txt	KUM519N002f1*
co2_kzd_surface-flask_2_3001-9999_monthly.txt	KZD244N002f1*
co2_kzm_surface-flask_2_3001-9999_monthly.txt	KZM243N002f1*
co2_llb_surface-flask_2_3001-9999_monthly.txt	LLB454N002f1
co2_lln_surface-flask_2_3001-9999_monthly.txt	LLN223N002f1*
co2_lmp_surface-flask_2_3001-9999_monthly.txt	LMP635N002f1*
co2_mbc_surface-flask_2_3001-9999_monthly.txt	MBC476N002f1*
co2_mex_surface-flask_2_3001-9999_monthly.txt	MEX418N002f1*
co2_mhd_surface-flask_2_3001-9999_monthly.txt	MHD653N002f1*
co2_mid_surface-flask_2_3001-9999_monthly.txt	MID528N002f1*
co2_mkn_surface-flask_2_3001-9999_monthly.txt	MKN100S002f1*
co2_mlo_surface-flask_2_3001-9999_monthly.txt	MLO519N002f1
co2_mlo_surface-insitu_2_3001-9999_monthly.txt	MLO519N002f1*
co2_nat_surface-flask_2_3001-9999_monthly.txt	NAT306S002f1*
co2_nmb_surface-flask_2_3001-9999_monthly.txt	NMB123S002f1*
co2_nwr_surface-flask_2_3001-9999_monthly.txt	NWR440N002f1*
co2_opw_surface-flask_2_3001-9999_monthly.txt	OPW448N002f1*
co2_oxk_surface-flask_2_3001-9999_monthly.txt	OXK650N002f1*
co2_pal_surface-flask_2_3001-9999_monthly.txt	PAL667N002f1
co2_poc_ship-flask_2_3001-3001_monthly.txt	POC800N002f1*
co2_poc_ship-flask_2_3001-3002_monthly.txt	POC805N002f1*
co2_poc_ship-flask_2_3001-3003_monthly.txt	POC810N002f1*
co2_poc_ship-flask_2_3001-3004_monthly.txt	POC815N002f1*
co2_poc_ship-flask_2_3001-3005_monthly.txt	POC820N002f1*
co2_poc_ship-flask_2_3001-3006_monthly.txt	POC825N002f1*
co2_poc_ship-flask_2_3001-3007_monthly.txt	POC830N002f1*
co2_poc_ship-flask_2_3001-3012_monthly.txt	POC805S002f1*
co2_poc_ship-flask_2_3001-3013_monthly.txt	POC810S002f1*
co2_poc_ship-flask_2_3001-3014_monthly.txt	POC815S002f1*
co2_poc_ship-flask_2_3001-3015_monthly.txt	POC820S002f1*
co2_poc_ship-flask_2_3001-3016_monthly.txt	POC825S002f1*
co2_poc_ship-flask_2_3001-3017_monthly.txt	POC830S002f1*
co2_poc_ship-flask_2_3001-3018_monthly.txt	POC835S002f1*
co2_psa_surface-flask_2_3001-9999_monthly.txt	PSA764S002f1*
co2_pta_surface-flask_2_3001-9999_monthly.txt	PTA438N002f1*
co2_rpb_surface-flask_2_3001-9999_monthly.txt	RPB413N002f1*
co2_scs_ship-flask_2_3001-3101_monthly.txt	SCS803N002f1*
co2_scs_ship-flask_2_3001-3102_monthly.txt	SCS806N002f1*
co2_scs_ship-flask_2_3001-3103_monthly.txt	SCS809N002f1*
co2_scs_ship-flask_2_3001-3104_monthly.txt	SCS812N002f1*

	co2_scs_ship-flask_2_3001-3105_monthly.txt co2_scs_ship-flask_2_3001-3106_monthly.txt co2_scs_ship-flask_2_3001-3107_monthly.txt co2_sdz_surface-flask_2_3001-9999_monthly.txt co2_sey_surface-flask_2_3001-9999_monthly.txt co2_sgp_surface-flask_2_3001-9999_monthly.txt co2_shm_surface-flask_2_3001-9999_monthly.txt co2_smo_surface-flask_2_3001-9999_monthly.txt co2_smo_surface-insitu_2_3001-9999_monthly.txt co2_spo_surface-flask_2_3001-9999_monthly.txt co2_spo_surface-insitu_2_3001-9999_monthly.txt co2_stc_surface-flask_2_3001-9999_monthly.txt co2_stm_surface-flask_2_3001-9999_monthly.txt co2_sum_surface-flask_2_3001-9999_monthly.txt co2_syo_surface-flask_2_3001-9999_monthly.txt co2_tap_surface-flask_2_3001-9999_monthly.txt co2_thd_surface-flask_2_3001-9999_monthly.txt co2_tik_surface-flask_2_3001-9999_monthly.txt co2_ush_surface-flask_2_3001-9999_monthly.txt co2_uta_surface-flask_2_3001-9999_monthly.txt co2_uum_surface-flask_2_3001-9999_monthly.txt co2_wis_surface-flask_2_3001-9999_monthly.txt co2_wlg_surface-flask_2_3001-9999_monthly.txt co2_zep_surface-flask_2_3001-9999_monthly.txt	SCS815N002f1* SCS818N002f1* SCS821N002f1* SDZ240N002f1 SEY104S002f1* SGP436N002f1* SHM452N002f1* SMO514S002f1 SMO514S002i1* SPO789S002f1 SPO789S002i1* STC654N002f1 STM666N002f1* SUM672N002f1* SYO769S002f1* TAP236N002f1* THD441N002f1* TIK271N002f1* USH354S002f1* UTA439N002f1* UUM244N002f1* WIS631N002f1* WLG236N002f1* ZEP678N002f1*		
NPL	co2_hfd_tower-insitu_154_6101-9999_monthly.txt	HFD650N154it*	WMO X2007	
OSAKAU	co2_sui_surface-insitu_60_9999-9999_monthly.txt	SUI234N060iz		
RIVM	co2_kmw_surface-insitu_63_9999-9999_monthly.txt	KMW653N063iz	NIST	
RSE	co2_prs_surface-insitu_64_9999-9999_monthly.txt	PRS645N064iz*	WMO X1993 WMO X2007 ICOS	99/00, 02/06 14/15
SAIPF	co2_ddr_surface-insitu_65_9999-9999_monthly.txt co2_kis_surface-insitu_65_9999-9999_monthly.txt co2_urw_surface-insitu_65_9999-9999_monthly.txt	DDR236N065iz* KIS236N065iz URW235N065iz	WMO X2007	
SAWS	co2_cpt_surface-insitu_66_9999-1001_monthly.txt	CPT134S066iz*	WMO X2019	99/00, 02/06, 09/12, 14/15
SHIZU	co2_hmm_surface-insitu_67_9999-9999_monthly.txt	HMM234N067iz		
TU	co2_syo_surface-insitu_70_9999-9999_monthly.txt	SYO769S070iz	Tohoku Univ. 2010	91/92, 96/97, 99/00, 02/06, 09/12
UBAA	co2_snb_surface-insitu_72_9999-9999_monthly.txt	SNB647N072iz*	WMO X2007	
UBAG	co2_brt_surface-insitu_71_9999-9999_monthly.txt co2_deu_surface-insitu_71_9999-9999_monthly.txt co2_ngl_surface-insitu_71_9999-9999_monthly.txt co2_wal_surface-insitu_71_9999-9999_monthly.txt co2_wes_surface-insitu_71_9999-9999_monthly.txt co2_zgt_surface-insitu_71_9999-9999_monthly.txt	BRT648N071iz* DEU649N071iz NGL653N071iz WAL652N071iz WES654N071iz* ZGT654N071iz	WMO	91/92, 96/97, 99/00, 02/06, 09/12, 14/15
	co2_ssl_surface-insitu_71_9998-9999_monthly.txt co2_ssl_surface-insitu_71_9999-9999_monthly.txt	SSL647N071iy SSL647N071iz*	WMO X2007	
	co2_zsf_surface-insitu_71_9999-9999_monthly.txt	ZSF647N071iz*	WMO X2019	

	co2_zug_surface-insitu_71_9999-9999_monthly.txt	ZUG647N071iz*	WMO X1985	
UMLT	co2_glh_surface-insitu_75_9999-9999_monthly.txt	GLH636N075iz		
UNIVBRI S	co2_rgl_tower-insitu_77_6091-9999_monthly.txt co2_tac_tower-insitu_77_6186-9999_monthly.txt	RGL651N077iz* TAC652N077iz*	WMO X2019	
UoE	co2_cvo_surface-insitu_151_9999-9999_monthly.txt	CVO116N151iz*	WMO X2007	
UYRK	co2_cvo_surface-insitu_76_9999-9999_monthly.txt	CVO116N076iz	WMO X2019	
VNMHA	co2_pdi_surface-insitu_51_9999-9999_monthly.txt	PDI221N051iz	WMO X2019	

\* Stations marked with an asterisk are used for the calculation of globally averaged mole fractions and related quantities.

The site selection procedure is described in Appendix A.

\*\* NIES 95 CO<sub>2</sub> scale is 0.10 to 0.14 ppm lower than that of WMO in the range 355 to 385 ppm.

(Machida *et al.*, WMO/GAW Report No. 186, 26-29, 2009.)

### 3. Methane (CH<sub>4</sub>)

The GAW Programme has a CCL for CH<sub>4</sub> at NOAA/ESRL (Dlugokencky *et al.*, 2005; WMO, 2017). Two WCCs for CH<sub>4</sub> are also run by the Swiss Federal Laboratory for Materials Testing and Research (Empa; Dübendorf, Switzerland) and the Japan Meteorological Agency (JMA; Tokyo, Japan) (WMO, 2017).

The current WMO Mole Fraction Scale is X2004A, which consists of 16 existing standards covering the range of the previous WMO X2004 scale and 6 new standards to expand the range of the scale ([https://gml.noaa.gov/ccl/ch4\\_scale.html](https://gml.noaa.gov/ccl/ch4_scale.html)). Table B3 summarizes the CH<sub>4</sub> standard scales used by stations contributing to the WDCGG. In this issue, the multiplying factor for conversion between X2004A and X2004 is

taken as 1 because the related difference is minor.

Mole fractions on the WMO X2004 scale are 1.0124 times higher than those on the NOAA 1983 scale (Dlugokencky *et al.*, 2005). The value on the NOAA 1983 scale is 1.0151 times lower than that on the scale of the Atmospheric Environment Service (AES, now known as Environment and Climate Change Canada (ECCC)) (Worthy *et al.*, 1998). The multiplying conversion factor of 1.0124 / 1.0151 = 0.9973 is adopted for comparison of the ECCC scale with the WMO X2004 scale. Mole fractions of the WMO X2004A scale are higher than those on the Tohoku University 1987 scale by around 0.5 ppb (Fujita *et al.*, 2018).

**Table B3. Status of the standard scales of CH<sub>4</sub>.**

Organiza-tion	WDCGG Filename	Filename Code in Plate 2.1	Calibration Scale
AEMET	ch4_izo_surface-insitu_3_9999-9999_monthly.txt	IZO128N003iz*	WMO X2004A
AGAGE	ch4_cgo_surface-insitu_4_2011-2016_monthly.txt ch4_cgo_surface-insitu_4_2021-2021_monthly.txt ch4_cmo_surface-insitu_4_2011-2016_monthly.txt ch4_mhd_surface-insitu_4_2011-2016_monthly.txt ch4_mhd_surface-insitu_4_2021-2021_monthly.txt ch4_rpb_surface-insitu_4_2021-2021_monthly.txt ch4_smo_surface-insitu_4_2011-2016_monthly.txt ch4_smo_surface-insitu_4_2021-2021_monthly.txt ch4_thd_surface-insitu_4_2021-2021_monthly.txt	CGO540S004ib CGO540S004ic* CMO445N004ib MHD653N004ib* MHD653N004ic* RPB413N004ic* SMO514S004ib SMO514S004ic* THD441N004ic*	TU-1987
BMKG	ch4_bkt_surface-insitu_10_9999-9999_monthly.txt	BKT500S010iz	WMO X2004 WMO X2004A
CHMI	ch4_kos_surface-insitu_12_9999-9999_monthly.txt	KOS649N012iz	
CMA	ch4_wlg_surface-insitu_13_9999-9999_monthly.txt	WLG236N013iz	WMO X2004
CSIRO	ch4_alt_surface-flask_16_9999-9999_monthly.txt ch4_cfa_surface-flask_16_9999-9999_monthly.txt ch4_cgo_surface-flask_16_9999-9999_monthly.txt	ALT482N016fz CFA519S016fz* CGO540S016fz	WMO X2004A

	ch4_cri_surface-flask_16_9999-9999_monthly.txt ch4_cya_surface-flask_16_9999-9999_monthly.txt ch4_esp_surface-flask_16_9999-9999_monthly.txt ch4_maa_surface-flask_16_9999-9999_monthly.txt ch4_mlo_surface-flask_16_9999-9999_monthly.txt ch4_mqa_surface-flask_16_9999-9999_monthly.txt ch4_sis_surface-flask_16_9999-9999_monthly.txt ch4_spo_surface-flask_16_9999-9999_monthly.txt	CRI215N016fz* CYA766S016fz* ESP449N016fz* MAA767S016fz* MLO519N016fz MQA554S016fz* SIS660N016fz* SPO789S016fz	
DMC	ch4_tll_surface-insitu_17_9999-9999_monthly.txt	TLL330S017iz*	WMO X2004A
DWD	ch4_gat_tower-insitu_19_6342-9999_monthly.txt ch4_hpb_tower-insitu_19_6132-9999_monthly.txt ch4_kit_tower-insitu_19_6201-9999_monthly.txt ch4_lin_tower-insitu_19_6099-9999_monthly.txt ch4_toh_tower-insitu_19_6148-9999_monthly.txt	GAT653N019it* HPB647N019it KIT649N019it* LIN652N019it* TOH651N019it*	WMO X2004A
ECCC	ch4_alt_surface-insitu_20_9999-9999_monthly.txt ch4_cdl_surface-insitu_20_9999-9999_monthly.txt ch4_chl_surface-insitu_20_9999-9999_monthly.txt ch4_chm_surface-insitu_20_9999-9999_monthly.txt ch4_egb_surface-insitu_20_9999-9999_monthly.txt ch4_esp_surface-insitu_20_9999-9999_monthly.txt ch4_etl_surface-insitu_20_9999-9999_monthly.txt ch4_fsd_surface-insitu_20_9999-9999_monthly.txt ch4_llb_surface-insitu_20_9999-9999_monthly.txt ch4_wsa_surface-insitu_20_9999-9999_monthly.txt	ALT482N020iz CDL453N020iz* CHL458N020iz* CHM449N020iz* EGB444N020iz* ESP449N020iz* ETL454N020iz* FSD449N020iz* LLB454N020iz* WSA443N020iz*	WMO X2004A
Empa	ch4_jfj_surface-insitu_23_9999-9999_monthly.txt	JFJ646N023iz*	WMO X2004A
ENEA	ch4_lmp_surface-flask_24_9999-9999_monthly.txt	LMP635N024fz*	WMO X2004
FMI	ch4_pal_surface-insitu_25_9999-9999_monthly.txt ch4_tik_surface-insitu_25_9999-9999_monthly.txt	PAL667N025iz TIK271N025iz*	WMO X2004A
GERC	ch4_gsn_surface-insitu_52_9999-9999_monthly.txt	GSN233N052iz*	WMO X2004
IAFMS	ch4_cmn_surface-insitu_29_9999-9999_monthly.txt	CMN644N029iz*	WMO X2004
INSTAAR	ch4_sum_surface-insitu_34_9999-9999_monthly.txt	SUM672N034iz	
ISAC	ch4_cgr_surface-insitu_37_9999-9999_monthly.txt ch4_lmt_surface-insitu_37_9999-9999_monthly.txt	CGR637N037iz* LMT638N037iz	WMO X2004A
	ch4_eco_surface-insitu_37_9999-9999_monthly.txt	ECO640N037iz	
JMA	ch4_mnm_surface-insitu_1_9999-9999_monthly.txt ch4_ryo_surface-insitu_1_9999-9999_monthly.txt ch4_yon_surface-insitu_1_9999-9999_monthly.txt	MNM224N001iz* RYO239N001iz* YON224N001iz*	WMO X2004A
KMA	ch4_amy_surface-insitu_39_9999-9999_monthly.txt	AMY236N039iz*	WMO X2004 WMO X2004A KRISS
KMD	ch4_mkn_surface-insitu_40_9999-9999_monthly.txt	MKN100S040iz*	WMO X2004A
KSNU	ch4_isk_surface-remote_41_9999-9999_monthly.txt	ISK242N041rz	
Kyrgyzh ydromet	ch4_cpa_surface-insitu_155_9999-9999_monthly.txt	CPA242N155iz*	WMO X2004A
LSCE	ch4_ams_surface-flask_45_9999-9999_monthly.txt ch4_bgu_surface-flask_45_9999-9999_monthly.txt ch4_lpo_surface-flask_45_9999-9999_monthly.txt ch4_pdm_surface-flask_45_9999-9999_monthly.txt ch4_puy_surface-flask_45_9999-9999_monthly.txt	AMS137S045fz* BGU641N045fz* LPO648N045fz PDM642N045fz PUY645N045fz*	NOAA 1983

	ch4_fkl_surface-flask_45_9999-9999_monthly.txt ch4_mhd_surface-flask_45_9999-9999_monthly.txt	FKL635N045fz MHD653N045fz	
METRI	ch4_gsn_surface-flask_55_9999-9999_monthly.txt	GSN233N055fz	SIO-97
MGO	ch4_ter_surface-flask_46_9999-9999_monthly.txt ch4_tik_surface-flask_46_9999-9999_monthly.txt	TER669N046fz* TIK271N046fz	WMO X2004A
MRI	ch4_tkb_surface-insitu_48_9999-9999_monthly.txt	TKB236N048iz*	MRI
NIES	ch4_coi_surface-insitu_53_9999-9999_monthly.txt ch4_hat_surface-insitu_53_9999-9999_monthly.txt	COI243N053iz* HAT224N053iz*	NIES
NIWA	ch4_arh_surface-flask_57_9999-9999_monthly.txt ch4_bhd_surface-flask_57_9999-9999_monthly.txt ch4_bhd_surface-insitu_57_9999-9999_monthly.txt ch4_lau_surface-flask_57_9999-9999_monthly.txt ch4_lau_surface-insitu_57_9999-9999_monthly.txt	ARH777S057fz* BHD541S057fz* BHD541S057iz* LAU545S057fz* LAU545S057iz*	WMO X2004A
NOAA	ch4_abp_surface-flask_2_3001-9999_monthly.txt ch4_alt_surface-flask_2_3001-9999_monthly.txt ch4_ams_surface-flask_2_3001-9999_monthly.txt ch4_amy_surface-flask_2_3001-9999_monthly.txt ch4_asc_surface-flask_2_3001-9999_monthly.txt ch4_ask_surface-flask_2_3001-9999_monthly.txt ch4_avi_surface-flask_2_3001-9999_monthly.txt ch4_azr_surface-flask_2_3001-9999_monthly.txt ch4_bal_surface-flask_2_3001-9999_monthly.txt ch4_bhd_surface-flask_2_3001-9999_monthly.txt ch4_bkt_surface-flask_2_3001-9999_monthly.txt ch4_bme_surface-flask_2_3001-9999_monthly.txt ch4_bmw_surface-flask_2_3001-9999_monthly.txt ch4_brw_surface-flask_2_3001-9999_monthly.txt ch4_brw_surface-insitu_2_3001-9999_monthly.txt ch4_bsc_surface-flask_2_3001-9999_monthly.txt ch4_cba_surface-flask_2_3001-9999_monthly.txt ch4_cgo_surface-flask_2_3001-9999_monthly.txt ch4_chr_surface-flask_2_3001-9999_monthly.txt ch4_cmo_surface-flask_2_3001-9999_monthly.txt ch4_cpt_surface-flask_2_3001-9999_monthly.txt ch4_crz_surface-flask_2_3001-9999_monthly.txt ch4_drp_ship-flask_2_3001-9999_monthly.txt ch4_eic_surface-flask_2_3001-9999_monthly.txt ch4_gmi_surface-flask_2_3001-9999_monthly.txt ch4_goz_surface-flask_2_3001-9999_monthly.txt ch4_hba_surface-flask_2_3001-9999_monthly.txt ch4_hpb_surface-flask_2_3001-9999_monthly.txt ch4_hun_surface-flask_2_3001-9999_monthly.txt ch4_ice_surface-flask_2_3001-9999_monthly.txt ch4_itn_surface-flask_2_3001-9999_monthly.txt ch4_izo_surface-flask_2_3001-9999_monthly.txt ch4_key_surface-flask_2_3001-9999_monthly.txt ch4_kum_surface-flask_2_3001-9999_monthly.txt ch4_kzd_surface-flask_2_3001-9999_monthly.txt ch4_kzm_surface-flask_2_3001-9999_monthly.txt ch4_llb_surface-flask_2_3001-9999_monthly.txt ch4_lln_surface-flask_2_3001-9999_monthly.txt ch4_lmp_surface-flask_2_3001-9999_monthly.txt ch4_mbc_surface-flask_2_3001-9999_monthly.txt ch4_mex_surface-flask_2_3001-9999_monthly.txt ch4_mhd_surface-flask_2_3001-9999_monthly.txt	ABP312S002f1* ALT482N002f1* AMS137S002f1* AMY236N002f1 ASC107S002f1* ASK123N002f1* AVI417N002f1* AZR638N002f1* BAL655N002f1* BHD541S002f1* BKT500S002f1 BME432N002f1* BMW432N002f1* BRW471N002f1* BRW471N002i1* BSC644N002f1 CBA455N002f1* CGO540S002f1* CHR501N002f1* CMO445N002f1* CPT134S002f1 CRZ146S002f1* DRP859S002f1* EIC327S002f1* GMI513N002f1* GOZ636N002f1* HBA775S002f1* HPB647N002f1* HUN646N002f1* ICE663N002f1* ITN435N002f1* IZO128N002f1* KEY425N002f1* KUM519N002f1* KZD244N002f1* KZM243N002f1* LLB454N002f1 LLN223N002f1* LMP635N002f1* MBC476N002f1* MEX418N002f1* MHD653N002f1*	WMO X2004A



RSE	ch4_prs_surface-insitu_64_9999-9999_monthly.txt	PRS645N064iz*	WMO X2004 ICOS
SAWS	ch4_cpt_surface-insitu_66_9999-1001_monthly.txt	CPT134S066iz*	WMO X2004 WMO X2004A
TU	ch4_syo_surface-insitu_70_9999-9999_monthly.txt	SYO769S070iz*	TU-1987
UBAA	ch4_snb_surface-insitu_72_9999-9999_monthly.txt	SNB647N072iz*	WMO X2004
UBAG	ch4_deu_surface-insitu_71_9999-9999_monthly.txt ch4_ngl_surface-insitu_71_9999-9999_monthly.txt ch4_ssl_surface-insitu_71_9999-9999_monthly.txt ch4_zgt_surface-insitu_71_9999-9999_monthly.txt ch4_zsf_surface-insitu_71_9999-9999_monthly.txt ch4 zug surface-insitu 71 9999-9999 monthly.txt	DEU649N071iz* NGL653N071iz* SSL647N071iz* ZGT654N071iz* ZSF647N071iz* ZUG647N071iz*	WMO X2004
UMLT	ch4_glh_surface-insitu_75_9999-9999_monthly.txt	GLH636N075iz	
UNIURB	ch4_cmn_surface-insitu_74_9999-9999_monthly.txt	CMN644N074iz*	WMO X2004A
UNIVBRI S	ch4_rgl_tower-insitu_77_6091-9999_monthly.txt ch4_tac tower-insitu 77 6186-9999 monthly.txt	RGL651N077it* TAC652N077it*	WMO X2004
UoE	ch4_cvo_surface-insitu_151_9999-9999_monthly.txt	CVO116N151iz*	WMO X2004A
UYRK	ch4_cvo_surface-insitu_76_9999-9999_monthly.txt	CVO116N076iz	WMO X2004
VNMHA	ch4_pdi_surface-insitu_51_9999-9999_monthly.txt	PDI221N051iz	WMO X2004A

\* Stations with an asterisk are used for the calculation of the globally averaged mole fractions and related quantities. The site selection procedure is described in Appendix A.

#### 4. Nitrous Oxide (N<sub>2</sub>O)

The Halocarbons and Other Atmospheric Trace Species (HATS) Group of NOAA/ESRL maintains a set of standards for N<sub>2</sub>O (Hall *et al.*, 2001) and serves as a CCL for N<sub>2</sub>O. The WMO X2006 scale (Hall *et al.*, 2007) was revised and updated to WMO X2006A in 2011 to deal with drifting in secondary standards, and is now designated as the primary scale for the GAW Programme. CCL compares its standards with those of other laboratories, including ECCC and the Australian Commonwealth Scientific and Industrial Research Organisation (CSIRO). The Karlsruhe Institute of

Technology under the Institute for Meteorology and Climate Research (KIT/IMK-IFU) in Germany serves as the GAW WCC for N<sub>2</sub>O.

The SIO-98 scale is approximately equivalent to the WMO X2006 scale, with an average difference of 0.01% over the range of 299 – 319 ppb. SIO-16 scale values can be converted to WMO X2006A via multiplication by a factor of 0.9983 (Prinn *et al.*, 2018). The WMO X2000 scale can be converted to WMO X2006 values using a multiplication factor of 0.999402 (Hall *et al.*, 2007).

**Table B4. Status of the standard scales of N<sub>2</sub>O.**

Organ-ization	WDCGG Filename	Filename Code in Plate 3.1	Calibration Scale
AEMET	n2o_izo_surface-insitu_3_9999-9999_monthly.txt	IZO128N003iz*	WMO X2006A
AGAGE	n2o_cgo_surface-insitu_4_2021-2021_monthly.txt n2o_mhd_surface-insitu_4_2021-2021_monthly.txt n2o_rpb_surface-insitu_4_2021-2021_monthly.txt n2o_smo_surface-insitu_4_2021-2021_monthly.txt n2o_thd_surface-insitu_4_2021-2021_monthly.txt	CGO540S004ic* MHD653N004ic* RPB413N004ic* SMO514S004ic* THD441N004ic*	SIO-16
	n2o_adr_surface-insitu_4_2001-2004_monthly.txt n2o_cgo_surface-insitu_4_2001-2004_monthly.txt n2o_cgo_surface-insitu_4_2011-2015_monthly.txt n2o_cmo_surface-insitu_4_2001-2004_monthly.txt	ADR651N004ia* CGO540S004ia* CGO540S004ib* CMO445N004ia*	SIO-98

	n2o_cmo_surface-insitu_4_2011-2015_monthly.txt n2o_mhd_surface-insitu_4_2011-2015_monthly.txt n2o_rpb_surface-insitu_4_2001-2004_monthly.txt n2o_rpb_surface-insitu_4_2011-2015_monthly.txt n2o_smo_surface-insitu_4_2001-2004_monthly.txt n2o_smo_surface-insitu_4_2011-2015_monthly.txt	CMO445N004ib* MHD653N004ib* RPB413N004ia* RPB413N004ib* SMO514S004ia* SMO514S004ib*	
CSIRO	n2o_alt_surface-flask_16_9999-9999_monthly.txt n2o_cfa_surface-flask_16_9999-9999_monthly.txt n2o_cgo_surface-flask_16_9999-9999_monthly.txt n2o_cri_surface-flask_16_9999-9999_monthly.txt n2o_cya_surface-flask_16_9999-9999_monthly.txt n2o_esp_surface-flask_16_9999-9999_monthly.txt n2o_maa_surface-flask_16_9999-9999_monthly.txt n2o_mlo_surface-flask_16_9999-9999_monthly.txt n2o_mqa_surface-flask_16_9999-9999_monthly.txt n2o_sis_surface-flask_16_9999-9999_monthly.txt n2o_spo_surface-flask_16_9999-9999_monthly.txt	ALT482N016fz* CFA519S016fz* CGO540S016fz CRI215N016fz* CYA766S016fz* ESP449N016fz* MAA767S016fz* MLO519N016fz* MQA554S016fz* SIS660N016fz* SPO789S016fz	WMO X2006A
DWD	n2o_gat_tower-insitu_19_6342-9999_monthly.txt n2o_hpb_tower-insitu_19_6132-9999_monthly.txt n2o_kit_tower-insitu_19_6201-9999_monthly.txt n2o_lin_tower-insitu_19_6099-9999_monthly.txt n2o_toh_tower-insitu_19_6148-9999_monthly.txt	GAT653N019it* HPB647N019it KIT649N019it* LIN652N019it* TOH651N019it*	WMO X2006A
Empa	n2o_jfj_surface-insitu_23_9999-9999_monthly.txt	JFJ646N023iz*	WMO X2006A SIO-98
ENEA	n2o_lmp_surface-flask_24_9999-9999_monthly.txt	LMP635N024fz	WMO X2006
GERC	n2o_gsn_surface-insitu_52_9999-9999_monthly.txt	GSN233N052iz	WMO X2006
JMA	n2o_ryo_surface-insitu_1_9999-9999_monthly.txt	RYO239N001iz*	WMO X2006A
KMA	n2o_amy_surface-insitu_39_9999-9999_monthly.txt	AMY236N039iz	WMO X2006 KRISS
METRI	n2o_gsn_surface-flask_55_9999-9999_monthly.txt	GSN233N055fz	WMO X1997
MRI	n2o_mmb_surface-insitu_48_9999-9999_monthly.txt	MMB243N048iz	
NAGOU	n2o_ngy_surface-insitu_49_9999-9999_monthly.txt	NGY235N049iz	
NIES	n2o_coi_surface-insitu_53_9999-9999_monthly.txt n2o_hat_surface-insitu_53_9999-9999_monthly.txt	COI243N053iz* HAT224N053iz*	NIES 96**
NILU	n2o_zep_surface-insitu_54_9999-9999_monthly.txt	ZEP678N054iz	
NIWA	n2o_arh_surface-flask_57_9999-9999_monthly.txt n2o_bhd_surface-flask_57_9999-9999_monthly.txt	ARH777S057fz* BHD541S057fz*	WMO X2006A
NOAA	n2o_brw_surface-insitu_2_3003-9999_monthly.txt n2o_mlo_surface-insitu_2_3003-9999_monthly.txt n2o_nwr_surface-insitu_2_3003-9999_monthly.txt n2o_smo_surface-insitu_2_3003-9999_monthly.txt n2o_spo_surface-insitu_2_3003-9999_monthly.txt	BRW471N002i3* MLO519N002i3* NWR440N002i3* SMO514S002i3* SPO789S002i3*	WMO X2006
	n2o_abp_surface-flask_2_3001-9999_monthly.txt n2o_alt_surface-flask_2_3001-9999_monthly.txt n2o_alt_surface-flask_2_3004-9999_monthly.txt n2o_alt_surface-flask_2_3005-9999_monthly.txt n2o_amy_surface-flask_2_3001-9999_monthly.txt n2o_asc_surface-flask_2_3001-9999_monthly.txt	ABP312S002f1* ALT482N002f1 ALT482N002f4* ALT482N002f5 AMY236N002f1* ASC107S002f1*	WMO X2006A

n2o_ask_surface-flask_2_3001-9999_monthly.txt	ASK123N002f1*
n2o_azr_surface-flask_2_3001-9999_monthly.txt	AZR638N002f1*
n2o_bal_surface-flask_2_3001-9999_monthly.txt	BAL655N002f1*
n2o_bhd_surface-flask_2_3001-9999_monthly.txt	BHD541S002f1
n2o_bkt_surface-flask_2_3001-9999_monthly.txt	BKT500S002f1*
n2o_bme_surface-flask_2_3001-9999_monthly.txt	BME432N002f1*
n2o_bmw_surface-flask_2_3001-9999_monthly.txt	BMW432N002f1*
n2o_brw_surface-flask_2_3001-9999_monthly.txt	BRW471N002f1
n2o_brw_surface-flask_2_3004-9999_monthly.txt	BRW471N002f4*
n2o_brw_surface-flask_2_3005-9999_monthly.txt	BRW471N002f5
n2o_brw_surface-insitu_2_3002-9999_monthly.txt	BRW471N002i2*
n2o_bsc_surface-flask_2_3001-9999_monthly.txt	BSC644N002f1*
n2o_cba_surface-flask_2_3001-9999_monthly.txt	CBA455N002f1*
n2o_cg0_surface-flask_2_3001-9999_monthly.txt	CGO540S002f1*
n2o_cg0_surface-flask_2_3004-9999_monthly.txt	CGO540S002f4
n2o_cg0_surface-flask_2_3005-9999_monthly.txt	CGO540S002f5
n2o_chr_surface-flask_2_3001-9999_monthly.txt	CHR501N002f1*
n2o_cpt_surface-flask_2_3001-9999_monthly.txt	CPT134S002f1*
n2o_crz_surface-flask_2_3001-9999_monthly.txt	CRZ146S002f1*
n2o_drp_ship-flask_2_3001-9999_monthly.txt	DRP859S002f1*
n2o_eic_surface-flask_2_3001-9999_monthly.txt	EIC327S002f1*
n2o_gmi_surface-flask_2_3001-9999_monthly.txt	GMI513N002f1*
n2o_hba_surface-flask_2_3001-9999_monthly.txt	HBA775S002f1*
n2o_hfm_surface-flask_2_3005-9999_monthly.txt	HFM442N002f5*
n2o_hpб_surface-flask_2_3001-9999_monthly.txt	HPB647N002f1*
n2o_hun_surface-flask_2_3001-9999_monthly.txt	HUN646N002f1*
n2o_ice_surface-flask_2_3001-9999_monthly.txt	ICE663N002f1*
n2o_itn_surface-flask_2_3001-9999_monthly.txt	ITN435N002f1
n2o_itn_surface-flask_2_3005-9999_monthly.txt	ITN435N002f5*
n2o_izo_surface-flask_2_3001-9999_monthly.txt	IZO128N002f1*
n2o_key_surface-flask_2_3001-9999_monthly.txt	KEY425N002f1*
n2o_kum_surface-flask_2_3001-9999_monthly.txt	KUM519N002f1*
n2o_kum_surface-flask_2_3005-9999_monthly.txt	KUM519N002f5*
n2o_kzd_surface-flask_2_3001-9999_monthly.txt	KZD244N002f1*
n2o_kzm_surface-flask_2_3001-9999_monthly.txt	KZM243N002f1*
n2o_lef_surface-flask_2_3005-9999_monthly.txt	LEF445N002f5*
n2o_llb_surface-flask_2_3001-9999_monthly.txt	LLB454N002f1*
n2o_lln_surface-flask_2_3001-9999_monthly.txt	LLN223N002f1*
n2o_lmp_surface-flask_2_3001-9999_monthly.txt	LMP635N002f1*
n2o_mex_surface-flask_2_3001-9999_monthly.txt	MEX418N002f1*
n2o_mhd_surface-flask_2_3001-9999_monthly.txt	MHD653N002f1*
n2o_mhd_surface-flask_2_3005-9999_monthly.txt	MHD653N002f5
n2o_mid_surface-flask_2_3001-9999_monthly.txt	MID528N002f1*
n2o_mkn_surface-flask_2_3001-9999_monthly.txt	MKN100S002f1*
n2o_mlo_surface-flask_2_3001-9999_monthly.txt	MLO519N002f1*
n2o_mlo_surface-flask_2_3004-9999_monthly.txt	MLO519N002f4*
n2o_mlo_surface-flask_2_3005-9999_monthly.txt	MLO519N002f5
n2o_mlo_surface-insitu_2_3002-9999_monthly.txt	MLO519N002i2*
n2o_nat_surface-flask_2_3001-9999_monthly.txt	NAT306S002f1*
n2o_nmb_surface-flask_2_3001-9999_monthly.txt	NMB123S002f1*
n2o_nwr_surface-flask_2_3001-9999_monthly.txt	NWR440N002f1*
n2o_nwr_surface-flask_2_3004-9999_monthly.txt	NWR440N002f4*
n2o_nwr_surface-flask_2_3005-9999_monthly.txt	NWR440N002f5
n2o_nwr_surface-insitu_2_3002-9999_monthly.txt	NWR440N002i2
n2o_oxk_surface-flask_2_3001-9999_monthly.txt	OXK650N002f1*
n2o_pal_surface-flask_2_3001-9999_monthly.txt	PAL667N002f1*

	n2o_poc_ship-flask_2_3001-3001_monthly.txt n2o_poc_ship-flask_2_3001-3002_monthly.txt n2o_poc_ship-flask_2_3001-3003_monthly.txt n2o_poc_ship-flask_2_3001-3004_monthly.txt n2o_poc_ship-flask_2_3001-3005_monthly.txt n2o_poc_ship-flask_2_3001-3006_monthly.txt n2o_poc_ship-flask_2_3001-3007_monthly.txt n2o_poc_ship-flask_2_3001-3012_monthly.txt n2o_poc_ship-flask_2_3001-3013_monthly.txt n2o_poc_ship-flask_2_3001-3014_monthly.txt n2o_poc_ship-flask_2_3001-3015_monthly.txt n2o_poc_ship-flask_2_3001-3016_monthly.txt n2o_poc_ship-flask_2_3001-3017_monthly.txt n2o_psa_surface-flask_2_3001-9999_monthly.txt n2o_psa_surface-flask_2_3005-9999_monthly.txt n2o_pta_surface-flask_2_3001-9999_monthly.txt n2o_rpb_surface-flask_2_3001-9999_monthly.txt n2o_sdz_surface-flask_2_3001-9999_monthly.txt n2o_sey_surface-flask_2_3001-9999_monthly.txt n2o_sgp_surface-flask_2_3001-9999_monthly.txt n2o_shm_surface-flask_2_3001-9999_monthly.txt n2o_smo_surface-flask_2_3001-9999_monthly.txt n2o_smo_surface-flask_2_3004-9999_monthly.txt n2o_smo_surface-flask_2_3005-9999_monthly.txt n2o_smo_surface-insitu_2_3002-9999_monthly.txt n2o_spo_surface-flask_2_3001-9999_monthly.txt n2o_spo_surface-flask_2_3004-9999_monthly.txt n2o_spo_surface-flask_2_3005-9999_monthly.txt n2o_spo_surface-insitu_2_3002-9999_monthly.txt n2o_stm_surface-flask_2_3001-9999_monthly.txt n2o_sum_surface-flask_2_3001-9999_monthly.txt n2o_sum_surface-flask_2_3005-9999_monthly.txt n2o_sum_surface-insitu_2_3002-9999_monthly.txt n2o_syo_surface-flask_2_3001-9999_monthly.txt n2o_tap_surface-flask_2_3001-9999_monthly.txt n2o_thd_surface-flask_2_3001-9999_monthly.txt n2o_thd_surface-flask_2_3005-9999_monthly.txt n2o_tik_surface-flask_2_3001-9999_monthly.txt n2o_ush_surface-flask_2_3001-9999_monthly.txt n2o_ush_surface-flask_2_3005-9999_monthly.txt n2o_uta_surface-flask_2_3001-9999_monthly.txt n2o_uum_surface-flask_2_3001-9999_monthly.txt n2o_wis_surface-flask_2_3001-9999_monthly.txt n2o_wkt_surface-flask_2_3001-9999_monthly.txt n2o_wlg_surface-flask_2_3001-9999_monthly.txt n2o_zep_surface-flask_2_3001-9999_monthly.txt	POC800N002f1* POC805N002f1* POC810N002f1* POC815N002f1* POC820N002f1* POC825N002f1* POC830N002f1* POC805S002f1* POC810S002f1* POC815S002f1* POC820S002f1* POC825S002f1* POC830S002f1* PSA764S002f1* PSA764S002f5 PTA438N002f1* RPB413N002f1* SDZ240N002f1* SEY104S002f1* SGP436N002f1* SHM452N002f1* SMO514S002f1* SMO514S002f4 SMO514S002f5 SMO514S002i2 SPO789S002f1 SPO789S002f4* SPO789S002f5 SPO789S002i2* STM666N002f1* SUM672N002f1* SUM672N002f5 SUM672N002i2 SYO769S002f1* TAP236N002f1* THD441N002f1 THD441N002f5 TIK271N002f1* USH354S002f1* USH354S002f5 UTA439N002f1* UUM244N002f1* WIS631N002f1* WKT431N002f1* WLG236N002f1* ZEP678N002f1*	
NPL	n2o_hfd_tower-insitu_154_6101-9999_monthly.txt	HFD650N154it*	WMO X2006A
SAWS	n2o_cpt_surface-insitu_66_9999-1001_monthly.txt	CPT134S066iz*	NOAA
UBAG	n2o_ssl_surface-insitu_71_9999-9999_monthly.txt n2o_zsf_surface-insitu_71_9999-9999_monthly.txt	SSL647N071iz ZSF647N071iz*	WMO X2006A
UNIURB	n2o_cmn_surface-insitu_74_9999-9999_monthly.txt	CMN644N074iz*	WMO X2006A
UNIVBR IS	n2o_tac_tower-insitu_77_6186-9999_monthly.txt	TAC652N077it*	WMO X2006A

	n2o_rgl_surface-insitu_77_9999-9999_monthly.txt	RGL651N077iz*	SIO-16
UoE	n2o_cvo_surface-insitu_151_9999-9999_monthly.txt	CVO116N151iz*	WMO X2006A

\* Stations with an asterisk are used for the calculation of the globally averaged mole fractions and related quantities. The site selection procedure is described in Appendix A.

\*\* NIES 96 N<sub>2</sub>O scale is approximately 0.7 ppb lower than that of WMO X2006A in the range 325 to 326 ppb.  
[https://gml.noaa.gov/ccgg/wmorr/wmorr\\_results.php?rr=rr6&param=n2o](https://gml.noaa.gov/ccgg/wmorr/wmorr_results.php?rr=rr6&param=n2o))

## 5. Carbon Monoxide (CO)

NOAA/ESRL is the WMO/GAW CCL for carbon monoxide. Due to lack of stability of CO in high pressure cylinders, the CO scale has historically been defined by repeated sets of gravimetric standards made in 1996/1997, 1999/2000, 2006 and 2011. The CCL makes revisions in the CO scale whenever new gravimetric standard sets indicate a significant drift in the scale. Scale revisions are indicated with date codes (WMO X2000, WMO X2004, WMO X2014) with the most recent made in December 2015 being WMO X2014A (WMO, 2020).

Empa serves as the WCC under GAW based on its secondary standards calibrated against the standard at NOAA/ESRL designated as the Primary Standard for GAW. Empa, as WCC for CO, has developed an audit system for CO measurements at GAW stations.

A small fraction of the data is reported in units of  $\mu\text{g}/\text{m}^3$  or  $\text{mg}/\text{m}^3$ . In WDCGG analysis, these units are converted

to ppb using the following formulas:

$$X_p [\text{ppb}] = (R \times T / M / P_0) \times 10 \times X_g [\mu\text{g}/\text{m}^3]$$

and

$$X_p [\text{ppb}] = (R \times T / M / P_0) \times 10^4 \times X_g [\text{mg}/\text{m}^3],$$

where

$R$  is the molar gas constant (8.31451 [J/K/mol]),

$T$  is the reported temperature for conversion (293.15 [K] or 298.15 [K]),

$M$  is the molecular weight of CO (28.0101) and

$P_0$  is the standard pressure (1013.25 [hPa]).

It is highly desirable to report CO concentration data in mole fractions (mostly in ppb) traceable to the WMO Mole Fraction Scale.

**Table B5. Status of CO standard scales.**

Organization	WDCGG Filename	Filename Code in Plate 5.1	Calibration Scale / Units except for using ppb	Audit Empa-WCC
AEMET	co_izo_surface-insitu_3_9999-9999_monthly.txt	IZO128N003iz	WMO X2014A	00, 04, 09, 13, 19
AGAGE	co_cgo_surface-insitu_4_2021-2021_monthly.txt co_mhd_surface-insitu_4_2021-2021_monthly.txt	CGO540S004ic MHD653N004ic*	CSIRO-94	
ARSO	co_kvv_surface-insitu_8_9999-9999_monthly.txt	KVV646N008iz*		
BAS	co_hba_surface-insitu_9_9999-9999_monthly.txt	HBA775S009iz	WMO X2014A	
BMKG	co_bkt_surface-insitu_10_9999-9999_monthly.txt	BKT500S010iz	WMO X2000 WMO X2014A	01, 04, 07, 08, 11, 14, 19
CHMI	co_kos_surface-insitu_12_9999-9999_monthly.txt	KOS649N012iz	$\mu\text{g}/\text{m}^3$ -20°C	
CSIRO	co_alt_surface-flask_16_9999-9999_monthly.txt co_cfa_surface-flask_16_9999-9999_monthly.txt co_cgo_surface-flask_16_9999-9999_monthly.txt co_cri_surface-flask_16_9999-9999_monthly.txt co_cya_surface-flask_16_9999-9999_monthly.txt co_esp_surface-flask_16_9999-9999_monthly.txt co_maa_surface-flask_16_9999-9999_monthly.txt co_mlo_surface-flask_16_9999-9999_monthly.txt co_mqa_surface-flask_16_9999-9999_monthly.txt co_sis_surface-flask_16_9999-9999_monthly.txt co_spo_surface-flask_16_9999-9999_monthly.txt	ALT482N016fz* CFA519S016fz* CGO540S016fz* CRI215N016fz* CYA766S016fz* ESP449N016fz* MAA767S016fz* MLO519N016fz MQA554S016fz* SIS660N016fz* SPO789S016fz*	CSIRO-2020	Cape Grim: 02, 16

DMC	co_tll_surface-insitu_17_9999-9999_monthly.txt	TLL330S017iz*	WMO X2014A	
DWD	co_hpb_surface-insitu_19_9999-9999_monthly.txt	HPB647N019iz*	WMO X2004	97, 06, 11, 20
	co_gat_tower-insitu_19_6342-9999_monthly.txt co_hpb_tower-insitu_19_6132-9999_monthly.txt co_kit_tower-insitu_19_6201-9999_monthly.txt co_lin_tower-insitu_19_6099-9999_monthly.txt co_toh_tower-insitu_19_6148-9999_monthly.txt	GAT653N019it* HPB647N019it* KIT649N019it* LIN652N019it* TOH651N019it*	WMO X2014A	
ECCC	co_alt_surface-insitu_20_9999-9999_monthly.txt co_cdl_surface-insitu_20_9999-9999_monthly.txt co_chl_surface-insitu_20_9999-9999_monthly.txt co_chm_surface-insitu_20_9999-9999_monthly.txt co_egb_surface-insitu_20_9999-9999_monthly.txt co_esp_surface-insitu_20_9999-9999_monthly.txt co_etl_surface-insitu_20_9999-9999_monthly.txt co_fsd_surface-insitu_20_9999-9999_monthly.txt co_llb_surface-insitu_20_9999-9999_monthly.txt co_wsa_surface-insitu_20_9999-9999_monthly.txt	ALT482N020iz CDL453N020iz* CHL458N020iz CHM449N020iz* EGB444N020iz* ESP449N020iz* ETL454N020iz* FSD449N020iz* LLB454N020iz* WSA443N020iz*	WMO X2014A	Alert: 04
Empa	co_jfj_surface-insitu_23_9999-9999_monthly.txt	JFJ646N023iz*	NIST SRM 1677c NMI PRM AC11 NIST SRM 2612a NPL PRGM in synth. Air WMO X2000 WMO X2004 WMO X2014A	99, 06, 15
	co_pay_surface-insitu_23_9999-9999_monthly.txt co_rig_surface-insitu_23_9999-9999_monthly.txt	PAY646N023iz* RIG647N023iz*	NMI PRM AC11 NIST SRM 1677c NIST SRM 2612a NPL PRGM in synth. Air NPL PRGM NG677 in synth. Air	
INRNE	co_beo_surface-insitu_33_9999-9999_monthly.txt	BEO642N033iz*		
ISAC	co_cmn_surface-insitu_37_9999-9999_monthly.txt	CMN644N037iz	WMO X2004 WMO X2014A	12, 18
	co_cgr_surface-insitu_37_9999-9999_monthly.txt co_lmt_surface-insitu_37_9999-9999_monthly.txt	CGR637N037iz* LMT638N037iz*	WMO X2014A	
	co_eco_surface-insitu_37_9999-9999_monthly.txt	ECO640N037iz		
JMA	co_mnm_surface-insitu_1_9999-9999_monthly.txt co_ryo_surface-insitu_1_9999-9999_monthly.txt co_yon_surface-insitu_1_9999-9999_monthly.txt	MNM224N001iz* RYO239N001iz* YON224N001iz*	WMO X2014A	Ryori: 05
KMA	co_amy_surface-insitu_39_9999-9999_monthly.txt co_jgs_surface-insitu_39_9999-9999_monthly.txt	AMY236N039iz JGS233N039iz*	KRISS	Anmye on-do:

				17 Jeju Gosan: 17
KMD	co_mkn_surface-insitu_40_9999-9999_monthly.txt	MKN100S040iz*	WMO X2000 WMO X2014A	05, 06, 08, 10, 15, 19
Kyrgyz hydro met	co_cpa_surface-insitu_155_9999-9999_monthly.txt	CPA242N155iz*	WMO X2014A	
LA	co_pdm_surface-insitu_43_9999-9999_monthly.txt	PDM642N043iz		
LAMP	co_puy_surface-insitu_44_9999-9999_monthly.txt	PUY645N044iz		16
LSCE	co_ams_surface-insitu_45_9999-9999_monthly.txt	AMS137S045iz		08
NIWA	co_arh_surface-flask_57_9999-9999_monthly.txt co_bhd_surface-flask_57_9999-9999_monthly.txt co_lau_surface-flask_57_9999-9999_monthly.txt co_lau_surface-insitu_57_9999-9999_monthly.txt	ARH777S057fz* BHD541S057fz* LAU545S057fz* LAU545S057iz*	WMO X2014A	10, 16
NOAA	co_abp_surface-flask_2_3001-9999_monthly.txt co_alt_surface-flask_2_3001-9999_monthly.txt co_amy_surface-flask_2_3001-9999_monthly.txt co_asc_surface-flask_2_3001-9999_monthly.txt co_ask_surface-flask_2_3001-9999_monthly.txt co_azr_surface-flask_2_3001-9999_monthly.txt co_bal_surface-flask_2_3001-9999_monthly.txt co_bhd_surface-flask_2_3001-9999_monthly.txt co_bkt_surface-flask_2_3001-9999_monthly.txt co_bme_surface-flask_2_3001-9999_monthly.txt co_bmw_surface-flask_2_3001-9999_monthly.txt co_brw_surface-flask_2_3001-9999_monthly.txt co_bsc_surface-flask_2_3001-9999_monthly.txt co_cba_surface-flask_2_3001-9999_monthly.txt co_cgo_surface-flask_2_3001-9999_monthly.txt co_chr_surface-flask_2_3001-9999_monthly.txt co_cmo_surface-flask_2_3001-9999_monthly.txt co_cpt_surface-flask_2_3001-9999_monthly.txt co_crz_surface-flask_2_3001-9999_monthly.txt co_drp_ship-flask_2_3001-9999_monthly.txt co_eic_surface-flask_2_3001-9999_monthly.txt co_gmi_surface-flask_2_3001-9999_monthly.txt co_goz_surface-flask_2_3001-9999_monthly.txt co_hba_surface-flask_2_3001-9999_monthly.txt co_hpb_surface-flask_2_3001-9999_monthly.txt co_hun_surface-flask_2_3001-9999_monthly.txt co_ice_surface-flask_2_3001-9999_monthly.txt co_itn_surface-flask_2_3001-9999_monthly.txt co_izo_surface-flask_2_3001-9999_monthly.txt co_key_surface-flask_2_3001-9999_monthly.txt co_kum_surface-flask_2_3001-9999_monthly.txt co_kzd_surface-flask_2_3001-9999_monthly.txt co_kzm_surface-flask_2_3001-9999_monthly.txt co_llb_surface-flask_2_3001-9999_monthly.txt co_lln_surface-flask_2_3001-9999_monthly.txt co_lmp_surface-flask_2_3001-9999_monthly.txt co_mbc_surface-flask_2_3001-9999_monthly.txt co_mex_surface-flask_2_3001-9999_monthly.txt	ABP312S002f1* ALT482N002f1 AMY236N002f1* ASC107S002f1* ASK123N002f1* AZR638N002f1* BAL655N002f1* BHD541S002f1* BKT500S002f1* BME432N002f1* BMW432N002f1* BRW471N002f1* BSC644N002f1 CBA455N002f1* CGO540S002f1 CHR501N002f1* CMO445N002f1* CPT134S002f1* CRZ146S002f1* DRP859S002f1* EIC327S002f1* GMI513N002f1* GOZ636N002f1* HBA775S002f1* HPB647N002f1* HUN646N002f1* ICE663N002f1* ITN435N002f1* IZO128N002f1* KEY425N002f1* KUM519N002f1* KZD244N002f1* KZM243N002f1* LLB454N002f1 LLN223N002f1* LMP635N002f1* MBC476N002f1* MEX418N002f1*	WMO X2014A	

	co_mhd_surface-flask_2_3001-9999_monthly.txt co_mid_surface-flask_2_3001-9999_monthly.txt co_mkn_surface-flask_2_3001-9999_monthly.txt co_mlo_surface-flask_2_3001-9999_monthly.txt co_nat_surface-flask_2_3001-9999_monthly.txt co_nmb_surface-flask_2_3001-9999_monthly.txt co_nwr_surface-flask_2_3001-9999_monthly.txt co_oxk_surface-flask_2_3001-9999_monthly.txt co_pal_surface-flask_2_3001-9999_monthly.txt co_poc_ship-flask_2_3001-3001_monthly.txt co_poc_ship-flask_2_3001-3002_monthly.txt co_poc_ship-flask_2_3001-3003_monthly.txt co_poc_ship-flask_2_3001-3004_monthly.txt co_poc_ship-flask_2_3001-3005_monthly.txt co_poc_ship-flask_2_3001-3006_monthly.txt co_poc_ship-flask_2_3001-3007_monthly.txt co_poc_ship-flask_2_3001-3012_monthly.txt co_poc_ship-flask_2_3001-3013_monthly.txt co_poc_ship-flask_2_3001-3014_monthly.txt co_poc_ship-flask_2_3001-3015_monthly.txt co_poc_ship-flask_2_3001-3016_monthly.txt co_poc_ship-flask_2_3001-3017_monthly.txt co_psa_surface-flask_2_3001-9999_monthly.txt co_pta_surface-flask_2_3001-9999_monthly.txt co_rpb_surface-flask_2_3001-9999_monthly.txt co_scs_ship-flask_2_3001-3101_monthly.txt co_scs_ship-flask_2_3001-3102_monthly.txt co_scs_ship-flask_2_3001-3103_monthly.txt co_scs_ship-flask_2_3001-3104_monthly.txt co_scs_ship-flask_2_3001-3105_monthly.txt co_scs_ship-flask_2_3001-3106_monthly.txt co_scs_ship-flask_2_3001-3107_monthly.txt co_sdz_surface-flask_2_3001-9999_monthly.txt co_sey_surface-flask_2_3001-9999_monthly.txt co_sgp_surface-flask_2_3001-9999_monthly.txt co_shm_surface-flask_2_3001-9999_monthly.txt co_smo_surface-flask_2_3001-9999_monthly.txt co_spo_surface-flask_2_3001-9999_monthly.txt co_stm_surface-flask_2_3001-9999_monthly.txt co_sum_surface-flask_2_3001-9999_monthly.txt co_syo_surface-flask_2_3001-9999_monthly.txt co_tap_surface-flask_2_3001-9999_monthly.txt co_thd_surface-flask_2_3001-9999_monthly.txt co_tik_surface-flask_2_3001-9999_monthly.txt co_ush_surface-flask_2_3001-9999_monthly.txt co_uta_surface-flask_2_3001-9999_monthly.txt co_uum_surface-flask_2_3001-9999_monthly.txt co_wis_surface-flask_2_3001-9999_monthly.txt co_wkt_surface-flask_2_3001-9999_monthly.txt co_wlg_surface-flask_2_3001-9999_monthly.txt co_zep_surface-flask_2_3001-9999_monthly.txt	MHD653N002f1* MID528N002f1* MKN100S002f1* MLO519N002f1* NAT306S002f1* NMB123S002f1* NWR440N002f1* OXK650N002f1* PAL667N002f1* POC800N002f1* POC805N002f1* POC810N002f1* POC815N002f1* POC820N002f1* POC825N002f1* POC830N002f1* POC805S002f1* POC810S002f1* POC815S002f1* POC820S002f1* POC825S002f1* POC830S002f1* PSA764S002f1* PTA438N002f1* RPB413N002f1* SCS803N002f1* SCS806N002f1* SCS809N002f1* SCS812N002f1* SCS815N002f1* SCS818N002f1* SCS821N002f1 SDZ240N002f1* SEY104S002f1* SGP436N002f1* SHM452N002f1* SMO514S002f1* SPO789S002f1 STM666N002f1* SUM672N002f1* SYO769S002f1* TAP236N002f1 THD441N002f1* TIK271N002f1* USH354S002f1* UTA439N002f1* UUM244N002f1* WIS631N002f1* WKT431N002f1* WLG236N002f1* ZEP678N002f1*		
NPL	co_hfd_tower-insitu_154_6101-9999_monthly.txt	HFD650N154it*	WMO X2014A	
ONM	co_ask_surface-insitu_59_9999-9999_monthly.txt	ASK123N059iz		07, 15
PolyU	co_hkg_surface-insitu_61_9999-9999_monthly.txt	HKG222N061iz		

RIVM	co_kmw_surface-insitu_63_9999-9999_monthly.txt co_ktb_surface-insitu_63_9999-9999_monthly.txt	KMW653N063iz*		
SAWS	co_cpt_surface-insitu_66_9999-1001_monthly.txt	CPT134S066iz*	WMO X2004 WMO X2014A CPT	98, 02, 06, 11, 15
SMNA	co_ush_surface-insitu_69_9999-9999_monthly.txt	USH354S069iz	WMO X1988 WMO X2000	98, 03, 08, 16, 19
UBAA	co_snb_surface-insitu_72_9999-9999_monthly.txt	SNB647N072iz*	NIST	98, 20
UBAG	co_zsf_surface-insitu_71_9999-9999_monthly.txt co_ssl_surface-insitu_71_9999-9999_monthly.txt co_ngl_surface-insitu_71_9999-9999_monthly.txt co zug_surface-insitu_71_9999-9999_monthly.txt	ZSF647N071iz* SSL647N071iz* NGL653N071iz* ZUG647N071iz*	WMO X2000 WMO X2004 WMO X2014 WMO X2014A	01, 06, 11, 20
UMLT	co_glh_surface-insitu_75_9999-9999_monthly.txt	GLH636N075iz*		
UNIURB	co_cmn_surface-insitu_74_9999-9999_monthly.txt	CMN644N074iz*	WMO X2014	12, 18
UoE	co_cvo_surface-insitu_151_9999-9999_monthly.txt	CVO116N151iz	WMO X2014A	
UYRK	co_cvo_surface-insitu_76_9999-9999_monthly.txt	CVO116N076iz*	WMO X2014	12
VNMHA	co_pdi_surface-insitu_51_9999-9999_monthly.txt	PDI221N051iz	WMO X2014A	

\* Stations with an asterisk are used for the calculation of the globally averaged mole fractions and related quantities. The site selection procedure is described in Appendix A.

## 6. Sulfur Hexafluoride (SF<sub>6</sub>)

NOAA/ESRL is the WMO/GAW CCL for sulfur hexafluoride. The most current WMO Mole Fraction Scale is the WMO X2014 version defined using 17 primary standards over the 2 – 20 ppt range, with calibration performed using GC-ECD (Hall *et al.*, 2011). The Korea Meteorological Administration (KMA), assisted by the Korea Research Institute of Standards and Science (KRISS), serves as a WCC for SF<sub>6</sub>. The first SF<sub>6</sub> intercomparison experiment was implemented by KMA WCC-SF<sub>6</sub> from 2016 to 2017 (Lee *et al.*, 2017; WMO, 2018).

SIO has developed and maintained a suite of standards for halogenated compounds at ppt levels since the 1990s (Weiss *et al.*, 1981; Prinn *et al.*, 2000). The SF<sub>6</sub> conversion factor between the WMO X2014 and SIO-05 calibration scales is reported as WMO X2014/SIO-05 = 1.0049 ± 0.0029 (Prinn *et al.*, 2018).

Table B6 summarizes the SF<sub>6</sub> standard scales used by stations contributing to the WDCGG.

**Table B6. Status of SF<sub>6</sub> standard scales.**

Organization	WDCGG Filename	Filename Code in Plate 4.2	Calibration Scale
AEMET	sf6_izo_surface-insitu_3_9999-9999_monthly.txt	IZO128N003iz	WMO X2014
AGAGE	sf6_cgo_surface-insitu_4_2021-2021_monthly.txt sf6_cgo_surface-insitu_4_2023-2021_monthly.txt sf6_gsn_surface-insitu_4_2023-2021_monthly.txt sf6_jfj_surface-insitu_4_2023-2021_monthly.txt sf6_mhd_surface-insitu_4_2023-2021_monthly.txt sf6_rpb_surface-insitu_4_2023-2021_monthly.txt	CGO540S004ic CGO540S004ie GSN233N004ie JFJ646N004ie MHD653N004ie RPB413N004ie	SIO-05

	sf6_smo_surface-insitu_4_2023-2021_monthly.txt sf6_thd_surface-insitu_4_2023-2021_monthly.txt sf6_zep_surface-insitu_4_2023-2021_monthly.txt	SMO514S004ie THD441N004ie ZEP678N004ie	
Empa	sf6_jfj_surface-insitu_23_9999-9999_monthly.txt	JFJ646N023iz	SIO-05
ENEA	sf6_lmp_surface-flask_24_9999-9999_monthly.txt	LMP635N024fz	
KMA	sf6_amy_surface-insitu_39_9999-9999_monthly.txt	AMY236N039iz	WMO X2006
NOAA	sf6_abp_surface-flask_2_3001-9999_monthly.txt sf6_alt_surface-flask_2_3001-9999_monthly.txt sf6_alt_surface-flask_2_3005-9999_monthly.txt sf6_amy_surface-flask_2_3001-9999_monthly.txt sf6_asc_surface-flask_2_3001-9999_monthly.txt sf6_ask_surface-flask_2_3001-9999_monthly.txt sf6_azr_surface-flask_2_3001-9999_monthly.txt sf6_bal_surface-flask_2_3001-9999_monthly.txt sf6_bhd_surface-flask_2_3001-9999_monthly.txt sf6_bkt_surface-flask_2_3001-9999_monthly.txt sf6_bme_surface-flask_2_3001-9999_monthly.txt sf6_bmw_surface-flask_2_3001-9999_monthly.txt sf6_brw_surface-flask_2_3001-9999_monthly.txt sf6_brw_surface-flask_2_3005-9999_monthly.txt sf6_brw_surface-insitu_2_3002-9999_monthly.txt sf6_bsc_surface-flask_2_3001-9999_monthly.txt sf6_cba_surface-flask_2_3001-9999_monthly.txt sf6_cgo_surface-flask_2_3001-9999_monthly.txt sf6_cgo_surface-flask_2_3005-9999_monthly.txt sf6_chr_surface-flask_2_3001-9999_monthly.txt sf6_cpt_surface-flask_2_3001-9999_monthly.txt sf6_crz_surface-flask_2_3001-9999_monthly.txt sf6_drp_ship-flask_2_3001-9999_monthly.txt sf6_eic_surface-flask_2_3001-9999_monthly.txt sf6_gmi_surface-flask_2_3001-9999_monthly.txt sf6_hba_surface-flask_2_3001-9999_monthly.txt sf6_hfm_surface-flask_2_3005-9999_monthly.txt sf6_hpб_surface-flask_2_3001-9999_monthly.txt sf6_hun_surface-flask_2_3001-9999_monthly.txt sf6_ice_surface-flask_2_3001-9999_monthly.txt sf6_itn_surface-flask_2_3001-9999_monthly.txt sf6_itn_surface-flask_2_3005-9999_monthly.txt sf6_izo_surface-flask_2_3001-9999_monthly.txt sf6_key_surface-flask_2_3001-9999_monthly.txt sf6_kum_surface-flask_2_3001-9999_monthly.txt sf6_kum_surface-flask_2_3005-9999_monthly.txt sf6_kzd_surface-flask_2_3001-9999_monthly.txt sf6_kzm_surface-flask_2_3001-9999_monthly.txt sf6_lef_surface-flask_2_3005-9999_monthly.txt sf6_llb_surface-flask_2_3001-9999_monthly.txt sf6_lln_surface-flask_2_3001-9999_monthly.txt sf6_lmp_surface-flask_2_3001-9999_monthly.txt sf6_mex_surface-flask_2_3001-9999_monthly.txt sf6_mhd_surface-flask_2_3001-9999_monthly.txt sf6_mhd_surface-flask_2_3005-9999_monthly.txt sf6_mid_surface-flask_2_3001-9999_monthly.txt sf6_mkn_surface-flask_2_3001-9999_monthly.txt sf6_mlo_surface-flask_2_3001-9999_monthly.txt sf6_mlo_surface-flask_2_3005-9999_monthly.txt	ABP312S002f1 ALT482N002f1 ALT482N002f5 AMY236N002f1 ASC107S002f1 ASK123N002f1 AZR638N002f1 BAL655N002f1 BHD541S002f1 BKT500S002f1 BME432N002f1 BMW432N002f1 BRW471N002f1 BRW471N002f5 BRW471N002i2 BSC644N002f1 CBA455N002f1 CGO540S002f1 CGO540S002f5 CHR501N002f1 CPT134S002f1 CRZ146S002f1 DRP859S002f1 EIC327S002f1 GMI513N002f1 HBA775S002f1 HFM442N002f5 HPB647N002f1 HUN646N002f1 ICE663N002f1 ITN435N002f1 ITN435N002f5 IZO128N002f1 KEY425N002f1 KUM519N002f1 KUM519N002f5 KZD244N002f1 KZM243N002f1 LEF445N002f5 LLB454N002f1 LLN223N002f1 LMP635N002f1 MEX418N002f1 MHD653N002f1 MHD653N002f5 MID528N002f1 MKN100S002f1 MLO519N002f1 MLO519N002f5	WMO X2014



UNIURB	sf6_cmn_surface-insitu_74_9999-9999_monthly.txt	CMN644N074iz	WMO X2014
UNIVBR IS	sf6_rgl_surface-insitu_77_9999-9999_monthly.txt sf6_tac_surface-insitu_77_9999-9999_monthly.txt	RGL651N077iz TAC652N077iz	SIO-05

## APPENDIX C LIST OF OBSERVATIONAL STATIONS

Station	Country/Territory	GAW ID	Organization	Latitude (°)	Longitude (°)	Altitude (m)	Parameter
<b>REGION I (Africa)</b>							
Amsterdam Island	France	AMS	NOAA	37.80 S	77.54 E	70	CO <sub>2</sub> , CH <sub>4</sub>
Amsterdam Island	France	AMS	LSCE	37.80 S	77.54 E	70	CO <sub>2</sub> , CH <sub>4</sub> , CO
Ascension Island	United Kingdom of Great Britain and Northern Ireland	ASC	NOAA	7.97 S	14.40 W	91	CO <sub>2</sub> , CH <sub>4</sub> , N <sub>2</sub> O, SF <sub>6</sub> , <sup>13</sup> CH <sub>4</sub> , <sup>13</sup> CO <sub>2</sub> , C <sup>18</sup> O <sub>2</sub> , CO, H <sub>2</sub>
Assekrem	Algeria	ASK	NOAA	23.27 N	5.63 E	2710	CO <sub>2</sub> , CH <sub>4</sub> , N <sub>2</sub> O, SF <sub>6</sub> , <sup>13</sup> CO <sub>2</sub> , C <sup>18</sup> O <sub>2</sub> , CO, H <sub>2</sub>
Assekrem	Algeria	ASK	ONM	23.27 N	5.63 E	2710	CO
Cairo	Egypt	CAI	EMA	30.08 N	31.28 E	35	CO <sub>2</sub>
Cape Point	South Africa	CPT	NOAA	34.35 S	18.49 E	230	CO <sub>2</sub> , CH <sub>4</sub> , N <sub>2</sub> O, SF <sub>6</sub> , <sup>13</sup> CO <sub>2</sub> , C <sup>18</sup> O <sub>2</sub> , CO
Cape Point	South Africa	CPT	ANSTO	34.35 S	18.49 E	230	<sup>222</sup> Rn
Cape Point	South Africa	CPT	SAWS	34.35 S	18.49 E	230	CO <sub>2</sub> , CH <sub>4</sub> , N <sub>2</sub> O, CO
Cape Verde Atmospheric Observatory	Cabo Verde	CVO	UYRK	16.86 N	24.87 W	10	CO <sub>2</sub> , CH <sub>4</sub> , CO
Cape Verde Atmospheric Observatory	Cabo Verde	CVO	UoE	16.86 N	24.87 W	10	CO <sub>2</sub> , CH <sub>4</sub> , N <sub>2</sub> O, CO
Crozet	France	CRZ	NOAA	46.43 S	51.83 E	120	CO <sub>2</sub> , CH <sub>4</sub> , N <sub>2</sub> O, SF <sub>6</sub> , <sup>13</sup> CO <sub>2</sub> , C <sup>18</sup> O <sub>2</sub> , CO, H <sub>2</sub>
Farafra	Egypt	FRF	EMA	27.06 N	27.99 E	92	CO <sub>2</sub>
Gobabeb	Namibia	NMB	NOAA	23.57 S	15.03 E	408	CO <sub>2</sub> , CH <sub>4</sub> , N <sub>2</sub> O, SF <sub>6</sub> , <sup>13</sup> CO <sub>2</sub> , C <sup>18</sup> O <sub>2</sub> , CO
Izaña (Tenerife)	Spain	IZO	NOAA	28.31 N	16.50 W	2373	CO <sub>2</sub> , CH <sub>4</sub> , N <sub>2</sub> O, SF <sub>6</sub> , <sup>13</sup> CO <sub>2</sub> , C <sup>18</sup> O <sub>2</sub> , CO, H <sub>2</sub>
Izaña (Tenerife)	Spain	IZO	AEMET	28.31 N	16.50 W	2373	CO <sub>2</sub> , CH <sub>4</sub> , N <sub>2</sub> O, SF <sub>6</sub> , CO
Mahé	Seychelles	SEY	NOAA	4.67 S	55.17 E	3	CO <sub>2</sub> , CH <sub>4</sub> , N <sub>2</sub> O, SF <sub>6</sub> , <sup>13</sup> CO <sub>2</sub> , C <sup>18</sup> O <sub>2</sub> , CO, H <sub>2</sub>
Mt. Kenya	Kenya	MKN	NOAA	0.06 S	37.30 E	3678	CO <sub>2</sub> , CH <sub>4</sub> , N <sub>2</sub> O, SF <sub>6</sub> , <sup>13</sup> CO <sub>2</sub> , C <sup>18</sup> O <sub>2</sub> , CO
Mt. Kenya	Kenya	MKN	KMD	0.06 S	37.30 E	3678	CO <sub>2</sub> , CH <sub>4</sub> , CO
<b>REGION II (Asia)</b>							
Anmyeon-do	Republic of Korea	AMY	NOAA	36.54 N	126.33 E	42	CO <sub>2</sub> , CH <sub>4</sub> , N <sub>2</sub> O, SF <sub>6</sub> , <sup>13</sup> CH <sub>4</sub> , HFCs, CBrF <sub>3</sub> , CO
Anmyeon-do	Republic of Korea	AMY	KMA	36.54 N	126.33 E	42	CO <sub>2</sub> , CH <sub>4</sub> , N <sub>2</sub> O, SF <sub>6</sub> , CFCs, CO
Bering Island	Russian Federation	BER	MGO	55.20 N	165.98 E	13	CO <sub>2</sub>
Cape Ochiishi	Japan	COI	NIES	43.17 N	145.50 E	49	CO <sub>2</sub> , CH <sub>4</sub> , N <sub>2</sub> O, SF <sub>6</sub> , CFCs, HCFCs, HFCs
Cape Rama	India	CRI	CSIRO	15.08 N	73.83 E	60	CO <sub>2</sub> , CH <sub>4</sub> , N <sub>2</sub> O, <sup>13</sup> CO <sub>2</sub> , CO, H <sub>2</sub>
Cholpon-Ata	Kyrgyzstan	CPA	Kyrgyzhydromet	42.64 N	77.07 E	1613	CO <sub>2</sub> , CH <sub>4</sub> , CO

## LIST OF OBSERVATIONAL STATIONS (continued)

Station	Country/Territory	GAW ID	Organization	Latitude (°)	Longitude (°)	Location Altitude (m)	Parameter
Gosan	Republic of Korea	GSN	AGAGE	33.29 N	126.16 E	71.39	SF <sub>6</sub> , CCl <sub>4</sub> , CH <sub>3</sub> CCl <sub>3</sub> , CFCs, HCFCs, HFCs, PFCs, CBrClF <sub>2</sub> , CBrF <sub>3</sub> , C <sub>2</sub> Br <sub>2</sub> F <sub>4</sub> , CHCl <sub>3</sub> , CH <sub>3</sub> Cl
Gosan	Republic of Korea	GSN	GERC	33.29 N	126.16 E	71.39	CO <sub>2</sub> , CH <sub>4</sub> , N <sub>2</sub> O
Gosan	Republic of Korea	GSN	METRI	33.29 N	126.16 E	71.39	CO <sub>2</sub> , CH <sub>4</sub> , N <sub>2</sub> O, CFCs
Hamamatsu	Japan	HMM	SHIZU	34.72 N	137.72 E	29	CO <sub>2</sub>
Hateruma Island	Japan	HAT	NIES	24.05 N	123.81 E	10	CO <sub>2</sub> , CH <sub>4</sub> , N <sub>2</sub> O, SF <sub>6</sub> , CFCs, HCFCs, HFCs
Hok Tsui / Cape d Aguilar	Hong Kong, China	HKG	HKO	22.21 N	114.25 E	53	CO <sub>2</sub>
Hok Tsui / Cape d Aguilar	Hong Kong, China	HKG	PolyU	22.21 N	114.25 E	53	CO
Issyk-Kul	Kyrgyzstan	ISK	KSNU	42.62 N	76.98 E	1640	CO <sub>2</sub> , CH <sub>4</sub>
Jeju Gosan	Republic of Korea	JGS	KMA	33.30 N	126.21 E	52	CO <sub>2</sub> , CO
Kaashidhoo (Male Atoll)	Maldives	KCO	NOAA	4.97 N	73.47 E	1	CO <sub>2</sub> , CH <sub>4</sub> , N <sub>2</sub> O, SF <sub>6</sub> , CO
King's Park	Hong Kong, China	HKO	HKO	22.31 N	114.17 E	65	CO <sub>2</sub>
Kisai	Japan	KIS	SAIPF	36.08 N	139.55 E	13	CO <sub>2</sub>
Kotelnyj Island	Russian Federation	KOT	MGO	76.00 N	137.87 E	5	CO <sub>2</sub>
Kyzylcha	Uzbekistan	KYZ	MGO	40.87 N	66.15 E	340	CO <sub>2</sub>
Lulin	Taiwan, Province of China	LLN	NOAA	23.47 N	120.87 E	2862	CO <sub>2</sub> , CH <sub>4</sub> , N <sub>2</sub> O, SF <sub>6</sub> , <sup>13</sup> CO <sub>2</sub> , C <sup>18</sup> O <sub>2</sub> , CO
Memanbetsu	Japan	MMB	MRI	43.92 N	144.20 E	33	N <sub>2</sub> O
Mikawa-Ichinomiya	Japan	MKW	AICH	34.85 N	137.43 E	50	CO <sub>2</sub>
Minamitorishima	Japan	MNM	JMA	24.29 N	153.98 E	7.1	CO <sub>2</sub> , CH <sub>4</sub> , HFCs, CO
Mt. Dodaira	Japan	DDR	SAIPF	36.00 N	139.20 E	840	CO <sub>2</sub>
Mt. Waliguan	China	WLG	NOAA	36.29 N	100.90 E	3810	CO <sub>2</sub> , CH <sub>4</sub> , N <sub>2</sub> O, SF <sub>6</sub> , <sup>13</sup> CH <sub>4</sub> , <sup>13</sup> CO <sub>2</sub> , C <sup>18</sup> O <sub>2</sub> , CO, H <sub>2</sub>
Mt. Waliguan	China	WLG	CMA	36.29 N	100.90 E	3810	CO <sub>2</sub> , CH <sub>4</sub>
Nagoya	Japan	NGY	NAGOU	35.15 N	136.97 E	35	N <sub>2</sub> O
Nepal Climate Observatory - Pyramid	Nepal	PYR	UNIURB	27.96 N	86.81 E	5079	SO <sub>2</sub> F <sub>2</sub> , COS, CCl <sub>4</sub> , CH <sub>3</sub> CCl <sub>3</sub> , CFCs, HCFCs, HFCs, PFCs, CBrClF <sub>2</sub> , CBrF <sub>3</sub> , CHCl <sub>3</sub> , CH <sub>3</sub> Cl, CH <sub>2</sub> Cl <sub>2</sub> , CH <sub>3</sub> I, CH <sub>3</sub> Br, CH <sub>2</sub> Br <sub>2</sub> , C <sub>2</sub> HCl <sub>3</sub> , C <sub>2</sub> Cl <sub>4</sub> , CHBr <sub>3</sub>
Pha Din Plateau Assy	Viet Nam Kazakhstan	PDI KZM	VNMHA NOAA	21.57 N 43.25 N	103.52 E 77.88 E	1466 2519	CO <sub>2</sub> , CH <sub>4</sub> , CO CO <sub>2</sub> , CH <sub>4</sub> , N <sub>2</sub> O, SF <sub>6</sub> , <sup>13</sup> CO <sub>2</sub> , C <sup>18</sup> O <sub>2</sub> , CO, H <sub>2</sub>
Ryori	Japan	RYO	JMA	39.03 N	141.82 E	260	CO <sub>2</sub> , CH <sub>4</sub> , N <sub>2</sub> O, CCl <sub>4</sub> , CH <sub>3</sub> CCl <sub>3</sub> , CFCs, CO
Sary Taukum	Kazakhstan	KZD	NOAA	44.45 N	77.57 E	412	CO <sub>2</sub> , CH <sub>4</sub> , N <sub>2</sub> O, SF <sub>6</sub> , <sup>13</sup> CO <sub>2</sub> , C <sup>18</sup> O <sub>2</sub> , CO, H <sub>2</sub>
Shangdianzi	China	SDZ	NOAA	40.65 N	117.12 E	287	CO <sub>2</sub> , CH <sub>4</sub> , N <sub>2</sub> O, SF <sub>6</sub> , <sup>13</sup> CO <sub>2</sub> , C <sup>18</sup> O <sub>2</sub> , CO
Suita Tae-ahn Peninsula	Japan Republic of Korea	SUI TAP	OSAKAU NOAA	34.82 N 36.73 N	135.52 E 126.13 E	63 20	CO <sub>2</sub> CO <sub>2</sub> , CH <sub>4</sub> , N <sub>2</sub> O, SF <sub>6</sub> , <sup>13</sup> CH <sub>4</sub> , <sup>13</sup> CO <sub>2</sub> , C <sup>18</sup> O <sub>2</sub> , CO, H <sub>2</sub>
Takayama	Japan	TKY	AIST	36.15 N	137.42 E	1420	CO <sub>2</sub>

## LIST OF OBSERVATIONAL STATIONS (continued)

Station	Country/Territory	GAW ID	Organization	Location			Parameter
				Latitude (°)	Longitude (°)	Altitude (m)	
Tateno (Tsukuba)	Japan	TKB	MRI	36.06 N	140.13 E	25.2	CO <sub>2</sub> , CH <sub>4</sub>
Tiksi	Russian Federation	TIK	NOAA	71.59 N	128.92 E	8	CO <sub>2</sub> , CH <sub>4</sub> , N <sub>2</sub> O, SF <sub>6</sub> , <sup>13</sup> CO <sub>2</sub> , C <sup>18</sup> O <sub>2</sub> , CO
Tiksi	Russian Federation	TIK	FMI	71.59 N	128.92 E	8	CO <sub>2</sub> , CH <sub>4</sub>
Tiksi	Russian Federation	TIK	MGO	71.59 N	128.92 E	8	CO <sub>2</sub> , CH <sub>4</sub>
Ulaan Uul	Mongolia	UUM	NOAA	44.44 N	111.09 E	992	CO <sub>2</sub> , CH <sub>4</sub> , N <sub>2</sub> O, SF <sub>6</sub> , <sup>13</sup> CO <sub>2</sub> , C <sup>18</sup> O <sub>2</sub> , CO, H <sub>2</sub>
Urawa	Japan	URW	SAIPF	35.87 N	139.62 E	10	CO <sub>2</sub>
Yonagunijima	Japan	YON	JMA	24.47 N	123.01 E	30	CO <sub>2</sub> , CH <sub>4</sub> , CO

### REGION III (South America)

Arembepe	Brazil	ABP	NOAA	12.77 S	38.17 W	0	CO <sub>2</sub> , CH <sub>4</sub> , N <sub>2</sub> O, SF <sub>6</sub> , <sup>13</sup> CO <sub>2</sub> , C <sup>18</sup> O <sub>2</sub> , CO
Arembepe	Brazil	ABP	INPE	12.77 S	38.17 W	0	CO <sub>2</sub> , CH <sub>4</sub> , N <sub>2</sub> O, CO
Bird Island (South Georgia)	United Kingdom of Great Britain and Northern Ireland	SGI	NOAA	54.01 S	38.05 W	30	CO <sub>2</sub> , CH <sub>4</sub>
Easter Island	Chile	EIC	NOAA	27.17 S	109.42 W	41	CO <sub>2</sub> , CH <sub>4</sub> , N <sub>2</sub> O, SF <sub>6</sub> , <sup>13</sup> CO <sub>2</sub> , C <sup>18</sup> O <sub>2</sub> , CO, H <sub>2</sub>
El Tololo	Chile	TLL	DMC	30.17 S	70.80 W	2154	CO <sub>2</sub> , CH <sub>4</sub> , CO
Huancayo	Peru	HUA	IGP	12.15 S	75.57 W	4575	CO <sub>2</sub>
Natal	Brazil	NAT	NOAA	6.00 S	35.20 W	0	CO <sub>2</sub> , CH <sub>4</sub> , N <sub>2</sub> O, SF <sub>6</sub> , <sup>13</sup> CO <sub>2</sub> , C <sup>18</sup> O <sub>2</sub> , CO
Ushuaia	Argentina	USH	NOAA	54.85 S	68.31 W	18	CO <sub>2</sub> , CH <sub>4</sub> , N <sub>2</sub> O, SF <sub>6</sub> , <sup>13</sup> CO <sub>2</sub> , C <sup>18</sup> O <sub>2</sub> , CCl <sub>4</sub> , CH <sub>3</sub> CCl <sub>3</sub> , CFCs, CO
Ushuaia	Argentina	USH	SMNA	54.85 S	68.31 W	18	CO

### REGION IV (North and Central America)

Alert	Canada	ALT	NOAA	82.50 N	62.34 W	185	CO <sub>2</sub> , CH <sub>4</sub> , N <sub>2</sub> O, SF <sub>6</sub> , <sup>13</sup> CH <sub>4</sub> , <sup>13</sup> CO <sub>2</sub> , C <sup>18</sup> O <sub>2</sub> , CCl <sub>4</sub> , CH <sub>3</sub> CCl <sub>3</sub> , CFCs, HCFCs, HFCs, CBrClF <sub>2</sub> , CBrF <sub>3</sub> , C <sub>2</sub> Br <sub>2</sub> F <sub>4</sub> , CO, CH <sub>3</sub> Cl, CH <sub>2</sub> Cl <sub>2</sub> , CH <sub>3</sub> Br, C <sub>2</sub> Cl <sub>4</sub> , H <sub>2</sub>
Alert	Canada	ALT	CSIRO	82.50 N	62.34 W	185	CO <sub>2</sub> , CH <sub>4</sub> , N <sub>2</sub> O, <sup>13</sup> CO <sub>2</sub> , CO, H <sub>2</sub>
Alert	Canada	ALT	ECCC	82.50 N	62.34 W	185	CO <sub>2</sub> , CH <sub>4</sub> , N <sub>2</sub> O, <sup>13</sup> CO <sub>2</sub> , C <sup>18</sup> O <sub>2</sub> , CO
Argyle (ME)	United States of America	AMT	NOAA	45.03 N	68.68 W	50	CH <sub>4</sub> , N <sub>2</sub> O, SF <sub>6</sub> , <sup>13</sup> CO <sub>2</sub> , C <sup>18</sup> O <sub>2</sub> , CO
Barrow (AK)	United States of America	BRW	NOAA	71.32 N	156.61 W	11	CO <sub>2</sub> , CH <sub>4</sub> , N <sub>2</sub> O, SF <sub>6</sub> , <sup>13</sup> CH <sub>4</sub> , <sup>13</sup> CO <sub>2</sub> , C <sup>18</sup> O <sub>2</sub> , CCl <sub>4</sub> , CH <sub>3</sub> CCl <sub>3</sub> , CFCs, HCFCs, HFCs, CBrClF <sub>2</sub> , CBrF <sub>3</sub> , C <sub>2</sub> Br <sub>2</sub> F <sub>4</sub> , CO, CH <sub>3</sub> Cl, CH <sub>2</sub> Cl <sub>2</sub> , CH <sub>3</sub> Br,

## LIST OF OBSERVATIONAL STATIONS (continued)

Station	Country/Territory	GAW ID	Organization	Latitude (°)	Longitude (°)	Location Altitude (m)	Parameter
Candle Lake	Canada	CDL	ECCC	53.99 N	105.12 W	591	$\text{C}_2\text{Cl}_4$ , $\text{H}_2$ $\text{CO}_2$ , $\text{CH}_4$ , $\text{CO}$
Cape Meares (OR)	United States of America	CMO	NOAA	45.00 N	124.00 W	30	$\text{CO}_2$ , $\text{CH}_4$ , $^{13}\text{CO}_2$ , $\text{C}^{18}\text{O}_2$ , $\text{CO}$ , $\text{H}_2$
Cape Meares (OR)	United States of America	CMO	AGAGE	45.00 N	124.00 W	30	$\text{CH}_4$ , $\text{N}_2\text{O}$ , $\text{CCl}_4$ , $\text{CH}_3\text{CCl}_3$ , CFCs
Chibougamau	Canada	CHM	ECCC	49.69 N	74.34 W	383	$\text{CO}_2$ , $\text{CH}_4$ , $\text{CO}$
Churchill	Canada	CHL	ECCC	58.74 N	93.82 W	16	$\text{CO}_2$ , $\text{CH}_4$ , $\text{N}_2\text{O}$ , $^{13}\text{CO}_2$ , $\text{C}^{18}\text{O}_2$ , $\text{CO}$
Churchill	Canada	CHL	TU	58.74 N	93.82 W	16	$^{13}\text{CH}_4$
Cold Bay (AK)	United States of America	CBA	NOAA	55.20 N	162.72 W	25	$\text{CO}_2$ , $\text{CH}_4$ , $\text{N}_2\text{O}$ , $\text{SF}_6$ , $^{13}\text{CH}_4$ , $^{13}\text{CO}_2$ , $\text{C}^{18}\text{O}_2$ , $\text{CO}$ , $\text{H}_2$
East Trout Lake	Canada	ETL	ECCC	54.35 N	104.99 W	500	$\text{CO}_2$ , $\text{CH}_4$ , $^{13}\text{CO}_2$ , $\text{C}^{18}\text{O}_2$ , $\text{CO}$
Egbert	Canada	EGB	ECCC	44.23 N	79.78 W	255	$\text{CO}_2$ , $\text{CH}_4$ , $\text{CO}$
Estevan Point	Canada	ESP	CSIRO	49.38 N	126.54 W	7	$\text{CO}_2$ , $\text{CH}_4$ , $\text{N}_2\text{O}$ , $^{13}\text{CO}_2$ , $\text{CO}$ , $\text{H}_2$
Estevan Point	Canada	ESP	ECCC	49.38 N	126.54 W	7	$\text{CO}_2$ , $\text{CH}_4$ , $\text{N}_2\text{O}$ , $^{13}\text{CO}_2$ , $\text{C}^{18}\text{O}_2$ , $\text{CO}$
Fraserdale	Canada	FSD	ECCC	49.84 N	81.52 W	210	$\text{CO}_2$ , $\text{CH}_4$ , $^{13}\text{CO}_2$ , $\text{C}^{18}\text{O}_2$ , $\text{CO}$
Grifton - Georgia Station (NC)	United States of America	ITN	NOAA	35.35 N	77.38 W	505	$\text{CH}_4$ , $\text{N}_2\text{O}$ , $\text{SF}_6$ , $^{13}\text{CO}_2$ , $\text{C}^{18}\text{O}_2$ , $\text{CCl}_4$ , $\text{CH}_3\text{CCl}_3$ , CFCs, $\text{CO}$ , $\text{H}_2$
Harvard Forest (MA)	United States of America	HFM	NOAA	42.90 N	72.30 W	340	$\text{N}_2\text{O}$ , $\text{SF}_6$ , $\text{CCl}_4$ , $\text{CH}_3\text{CCl}_3$ , CFCs, HCFCs, HFCs, $\text{CBrClF}_2$ , $\text{CBrF}_3$ , $\text{C}_2\text{Br}_2\text{F}_4$ , $\text{CH}_3\text{Cl}$ , $\text{CH}_2\text{Cl}_2$ , $\text{CH}_3\text{Br}$ , $\text{C}_2\text{Cl}_4$
Key Biscane (FL)	United States of America	KEY	NOAA	25.67 N	80.20 W	3	$\text{CO}_2$ , $\text{CH}_4$ , $\text{N}_2\text{O}$ , $\text{SF}_6$ , $^{13}\text{CO}_2$ , $\text{C}^{18}\text{O}_2$ , $\text{CO}$ , $\text{H}_2$
Kitt Peak (AZ)	United States of America	KPA	NOAA	31.97 N	111.60 W	2083	$\text{CH}_4$
La Jolla (CA)	United States of America	SIO	NOAA	32.83 N	117.27 W	14	$\text{CH}_4$
Lac La Biche (Alberta)	Canada	LLB	NOAA	54.95 N	112.47 W	548	$\text{CO}_2$ , $\text{CH}_4$ , $\text{N}_2\text{O}$ , $\text{SF}_6$ , $^{13}\text{CH}_4$ , $^{13}\text{CO}_2$ , $\text{C}^{18}\text{O}_2$ , $\text{CO}$
Lac La Biche (Alberta)	Canada	LLB	ECCC	54.95 N	112.47 W	548	$\text{CO}_2$ , $\text{CH}_4$ , $\text{CO}$
Mex High Altitude Global Climate Observation Center	Mexico	MEX	NOAA	18.99 N	97.31 W	4560	$\text{CO}_2$ , $\text{CH}_4$ , $\text{N}_2\text{O}$ , $\text{SF}_6$ , $^{13}\text{CH}_4$ , $^{13}\text{CO}_2$ , $\text{C}^{18}\text{O}_2$ , $\text{CO}$
Moody (TX)	United States of America	WKT	NOAA	31.32 N	97.62 W	723	$\text{CH}_4$ , $\text{N}_2\text{O}$ , $\text{SF}_6$ , $^{13}\text{CO}_2$ , $\text{C}^{18}\text{O}_2$ , $\text{CO}$
Mould Bay	Canada	MBC	NOAA	76.25 N	119.35 W	58	$\text{CO}_2$ , $\text{CH}_4$ , $^{13}\text{CO}_2$ , $\text{C}^{18}\text{O}_2$ , $\text{CO}$ , $\text{H}_2$

## LIST OF OBSERVATIONAL STATIONS (continued)

Station	Country/Territory	GAW ID	Organization	Latitude (°)	Longitude (°)	Location Altitude (m)	Parameter
Niwot Ridge - T-van (CO)	United States of America	NWR	NOAA	40.05 N	105.59 W	3523	CO <sub>2</sub> , CH <sub>4</sub> , N <sub>2</sub> O, SF <sub>6</sub> , <sup>13</sup> CH <sub>4</sub> , <sup>13</sup> CO <sub>2</sub> , C <sup>18</sup> O <sub>2</sub> , CCl <sub>4</sub> , CH <sub>3</sub> CCl <sub>3</sub> , CFCs, HCFCs, HFCs, CBrClF <sub>2</sub> , CBrF <sub>3</sub> , C <sub>2</sub> Br <sub>2</sub> F <sub>4</sub> , CO, CH <sub>3</sub> Cl, CH <sub>2</sub> Cl <sub>2</sub> , CH <sub>3</sub> Br, C <sub>2</sub> Cl <sub>4</sub> , H <sub>2</sub> , <sup>14</sup> CO <sub>2</sub>
Olympic Peninsula (WA)	United States of America	OPW	NOAA	48.25 N	124.42 W	488	CO <sub>2</sub> , CH <sub>4</sub>
Park Falls (WI)	United States of America	LEF	NOAA	45.93 N	90.27 W	868	CO <sub>2</sub> , CH <sub>4</sub> , N <sub>2</sub> O, SF <sub>6</sub> , <sup>13</sup> CO <sub>2</sub> , C <sup>18</sup> O <sub>2</sub> , CCl <sub>4</sub> , CH <sub>3</sub> CCl <sub>3</sub> , CFCs, HCFCs, HFCs, CBrClF <sub>2</sub> , CBrF <sub>3</sub> , C <sub>2</sub> Br <sub>2</sub> F <sub>4</sub> , CO, CH <sub>3</sub> Cl, CH <sub>2</sub> Cl <sub>2</sub> , CH <sub>3</sub> Br, C <sub>2</sub> Cl <sub>4</sub> , H <sub>2</sub>
Point Arena (CA)	United States of America	PTA	NOAA	38.95 N	123.73 W	17	CO <sub>2</sub> , CH <sub>4</sub> , N <sub>2</sub> O, SF <sub>6</sub> , <sup>13</sup> CO <sub>2</sub> , C <sup>18</sup> O <sub>2</sub> , CO
Ragged Point	Barbados	RPB	NOAA	13.17 N	59.43 W	45	CO <sub>2</sub> , CH <sub>4</sub> , N <sub>2</sub> O, SF <sub>6</sub> , <sup>13</sup> CO <sub>2</sub> , C <sup>18</sup> O <sub>2</sub> , CO, H <sub>2</sub>
Ragged Point	Barbados	RPB	AGAGE	13.17 N	59.43 W	45	CH <sub>4</sub> , N <sub>2</sub> O, SF <sub>6</sub> , SO <sub>2</sub> F <sub>2</sub> , NF <sub>3</sub> , CCl <sub>4</sub> , CH <sub>3</sub> CCl <sub>3</sub> , CFCs, HCFCs, HFCs, PFCs, CBrClF <sub>2</sub> , CBrF <sub>3</sub> , C <sub>2</sub> Br <sub>2</sub> F <sub>4</sub> , CHCl <sub>3</sub> , CH <sub>3</sub> Cl, CH <sub>2</sub> Cl <sub>2</sub> , CH <sub>3</sub> Br, C <sub>2</sub> Cl <sub>4</sub>
Sable Island	Canada	WSA	ECCC	43.93 N	60.01 W	2	CO <sub>2</sub> , CH <sub>4</sub> , N <sub>2</sub> O, <sup>13</sup> CO <sub>2</sub> , C <sup>18</sup> O <sub>2</sub> , CO
Shemya Island	United States of America	SHM	NOAA	52.72 N	174.10 E	40	CO <sub>2</sub> , CH <sub>4</sub> , N <sub>2</sub> O, SF <sub>6</sub> , <sup>13</sup> CO <sub>2</sub> , C <sup>18</sup> O <sub>2</sub> , CO, H <sub>2</sub>
Southern Great Plains E13 (OK)	United States of America	SGP	NOAA	36.60 N	97.50 W	318	CO <sub>2</sub> , CH <sub>4</sub> , N <sub>2</sub> O, SF <sub>6</sub> , <sup>13</sup> CO <sub>2</sub> , C <sup>18</sup> O <sub>2</sub> , CO
St. Croix	United States of America	AVI	NOAA	17.75 N	64.75 W	3	CO <sub>2</sub> , CH <sub>4</sub>
St. David's Head	United Kingdom of Great Britain and Northern Ireland	BME	NOAA	32.37 N	64.65 W	30	CO <sub>2</sub> , CH <sub>4</sub> , N <sub>2</sub> O, SF <sub>6</sub> , <sup>13</sup> CO <sub>2</sub> , C <sup>18</sup> O <sub>2</sub> , CO, H <sub>2</sub>
Trinidad Head (CA)	United States of America	THD	NOAA	41.05 N	124.15 W	107	CO <sub>2</sub> , CH <sub>4</sub> , N <sub>2</sub> O, SF <sub>6</sub> , <sup>13</sup> CO <sub>2</sub> , C <sup>18</sup> O <sub>2</sub> , CCl <sub>4</sub> , CH <sub>3</sub> CCl <sub>3</sub> , CFCs, HCFCs, HFCs, CBrClF <sub>2</sub> , CBrF <sub>3</sub> , C <sub>2</sub> Br <sub>2</sub> F <sub>4</sub> , CO, CH <sub>3</sub> Cl, CH <sub>2</sub> Cl <sub>2</sub> , CH <sub>3</sub> Br, C <sub>2</sub> Cl <sub>4</sub>
Trinidad Head (CA)	United States of America	THD	AGAGE	41.05 N	124.15 W	107	CH <sub>4</sub> , N <sub>2</sub> O, SF <sub>6</sub> , SO <sub>2</sub> F <sub>2</sub> , NF <sub>3</sub> , CCl <sub>4</sub> , CH <sub>3</sub> CCl <sub>3</sub> , CFCs, HCFCs, HFCs, PFCs, CBrClF <sub>2</sub> , CBrF <sub>3</sub> , C <sub>2</sub> Br <sub>2</sub> F <sub>4</sub> , CHCl <sub>3</sub> , CH <sub>3</sub> Cl, CH <sub>2</sub> Cl <sub>2</sub> , CH <sub>3</sub> Br, C <sub>2</sub> Cl <sub>4</sub>
Tudor Hill (Bermuda)	United Kingdom of Great Britain and Northern Ireland	BMW	NOAA	32.27 N	64.88 W	30	CO <sub>2</sub> , CH <sub>4</sub> , N <sub>2</sub> O, SF <sub>6</sub> , <sup>13</sup> CO <sub>2</sub> , C <sup>18</sup> O <sub>2</sub> , CO, H <sub>2</sub>

## LIST OF OBSERVATIONAL STATIONS (continued)

Station	Country/Territory	GAW ID	Organization	Latitude (°)	Longitude (°)	Location Altitude (m)	Parameter
Wendover (UT)	United States of America	UTA	NOAA	39.90 N	113.72 W	1320	CO <sub>2</sub> , CH <sub>4</sub> , N <sub>2</sub> O, SF <sub>6</sub> , <sup>13</sup> CO <sub>2</sub> , C <sup>18</sup> O <sub>2</sub> , CO, H <sub>2</sub>
West Branch (Iowa)	United States of America	WBI	NOAA	41.72 N	91.35 W	242	C <sup>18</sup> O <sub>2</sub>

### REGION V (South-West Pacific)

Baring Head	New Zealand	BHD	NOAA	41.41 S	174.87 E	85	CO <sub>2</sub> , CH <sub>4</sub> , N <sub>2</sub> O, SF <sub>6</sub> , <sup>13</sup> CH <sub>4</sub> , <sup>13</sup> CO <sub>2</sub> , C <sup>18</sup> O <sub>2</sub> , CO
Baring Head	New Zealand	BHD	NIWA	41.41 S	174.87 E	85	CO <sub>2</sub> , CH <sub>4</sub> , N <sub>2</sub> O, <sup>13</sup> CH <sub>4</sub> , CO, <sup>14</sup> CO <sub>2</sub>
Bukit Kototabang	Indonesia	BKT	NOAA	0.20 S	100.32 E	864	CO <sub>2</sub> , CH <sub>4</sub> , N <sub>2</sub> O, SF <sub>6</sub> , <sup>13</sup> CO <sub>2</sub> , C <sup>18</sup> O <sub>2</sub> , CO
Bukit Kototabang	Indonesia	BKT	BMKG	0.20 S	100.32 E	864	CO <sub>2</sub> , CH <sub>4</sub> , CO
Cape Ferguson	Australia	CFA	CSIRO	19.28 S	147.06 E	2	CO <sub>2</sub> , CH <sub>4</sub> , N <sub>2</sub> O, <sup>13</sup> CO <sub>2</sub> , CO, H <sub>2</sub>
Cape Grim	Australia	CGO	NOAA	40.68 S	144.69 E	94	CO <sub>2</sub> , CH <sub>4</sub> , N <sub>2</sub> O, SF <sub>6</sub> , <sup>13</sup> CH <sub>4</sub> , <sup>13</sup> CO <sub>2</sub> , C <sup>18</sup> O <sub>2</sub> , CCl <sub>4</sub> , CH <sub>3</sub> CCl <sub>3</sub> , CFCs, HCFCs, HFCs, CBrClF <sub>2</sub> , CBrF <sub>3</sub> , C <sub>2</sub> Br <sub>2</sub> F <sub>4</sub> , CO, CH <sub>3</sub> Cl, CH <sub>2</sub> Cl <sub>2</sub> , CH <sub>3</sub> Br, C <sub>2</sub> Cl <sub>4</sub> , H <sub>2</sub>
Cape Grim	Australia	CGO	AGAGE	40.68 S	144.69 E	94	CH <sub>4</sub> , N <sub>2</sub> O, SF <sub>6</sub> , SO <sub>2</sub> F <sub>2</sub> , NF <sub>3</sub> , CCl <sub>4</sub> , CH <sub>3</sub> CCl <sub>3</sub> , CFCs, HCFCs, HFCs, PFCs, CBrClF <sub>2</sub> , CBrF <sub>3</sub> , C <sub>2</sub> Br <sub>2</sub> F <sub>4</sub> , CO, CHCl <sub>3</sub> , CH <sub>3</sub> Cl, CH <sub>2</sub> Cl <sub>2</sub> , CH <sub>3</sub> Br, C <sub>2</sub> Cl <sub>4</sub> , H <sub>2</sub>
Cape Grim	Australia	CGO	ANSTO	40.68 S	144.69 E	94	<sup>222</sup> Rn
Cape Grim	Australia	CGO	CSIRO	40.68 S	144.69 E	94	CO <sub>2</sub> , CH <sub>4</sub> , N <sub>2</sub> O, <sup>13</sup> CO <sub>2</sub> , CO, H <sub>2</sub>
Cape Kumukahi (HI)	United States of America	KUM	NOAA	19.52 N	154.82 W	3	CO <sub>2</sub> , CH <sub>4</sub> , N <sub>2</sub> O, SF <sub>6</sub> , <sup>13</sup> CH <sub>4</sub> , <sup>13</sup> CO <sub>2</sub> , C <sup>18</sup> O <sub>2</sub> , CCl <sub>4</sub> , CH <sub>3</sub> CCl <sub>3</sub> , CFCs, HCFCs, HFCs, CBrClF <sub>2</sub> , CBrF <sub>3</sub> , C <sub>2</sub> Br <sub>2</sub> F <sub>4</sub> , CO, CH <sub>3</sub> Cl, CH <sub>2</sub> Cl <sub>2</sub> , CH <sub>3</sub> Br, C <sub>2</sub> Cl <sub>4</sub> , H <sub>2</sub>
Christmas Island	Kiribati	CHR	NOAA	1.70 N	157.17 W	3	CO <sub>2</sub> , CH <sub>4</sub> , N <sub>2</sub> O, SF <sub>6</sub> , <sup>13</sup> CO <sub>2</sub> , C <sup>18</sup> O <sub>2</sub> , CO, H <sub>2</sub>
Danum Valley	Malaysia	DMV	MMD	4.98 N	117.84 E	426	CO <sub>2</sub>
Guam (Mariana Island)	United States of America	GMI	NOAA	13.43 N	144.78 E	2	CO <sub>2</sub> , CH <sub>4</sub> , N <sub>2</sub> O, SF <sub>6</sub> , <sup>13</sup> CO <sub>2</sub> , C <sup>18</sup> O <sub>2</sub> , CO, H <sub>2</sub>
Gunn Point	Australia	GPA	CSIRO	12.25 S	131.05 E	25	CO <sub>2</sub> , CH <sub>4</sub> , N <sub>2</sub> O, <sup>13</sup> CO <sub>2</sub> , CO, H <sub>2</sub>
Kaitorete Spit	New Zealand	NZL	NOAA	43.83 S	172.63 E	3	CH <sub>4</sub>
Lauder	New Zealand	LAU	NIWA	45.04 S	169.68 E	370	CH <sub>4</sub> , CO

## LIST OF OBSERVATIONAL STATIONS (continued)

Station	Country/Territory	GAW ID	Organization	Latitude (°)	Longitude (°)	Location Altitude (m)	Parameter
Macquarie Island	Australia	MQA	CSIRO	54.50 S	158.94 E	6	CO <sub>2</sub> , CH <sub>4</sub> , N <sub>2</sub> O, <sup>13</sup> CO <sub>2</sub> , CO, H <sub>2</sub>
Mauna Loa (HI)	United States of America	MLO	NOAA	19.54 N	155.58 W	3397	CO <sub>2</sub> , CH <sub>4</sub> , N <sub>2</sub> O, SF <sub>6</sub> , <sup>13</sup> CH <sub>4</sub> , <sup>13</sup> CO <sub>2</sub> , C <sup>18</sup> O <sub>2</sub> , CCl <sub>4</sub> , CH <sub>3</sub> CCl <sub>3</sub> , CFCs, HCFCs, HFCs, CBrClF <sub>2</sub> , CBrF <sub>3</sub> , C <sub>2</sub> Br <sub>2</sub> F <sub>4</sub> , CO, CH <sub>3</sub> Cl, CH <sub>2</sub> Cl <sub>2</sub> , CH <sub>3</sub> Br, C <sub>2</sub> Cl <sub>4</sub> , H <sub>2</sub>
Mauna Loa (HI)	United States of America	MLO	CSIRO	19.54 N	155.58 W	3397	CO <sub>2</sub> , CH <sub>4</sub> , N <sub>2</sub> O, <sup>13</sup> CO <sub>2</sub> , CO, H <sub>2</sub>
Samoa (Cape Matatula)	United States of America	SMO	NOAA	14.25 S	170.56 W	77	CO <sub>2</sub> , CH <sub>4</sub> , N <sub>2</sub> O, SF <sub>6</sub> , <sup>13</sup> CH <sub>4</sub> , <sup>13</sup> CO <sub>2</sub> , C <sup>18</sup> O <sub>2</sub> , CCl <sub>4</sub> , CH <sub>3</sub> CCl <sub>3</sub> , CFCs, HCFCs, HFCs, CBrClF <sub>2</sub> , CBrF <sub>3</sub> , C <sub>2</sub> Br <sub>2</sub> F <sub>4</sub> , CO, CH <sub>3</sub> Cl, CH <sub>2</sub> Cl <sub>2</sub> , CH <sub>3</sub> Br, C <sub>2</sub> Cl <sub>4</sub> , H <sub>2</sub>
Samoa (Cape Matatula)	United States of America	SMO	AGAGE	14.25 S	170.56 W	77	CH <sub>4</sub> , N <sub>2</sub> O, SF <sub>6</sub> , SO <sub>2</sub> F <sub>2</sub> , NF <sub>3</sub> , CCl <sub>4</sub> , CH <sub>3</sub> CCl <sub>3</sub> , CFCs, HCFCs, HFCs, PFCs, CBrClF <sub>2</sub> , CBrF <sub>3</sub> , C <sub>2</sub> Br <sub>2</sub> F <sub>4</sub> , CHCl <sub>3</sub> , CH <sub>3</sub> Cl, CH <sub>2</sub> Cl <sub>2</sub> , CH <sub>3</sub> Br, C <sub>2</sub> Cl <sub>4</sub>
Sand Island	United States of America	MID	NOAA	28.22 N	177.37 W	4	CO <sub>2</sub> , CH <sub>4</sub> , N <sub>2</sub> O, SF <sub>6</sub> , <sup>13</sup> CO <sub>2</sub> , C <sup>18</sup> O <sub>2</sub> , CO, H <sub>2</sub>

### REGION VI (Europe)

Adrigole	Ireland	ADR	AGAGE	51.68 N	9.73 W	50	N <sub>2</sub> O, CCl <sub>4</sub> , CH <sub>3</sub> CCl <sub>3</sub> , CFCs
BEO Moussala Baltic Sea	Bulgaria Poland	BEO BAL	INRNE NOAA	42.18 N 55.50 N	23.59 E 16.67 E	2925 7	CO <sub>2</sub> , CO CO <sub>2</sub> , CH <sub>4</sub> , N <sub>2</sub> O, SF <sub>6</sub> , <sup>13</sup> CH <sub>4</sub> , <sup>13</sup> CO <sub>2</sub> , C <sup>18</sup> O <sub>2</sub> , CO, H <sub>2</sub>
Begur Brotjacklriegel Capo Granitola Constanta (Black Sea)	Spain Germany Italy Romania	BGU BRT CGR BSC	LSCE UBAG ISAC NOAA	41.97 N 48.82 N 37.57 N 44.17 N	3.23 E 13.22 E 12.66 E 28.68 E	13 1016 5 3	CO <sub>2</sub> , CH <sub>4</sub> CO <sub>2</sub> CO <sub>2</sub> , CH <sub>4</sub> , CO CO <sub>2</sub> , CH <sub>4</sub> , N <sub>2</sub> O, SF <sub>6</sub> , <sup>13</sup> CO <sub>2</sub> , C <sup>18</sup> O <sub>2</sub> , CO, H <sub>2</sub>
Deuselbach Diabla Gora / Puszczna Borecka Dwejra Point	Germany Poland  Malta	DEU DIG  GOZ	UBAG IOEP  NOAA	49.77 N 54.15 N  36.05 N	7.05 E 22.07 E  14.18 E	480 157  30	CO <sub>2</sub> , CH <sub>4</sub> CO <sub>2</sub>  CO <sub>2</sub> , CH <sub>4</sub> , <sup>13</sup> CO <sub>2</sub> , C <sup>18</sup> O <sub>2</sub> , CO, H <sub>2</sub>
Finokalia Fundata Gartow Giordan Lighthouse	Greece Romania Germany Malta	FKL FDT GAT GLH	LSCE INMH DWD UMLT	35.34 N 45.43 N 53.07 N 36.07 N	25.67 E 25.27 E 11.44 E 14.22 E	150 1384 69 167	CO <sub>2</sub> , CH <sub>4</sub> CO <sub>2</sub> CO <sub>2</sub> , CH <sub>4</sub> , N <sub>2</sub> O, CO CO <sub>2</sub> , CH <sub>4</sub> , CO, <sup>222</sup> Rn

## LIST OF OBSERVATIONAL STATIONS (continued)

Station	Country/Territory	GAW ID	Organization	Latitude (°)	Longitude (°)	Location Altitude (m)	Parameter
Heathfield	United Kingdom of Great Britain and Northern Ireland	HFD	NPL	50.98 N	0.23 E	160	CO <sub>2</sub> , CH <sub>4</sub> , N <sub>2</sub> O, SF <sub>6</sub> , CO
Hegyhatsal	Hungary	HUN	NOAA	46.95 N	16.65 E	248	CO <sub>2</sub> , CH <sub>4</sub> , N <sub>2</sub> O, SF <sub>6</sub> , <sup>13</sup> CO <sub>2</sub> , C <sup>18</sup> O <sub>2</sub> , CO, H <sub>2</sub>
Hegyhatsal	Hungary	HUN	HMS	46.95 N	16.65 E	248	CO <sub>2</sub>
Hohenpeissenberg	Germany	HPB	NOAA	47.80 N	11.01 E	985	CO <sub>2</sub> , CH <sub>4</sub> , N <sub>2</sub> O, SF <sub>6</sub> , <sup>13</sup> CO <sub>2</sub> , C <sup>18</sup> O <sub>2</sub> , CO
Hohenpeissenberg	Germany	HPB	DWD	47.80 N	11.01 E	985	CO <sub>2</sub> , CH <sub>4</sub> , N <sub>2</sub> O, CO, <sup>222</sup> Rn
Ile Grande Jungfraujoch	France Switzerland	LPO JFJ	LSCE AGAGE	48.80 N 46.55 N	3.58 W 7.99 E	20 3580	CO <sub>2</sub> , CH <sub>4</sub> SF <sub>6</sub> , SO <sub>2</sub> F <sub>2</sub> , NF <sub>3</sub> , CCl <sub>4</sub> , CH <sub>3</sub> CCl <sub>3</sub> , CFCs, HCFCs, HFCs, PFCs, CBrClF <sub>2</sub> , CBrF <sub>3</sub> , C <sub>2</sub> Br <sub>2</sub> F <sub>4</sub> , CHCl <sub>3</sub> , CH <sub>3</sub> Cl, CH <sub>2</sub> Cl <sub>2</sub> , CH <sub>3</sub> Br, C <sub>2</sub> HCl <sub>3</sub> , C <sub>2</sub> Cl <sub>4</sub>
Jungfraujoch	Switzerland	JFJ	Empa	46.55 N	7.99 E	3580	CO <sub>2</sub> , CH <sub>4</sub> , N <sub>2</sub> O, SF <sub>6</sub> , CO
Jungfraujoch	Switzerland	JFJ	KUP	46.55 N	7.99 E	3580	CO <sub>2</sub>
K-Puszta	Hungary	KPS	HMS	46.97 N	19.58 E	125	CO <sub>2</sub>
Karlsruhe	Germany	KIT	DWD	49.10 N	8.44 E	111	CO <sub>2</sub> , CH <sub>4</sub> , N <sub>2</sub> O, CO
Kloosterburen	Netherlands	KTB	RIVM	53.40 N	6.42 E	0	CO
Kollumerwaard	Netherlands	KMW	RIVM	53.33 N	6.27 E	0	CO <sub>2</sub> , CH <sub>4</sub> , CO
Kosetice Observatory	Czech Republic	KOS	CHMI	49.58 N	15.08 E	534	CH <sub>4</sub> , CO
Krvavec	Slovenia	KVV	ARSO	46.30 N	14.53 E	1740	CO
Lamezia Terme	Italy	LMT	ISAC	38.88 N	16.23 E	6	CO <sub>2</sub> , CH <sub>4</sub> , CO
Lampedusa	Italy	LMP	NOAA	35.52 N	12.63 E	45	CO <sub>2</sub> , CH <sub>4</sub> , N <sub>2</sub> O, SF <sub>6</sub> , <sup>13</sup> CO <sub>2</sub> , C <sup>18</sup> O <sub>2</sub> , CO
Lampedusa	Italy	LMP	ENEA	35.52 N	12.63 E	45	CO <sub>2</sub> , CH <sub>4</sub> , N <sub>2</sub> O, SF <sub>6</sub> , CCl <sub>4</sub> , CH <sub>3</sub> CCl <sub>3</sub> , CFCs, HCFCs, HFCs, CBrClF <sub>2</sub> , CBrF <sub>3</sub> , CHCl <sub>3</sub> , CH <sub>3</sub> Cl, CH <sub>2</sub> Cl <sub>2</sub> , CH <sub>3</sub> I, CH <sub>3</sub> Br, CH <sub>2</sub> Br <sub>2</sub>
Lecce Environmental-Climate Observatory	Italy	ECO	ISAC	40.34 N	18.12 E	36	CO <sub>2</sub> , CH <sub>4</sub> , CO
Lerwick	United Kingdom of Great Britain and Northern Ireland	SIS	CSIRO	60.13 N	1.18 W	84	CO <sub>2</sub> , CH <sub>4</sub> , N <sub>2</sub> O, <sup>13</sup> CO <sub>2</sub> , CO, H <sub>2</sub>
Lindenberg	Germany	LIN	DWD	52.22 N	14.12 E	112	CO <sub>2</sub> , CH <sub>4</sub> , N <sub>2</sub> O, CO
Mace Head	Ireland	MHD	NOAA	53.33 N	9.90 W	8.4	CO <sub>2</sub> , CH <sub>4</sub> , N <sub>2</sub> O, SF <sub>6</sub> , <sup>13</sup> CH <sub>4</sub> , <sup>13</sup> CO <sub>2</sub> , C <sup>18</sup> O <sub>2</sub> , CCl <sub>4</sub> , CH <sub>3</sub> CCl <sub>3</sub> , CFCs, HCFCs, HFCs, CBrClF <sub>2</sub> , CBrF <sub>3</sub> , C <sub>2</sub> Br <sub>2</sub> F <sub>4</sub> , CO, CH <sub>3</sub> Cl, CH <sub>2</sub> Cl <sub>2</sub> , CH <sub>3</sub> Br, C <sub>2</sub> Cl <sub>4</sub> , H <sub>2</sub>
Mace Head	Ireland	MHD	AGAGE	53.33 N	9.90 W	8.4	CH <sub>4</sub> , N <sub>2</sub> O, SF <sub>6</sub> , SO <sub>2</sub> F <sub>2</sub> , NF <sub>3</sub> , CCl <sub>4</sub> , CH <sub>3</sub> CCl <sub>3</sub> , CFCs, HCFCs, HFCs, PFCs, CBrClF <sub>2</sub> , CBrF <sub>3</sub> , C <sub>2</sub> Br <sub>2</sub> F <sub>4</sub> , CO, CHCl <sub>3</sub> ,

## LIST OF OBSERVATIONAL STATIONS (continued)

Station	Country/Territory	GAW ID	Organization	Latitude (°)	Longitude (°)	Altitude (m)	Location Parameter
Mace Head	Ireland	MHD	LSCE	53.33 N	9.90 W	8.4	CH <sub>3</sub> Cl, CH <sub>2</sub> Cl <sub>2</sub> , CH <sub>3</sub> Br, C <sub>2</sub> HCl <sub>3</sub> , C <sub>2</sub> Cl <sub>4</sub> , H <sub>2</sub>
Madonie - Piano Battaglia	Italy	MDN	ENEA	37.88 N	14.03 E	1650	CO <sub>2</sub> , CH <sub>4</sub>
Monte Cimone	Italy	CMN	AGAGE	44.19 N	10.70 E	2165	SO <sub>2</sub> F <sub>2</sub> , CCl <sub>4</sub> , CH <sub>3</sub> CCl <sub>3</sub> , CFCs, HCFCs, HFCs, PFCs, CBrClF <sub>2</sub> , CBrF <sub>3</sub> , CHCl <sub>3</sub> , CH <sub>3</sub> Cl, CH <sub>2</sub> Cl <sub>2</sub> , CH <sub>3</sub> Br, C <sub>2</sub> Cl <sub>4</sub>
Monte Cimone	Italy	CMN	IAFMS	44.19 N	10.70 E	2165	CO <sub>2</sub> , CH <sub>4</sub>
Monte Cimone	Italy	CMN	ISAC	44.19 N	10.70 E	2165	CO, H <sub>2</sub>
Monte Cimone	Italy	CMN	UNIURB	44.19 N	10.70 E	2165	CH <sub>4</sub> , N <sub>2</sub> O, SF <sub>6</sub> , CO
Monte Curcio	Italy	CUR	IIA	39.32 N	16.42 E	1796	CO <sub>2</sub> , CH <sub>4</sub> , CO
Neuglobsow	Germany	NGL	UBAG	53.14 N	13.03 E	62	CO <sub>2</sub> , CH <sub>4</sub> , CO
Ny Ålesund	Norway	NYA	TU	78.92 N	11.92 E	0	CH <sub>4</sub> , <sup>13</sup> CH <sub>4</sub> , CH <sub>3</sub> D
Ocean Station Charlie	United States of America	STC	NOAA	54.00 N	35.00 W	0	CO <sub>2</sub>
Ocean Station Charlie	United States of America	STC	MGO	54.00 N	35.00 W	0	CO <sub>2</sub>
Ocean Station M	Norway	STM	NOAA	66.00 N	2.00 E	4	CO <sub>2</sub> , CH <sub>4</sub> , N <sub>2</sub> O, SF <sub>6</sub> , <sup>13</sup> CO <sub>2</sub> , C <sup>18</sup> O <sub>2</sub> , CO, H <sub>2</sub>
Ochsenkopf	Germany	OXK	NOAA	50.03 N	11.81 E	1185	CO <sub>2</sub> , CH <sub>4</sub> , N <sub>2</sub> O, SF <sub>6</sub> , <sup>13</sup> CO <sub>2</sub> , C <sup>18</sup> O <sub>2</sub> , CO
Pallas	Finland	PAL	NOAA	67.97 N	24.12 E	560	CO <sub>2</sub> , CH <sub>4</sub> , N <sub>2</sub> O, SF <sub>6</sub> , <sup>13</sup> CO <sub>2</sub> , C <sup>18</sup> O <sub>2</sub> , CO
Pallas	Finland	PAL	FMI	67.97 N	24.12 E	560	CO <sub>2</sub> , CH <sub>4</sub>
Payerne	Switzerland	PAY	Empa	46.81 N	6.94 E	490	CO
Pic du Midi	France	PDM	LA	42.94 N	0.14 E	2877	CO
Pic du Midi	France	PDM	LSCE	42.94 N	0.14 E	2877	CO <sub>2</sub> , CH <sub>4</sub>
Plateau Rosa	Italy	PRS	RSE	45.94 N	7.71 E	3480	CO <sub>2</sub> , CH <sub>4</sub>
Puy de Dôme	France	PUY	LAMP	45.77 N	2.97 E	1465	CO
Puy de Dôme	France	PUY	LSCE	45.77 N	2.97 E	1465	CO <sub>2</sub> , CH <sub>4</sub>
Ridge Hill	United Kingdom of Great Britain and Northern Ireland	RGL	UNIVBRIS	52.00 N	2.54 W	204	CO <sub>2</sub> , CH <sub>4</sub> , N <sub>2</sub> O, SF <sub>6</sub>
Rigi SONNBLICK Observatory	Switzerland Austria	RIG SNB	Empa UBAA	47.07 N 47.05 N	8.46 E 12.96 E	1031 3106	CO CO <sub>2</sub> , CH <sub>4</sub> , CO
Schauinsland	Germany	SSL	UBAG	47.90 N	7.92 E	1205	CO <sub>2</sub> , CH <sub>4</sub> , N <sub>2</sub> O, SF <sub>6</sub> , CO
Sede Boker	Israel	WIS	NOAA	31.13 N	34.88 E	400	CO <sub>2</sub> , CH <sub>4</sub> , N <sub>2</sub> O, SF <sub>6</sub> , <sup>13</sup> CO <sub>2</sub> , C <sup>18</sup> O <sub>2</sub> , CO, H <sub>2</sub>
Serreta (Terceira)	Portugal	AZR	NOAA	38.77 N	27.38 W	40	CO <sub>2</sub> , CH <sub>4</sub> , N <sub>2</sub> O, SF <sub>6</sub> , <sup>13</sup> CH <sub>4</sub> , <sup>13</sup> CO <sub>2</sub> , C <sup>18</sup> O <sub>2</sub> , CO, H <sub>2</sub>
Storhofdi	Iceland	ICE	NOAA	63.40 N	20.28 W	118	CO <sub>2</sub> , CH <sub>4</sub> , N <sub>2</sub> O, SF <sub>6</sub> , <sup>13</sup> CO <sub>2</sub> , C <sup>18</sup> O <sub>2</sub> , CO, H <sub>2</sub>
Summit	Denmark	SUM	NOAA	72.58 N	38.48 W	3238	CO <sub>2</sub> , CH <sub>4</sub> , N <sub>2</sub> O, SF <sub>6</sub> , <sup>13</sup> CH <sub>4</sub> , <sup>13</sup> CO <sub>2</sub> , C <sup>18</sup> O <sub>2</sub> , CCl <sub>4</sub> , CH <sub>3</sub> CCl <sub>3</sub> , CFCs, HCFCs, HFCs, CBrClF <sub>2</sub> , CBrF <sub>3</sub> , C <sub>2</sub> Br <sub>2</sub> F <sub>4</sub> , CO,

## LIST OF OBSERVATIONAL STATIONS (continued)

Station	Country/Territory	GAW ID	Organization	Location			Parameter
				Latitude (°)	Longitude (°)	Altitude (m)	
Summit	Denmark	SUM	INSTAAR	72.58 N	38.48 W	3238	CH <sub>3</sub> Cl, CH <sub>2</sub> Cl <sub>2</sub> , CH <sub>3</sub> Br, CH <sub>4</sub>
Tacolneston Tall Tower	United Kingdom of Great Britain and Northern Ireland	TAC	NOAA	52.52 N	1.14 E	56	CO <sub>2</sub> , CH <sub>4</sub> , N <sub>2</sub> O, SF <sub>6</sub> , CO
Tacolneston Tall Tower	United Kingdom of Great Britain and Northern Ireland	TAC	UNIVBRIS	52.52 N	1.14 E	56	CO <sub>2</sub> , CH <sub>4</sub> , N <sub>2</sub> O, SF <sub>6</sub> , SO <sub>2</sub> F <sub>2</sub> , CH <sub>3</sub> CCl <sub>3</sub> , CFCs, HCFCs, HFCs, PFCs, CBrClF <sub>2</sub> , CBrF <sub>3</sub> , CO, CHCl <sub>3</sub> , CH <sub>3</sub> Cl, CH <sub>2</sub> Cl <sub>2</sub> , CH <sub>3</sub> Br, C <sub>2</sub> HCl <sub>3</sub> , C <sub>2</sub> Cl <sub>4</sub> , H <sub>2</sub>
Teriberka	Russian Federation	TER	MGO	69.20 N	35.10 E	40	CO <sub>2</sub> , CH <sub>4</sub>
Torfhaus	Germany	TOH	DWD	51.81 N	10.53 E	801	CO <sub>2</sub> , CH <sub>4</sub> , N <sub>2</sub> O, CO
Waldhof-Langenbrügge	Germany	WAL	UBAG	52.80 N	10.76 E	74	CO <sub>2</sub>
Wank	Germany	WNK	IMKIFU	47.51 N	11.14 E	1780	CO <sub>2</sub>
Westerland	Germany	WES	UBAG	54.92 N	8.31 E	12	CO <sub>2</sub>
Zeppelin Mountain (Ny Ålesund)	Norway	ZEP	NOAA	78.91 N	11.89 E	475	CO <sub>2</sub> , CH <sub>4</sub> , N <sub>2</sub> O, SF <sub>6</sub> , <sup>13</sup> CH <sub>4</sub> , <sup>13</sup> CO <sub>2</sub> , C <sup>18</sup> O <sub>2</sub> , CO, H <sub>2</sub>
Zeppelin Mountain (Ny Ålesund)	Norway	ZEP	AGAGE	78.91 N	11.89 E	475	SF <sub>6</sub> , SO <sub>2</sub> F <sub>2</sub> , NF <sub>3</sub> , CH <sub>3</sub> CCl <sub>3</sub> , CFCs, HCFCs, HFCs, PFCs, CBrClF <sub>2</sub> , CBrF <sub>3</sub> , C <sub>2</sub> Br <sub>2</sub> F <sub>4</sub> , CHCl <sub>3</sub> , CH <sub>3</sub> Cl, CH <sub>2</sub> Cl <sub>2</sub> , CH <sub>3</sub> Br, C <sub>2</sub> Cl <sub>4</sub>
Zeppelin Mountain (Ny Ålesund)	Norway	ZEP	ITM	78.91 N	11.89 E	475	CO <sub>2</sub>
Zeppelin Mountain (Ny Ålesund)	Norway	ZEP	NILU	78.91 N	11.89 E	475	CO <sub>2</sub> , N <sub>2</sub> O, CFCs
Zingst	Germany	ZGT	UBAG	54.44 N	12.72 E	1	CO <sub>2</sub> , CH <sub>4</sub>
Zugspitze-Gipfel	Germany	ZUG	IMKIFU	47.42 N	10.99 E	2962	CO <sub>2</sub>
Zugspitze-Gipfel	Germany	ZUG	UBAG	47.42 N	10.99 E	2962	CO <sub>2</sub> , CH <sub>4</sub> , CO
Zugspitze-Schneefernerhaus	Germany	ZSF	DWD	47.42 N	10.98 E	2671	<sup>222</sup> Rn, <sup>7</sup> Be
Zugspitze-Schneefernerhaus	Germany	ZSF	UBAG	47.42 N	10.98 E	2671	CO <sub>2</sub> , CH <sub>4</sub> , N <sub>2</sub> O, SF <sub>6</sub> , CO

## LIST OF OBSERVATIONAL STATIONS (continued)

Station	Country/Territory	GAW ID	Organization	Latitude (°)	Longitude (°)	Altitude (m)	Parameter
<b>ANTARCTICA</b>							
Arrival Heights	New Zealand	ARH	NIWA	77.83 S	166.66 E	184	CH <sub>4</sub> , N <sub>2</sub> O, <sup>13</sup> CH <sub>4</sub> , CO
Casey	Australia	CYA	CSIRO	66.28 S	110.52 E	51	CO <sub>2</sub> , CH <sub>4</sub> , N <sub>2</sub> O, <sup>13</sup> CO <sub>2</sub> , CO, H <sub>2</sub>
Halley	United Kingdom of Great Britain and Northern Ireland	HBA	NOAA	75.57 S	25.50 W	30	CO <sub>2</sub> , CH <sub>4</sub> , N <sub>2</sub> O, SF <sub>6</sub> , <sup>13</sup> CO <sub>2</sub> , C <sup>18</sup> O <sub>2</sub> , CO, H <sub>2</sub>
Halley	United Kingdom of Great Britain and Northern Ireland	HBA	BAS	75.57 S	25.50 W	30	CO
Jubany	Argentina	JBN	IAA	62.24 S	58.67 W	15	CO <sub>2</sub>
King Sejong	Republic of Korea	KSG	KMA	62.22 S	58.78 W	0	CO <sub>2</sub>
Mawson	Australia	MAA	CSIRO	67.60 S	62.87 E	20	CO <sub>2</sub> , CH <sub>4</sub> , N <sub>2</sub> O, <sup>13</sup> CO <sub>2</sub> , CO, H <sub>2</sub>
McMurdo	United States of America	MCM	NOAA	77.85 S	166.67 E	11	CH <sub>4</sub>
Palmer Station	United States of America	PSA	NOAA	64.77 S	64.05 W	10	CO <sub>2</sub> , CH <sub>4</sub> , N <sub>2</sub> O, SF <sub>6</sub> , <sup>13</sup> CO <sub>2</sub> , C <sup>18</sup> O <sub>2</sub> , CCl <sub>4</sub> , CH <sub>3</sub> CCl <sub>3</sub> , CFCs, HCFCs, HFCs, CBrClF <sub>2</sub> , CBrF <sub>3</sub> , C <sub>2</sub> Br <sub>2</sub> F <sub>4</sub> , CO, CH <sub>3</sub> Cl, CH <sub>2</sub> Cl <sub>2</sub> , CH <sub>3</sub> Br, H <sub>2</sub>
South Pole	United States of America	SPO	NOAA	90.00 S	24.80 W	2841	CO <sub>2</sub> , CH <sub>4</sub> , N <sub>2</sub> O, SF <sub>6</sub> , <sup>13</sup> CH <sub>4</sub> , <sup>13</sup> CO <sub>2</sub> , C <sup>18</sup> O <sub>2</sub> , CCl <sub>4</sub> , CH <sub>3</sub> CCl <sub>3</sub> , CFCs, HCFCs, HFCs, CBrClF <sub>2</sub> , CBrF <sub>3</sub> , C <sub>2</sub> Br <sub>2</sub> F <sub>4</sub> , CO, CH <sub>3</sub> Cl, CH <sub>2</sub> Cl <sub>2</sub> , CH <sub>3</sub> Br, C <sub>2</sub> Cl <sub>4</sub> , H <sub>2</sub>
South Pole	United States of America	SPO	CSIRO	90.00 S	24.80 W	2841	CO <sub>2</sub> , CH <sub>4</sub> , N <sub>2</sub> O, <sup>13</sup> CO <sub>2</sub> , CO, H <sub>2</sub>
Syowa	Japan	SYO	NOAA	69.01 S	39.58 E	29.1	CO <sub>2</sub> , CH <sub>4</sub> , N <sub>2</sub> O, SF <sub>6</sub> , <sup>13</sup> CO <sub>2</sub> , C <sup>18</sup> O <sub>2</sub> , CO, H <sub>2</sub>
Syowa	Japan	SYO	TU	69.01 S	39.58 E	29.1	CO <sub>2</sub> , CH <sub>4</sub> , <sup>13</sup> CH <sub>4</sub> , CH <sub>3</sub> D
<b>MOBILE</b>							
Aircraft (Western North Pacific)	Japan	AOA	JMA				CO <sub>2</sub> , CH <sub>4</sub> , N <sub>2</sub> O, CO
Aircraft (off the coast of Sendai Plain)	Japan	PIP	TU				CH <sub>4</sub>
Aircraft (over Bass Strait and Cape Grim)	Australia	AIA	CSIRO				CO <sub>2</sub> , CH <sub>4</sub> , N <sub>2</sub> O, <sup>13</sup> CO <sub>2</sub> , CO, H <sub>2</sub>
Aircraft (over Japan and surroundings)	Japan	OAS	MRI				CH <sub>4</sub> , N <sub>2</sub> O, SF <sub>6</sub> , CFCs
Aircraft: Orleans Alligator liberty, M/V	France	ORL	LSCE				CO <sub>2</sub> , CH <sub>4</sub>
Atlantic Ocean	Japan	ALL	JMA				CO <sub>2</sub>
	United States of America	AOC	NOAA				CO <sub>2</sub> , CH <sub>4</sub>

## LIST OF OBSERVATIONAL STATIONS (continued)

Station	Country/Territory	GAW ID	Organization	Latitude (°)	Longitude (°)	Altitude (m)	Parameter
CONTRAIL	Japan	EOM	NIES				CO <sub>2</sub> , CH <sub>4</sub>
CONTRAIL	Japan	EOM	TU				<sup>13</sup> CH <sub>4</sub> , CH <sub>3</sub> D
Drake Passage	United States of America	DRP	NOAA				CO <sub>2</sub> , CH <sub>4</sub> , N <sub>2</sub> O, SF <sub>6</sub> , <sup>13</sup> CO <sub>2</sub> , C <sup>18</sup> O <sub>2</sub> , CO
INSTAC	Japan	INS	MRI				CO <sub>2</sub> , CH <sub>4</sub> , <sup>13</sup> CO <sub>2</sub>
Keifu Maru, R/V	Japan	KEF	JMA				CO <sub>2</sub> , CFCs, TIC
Kofu Maru, R/V	Japan	KOF	JMA				CO <sub>2</sub>
MRI Research, Hakuho Maru, R/V	Japan	HKH	MRI				CO <sub>2</sub> , CH <sub>4</sub>
MRI Research, Kaiyo Maru, R/V	Japan	KIY	MRI				CO <sub>2</sub> , CO
MRI Research, Natushima, R/V	Japan	NTU	MRI				CO <sub>2</sub> , CH <sub>4</sub>
MRI Research, Ryofu Maru, R/V	Japan	RFM	MRI				CO <sub>2</sub> , CH <sub>4</sub>
MRI Research, Ship observations	Japan	MRI	MRI				CH <sub>4</sub>
MRI Research, Wellington Maru, R/V	Japan	WLT	MRI				CO <sub>2</sub>
Mirai, R/V	Japan	MMR	MRI				CO <sub>2</sub>
Mirai, R/V	Japan	MMR	JAMSTEC				CO <sub>2</sub>
NOPACCS - Hakurei Maru - Northern and western Pacific	Japan	HAK	NEDO				TIC
Pacific Ocean	United States of America	NWP	TU				CH <sub>4</sub> , N <sub>2</sub> O, <sup>13</sup> CH <sub>4</sub> , CH <sub>3</sub> D
Pacific Ocean	New Zealand	POC	NOAA				CO <sub>2</sub> , CH <sub>4</sub> , N <sub>2</sub> O, SF <sub>6</sub> , <sup>13</sup> CO <sub>2</sub> , C <sup>18</sup> O <sub>2</sub> , CO, H <sub>2</sub>
Pacific-Atlantic Ocean	United States of America	BSL	NIWA				CH <sub>4</sub> , <sup>13</sup> CH <sub>4</sub>
Ryofu Maru, R/V	Japan	PAO	NOAA				CO <sub>2</sub> , CH <sub>4</sub> , N <sub>2</sub> O, SF <sub>6</sub> , CO
Santarem	Brazil	RYF	JMA				CO <sub>2</sub> , CH <sub>4</sub> , N <sub>2</sub> O, CFCs, TIC
Ship between Ishigaki Island and Hateruma Island	Japan	SAN	INPE				CO <sub>2</sub> , CH <sub>4</sub> , N <sub>2</sub> O, SF <sub>6</sub> , CO
South China Sea	Japan	SIH	TU				CO <sub>2</sub>
Soyo Maru, R/V	United States of America	SCS	NIWA				CO <sub>2</sub> , CH <sub>4</sub> , <sup>13</sup> CO <sub>2</sub> , C <sup>18</sup> O <sub>2</sub> , CO, H <sub>2</sub>
WEST COSMIC - Hakurei Maru No.2 - Wakataka-Maru	Japan	SOY	FRA				CO <sub>2</sub>
Western Pacific	Japan	HRM	NEDO				SF <sub>6</sub> , CFCs, TIC
over Japan between Sendai and Fukuoka	United States of America	WAK	FRA				CO <sub>2</sub>
	Japan	WPC	NOAA				CO <sub>2</sub> , CH <sub>4</sub> , N <sub>2</sub> O, SF <sub>6</sub> , <sup>13</sup> CH <sub>4</sub> , <sup>13</sup> CO <sub>2</sub> , C <sup>18</sup> O <sub>2</sub> , CO
	Japan	TDA	TU				CH <sub>4</sub>

## APPENDIX D LIST OF CONTRIBUTORS

Station Country/Territory	Name	Address
<b>REGION I (Africa)</b>		
Mt. Kenya (Kenya)	Martin Steinbacher	Swiss Federal Laboratories for Materials Science and Technology Ueberlandstrasse 129 CH-8600 Duebendorf Switzerland
	Jörg Klausen	Federal Office of Meteorology and Climatology MeteoSwiss 8058 ZH,Zürich-Flughafen Operation Center 1, Switzerland
	Christoph Zellweger	Swiss Federal Laboratories for Materials Science and Technology Ueberlandstrasse 129 CH-8600 Duebendorf
	Mathew Mutuku	Kenyan Meteorological Department Dagoretti Corner P.O. Box 30259 00100 Nairobi
	David Murithi Njiru	Kenya Meteorological Department MT KENYA GAW STATION P.O. Box 192 10400 NANYUKI Kenya
Izaña (Tenerife) (Spain)	Emilio Cuevas	State Meteorological Agency of Spain C/ La Marina, 20, Planta 6, 38001 Santa Cruz de Tenerife, Spain
	Pedro Rivas	State Meteorological Agency of Spain C/ La Marina, 20, Planta 6, 38001 Santa Cruz de Tenerife, Spain
Cape Point (South Africa)	Alastair Williams	ANSTO, Locked Bag 2001 Kirrawee DC, NSW 2232 Australia
	Scott Chambers	ANSTO, Locked Bag 2001 Kirrawee DC, NSW 2232 Australia
Assekrem (Algeria)	Sidi Baika	Office National de la Meteorologie POBox 31 Tamanrasset 11000, Algeria
Cairo Farafra (Egypt)	AbdElhamid Gouda Elawadi	Department of Air Pollution Study Egyptian Meteorological Authority P.O.Box:11784 Cairo, Egypt
	Zeinab Salah	Egyptian Meteorological Authority Al-Khalifa El-Maamoun St. Kobry Al-Qubba Cairo, Egypt P.O.Box: 11784
Amsterdam Island (France)	Michel Ramonet	LSCE - CEA Saclay - Orme des Merisiers - 91191 Gif-sur-Yvette, France

## LIST OF CONTRIBUTORS (continued)

Station Country/Territory	Name	Address
	Jean Sciare	LSCE - CEA Saclay - Orme des Merisiers - Bat.701 91191 Gif-sur-Yvette, France
Cape Point (South Africa)	Thumeka Mkololo	SAWS, c/o CSIR (Environmentek), P.O. Box 320, Stellenbosch 7599, South Africa
	Casper Labuschagne	SA Weather Service c/o CSIR (Environmentek) P.O. Box 320, Stellenbosch 7599, South Africa
	Lynwill Martin	SAWS, c/o CSIR (Environmentek), P.O. Box 320, Stellenbosch 7599, South Africa
	Warren Joubert	SAWS c/o CSIR (Environmentek) P.O. Box 320, Stellenbosch 7599, South Africa
Cape Verde Atmospheric Observatory (Cabo Verde)	E Kozlova	University of Exeter Hatherly Labs Prince Of Wales Road Exeter, EX4 4PS
Cape Verde Atmospheric Observatory (Cabo Verde)	Katie Read	Department of Chemistry University of York, Heslington York YO10 5DD United Kingdom
	Lucy Carpenter	Department of Chemistry University of York, Heslington York YO10 5DD United Kingdom

### REGION II (Asia)

Hamamatsu (Japan)	Mitsuo Toda	Shizuoka University 3-5-1 Jyohoku, Hamamatsu 432-8561, Japan
Cholpon-Ata (Kyrgyzstan)	Gulzhan Esenzhanova	Agency on Hydrometeorology under Ministry of Emergency Situations of the Kyrgyz Republic 1 Kerimbekov Bishkek
Cape Ochiishi Hateruma Island (Japan)	Yasunori TOHJIMA	National Institute for Environmental Studies Center for Global Environmental Research 16-2, Onogawa, Tsukuba-shi, Ibaraki 305-8506, Japan
	Hitoshi MUKAI	National Institute for Environmental Studies Center for Global Environmental Research 16-2, Onogawa, Tsukuba-shi, Ibaraki 305-8506, Japan
	Takuya Saito	National Institute for Environmental Studies 16-2 Onogawa, Tsukuba 305-8506, Japan

## LIST OF CONTRIBUTORS (continued)

Station Country/Territory	Name	Address
Memanbetsu Tateno (Tsukuba) (Japan)	Kazuhiro Tsuboi	Meteorological Research Institute 1-1, Nagamine Tsukuba Ibaraki 305-0052
Minamitorishima Ryori Yonagunijima (Japan)	SAITO Kazuyuki	Japan Meteorological Agency Atmosphere and Ocean Department Atmospheric Environment and Ocean Division 3-6-9 Toranomon, Minato City, Tokyo 105-8431
Bering Island Kotelnyj Island Tiksi (Russian Federation)	Nina Paramonova	Voeikov Main Geophysical Observatory St. Petersburg, Karbyshev Street 7, Russian Federation, 194021
Kyzylcha (Uzbekistan)		
Mt. Waliguan (China)	ZHANG Yong	China Meteorological Administration 46 Zhongguancun S. Ave., Haidian Dist., Beijing, 100081, China
Kisai Mt. Dodaira Urawa (Japan)	Yosuke MUTO	Center for Environmental Science in Saitama 914 Kamitanadare,Kazo,Saitama,Japan
Gosan (Republic of Korea)	Haeyoung Lee	National Institute of Meteorological Sciences/Korea Meteorological Administration 33 Seohobuk-ro, Seogwipo, Jeju, 63568 Rep.of Korea
Tiksi (Russian Federation)	Park Hyo-Jin	Climate Change Monitoring Division, Korea Meteorological Administration 61 Yeouidaebang-ro 16 gil, Dongjak-gu, Seoul, 07062, Republic of Korea
Ed Dlugokencky		NOAA GML 325 Broadway R/GML-1 Boulder, CO 80305-3328
Viktor Ivakhov		Voeikov Main Geophysical Observatory St. Petersburg, Karbyshev Street 7, Russian Federation, 194021
Tuomas Laurila		Finnish Meteorological Institute P.O. BOX 503 FI-00101 HELSINKI FINLAND
Takayama (Japan)	Shohei Murayama	AIST Tsukuba West, 16-1 Onogawa, Tsukuba, Ibaraki 305-8569, Japan

## LIST OF CONTRIBUTORS (continued)

Station Country/Territory	Name	Address
Nepal Climate Observatory - Pyramid (Nepal)	Igor Arduini	University of Urbino, Dep. of Pure and Applied Sciences (DISPEA) piazza Rinascimento 6, 61029 Urbino - Italy
Hok Tsui / Cape d Aguilar King's Park (Hong Kong, China)	David H.Y. Lam	Hong Kong Observatory 134A Nathan Road, Kowloon, Hong Kong.
	W.H. Leung	Hong Kong Observatory 134A Nathan Road, Kowloon, Hong Kong.
Anmyeon-do Jeju Gosan (Republic of Korea)	Haeyoung Lee	National Institute of Meteorological Sciences/Korea Meteorological Administration 33 Seohobuk-ro, Seogwipo, Jeju, 63568 Rep.of Korea
	Sumin Kim	National Institute of Meteorological Sciences 33, Seohobuk-ro, Seoqwipo. Jeju, 63568, Rep. of KOREA
Hok Tsui / Cape d Aguilar (Hong Kong, China)	Ka Se Lam	The Hong Kong Polytechnic University Hung Hom, Kowloon, Hong Kong, China
Pha Din (Viet Nam)	Martin Steinbacher	Swiss Federal Laboratories for Materials Science and Technology Ueberlandstrasse 129 CH-8600 Duebendorf Switzerland
	Nguyen Nhat Anh	Viet Nam Meteorological and Hydrological Administration No. 8 Phao Dai Lang street 100000 Ha Noi Viet Nam
Issyk-Kul (Kyrgyzstan)	V. Sinyakov	Kyrgyz National University Manas Street 101, Bishkek, 720033, Kyrgyz Republic
Gosan (Republic of Korea)	Jiyoung Kim	National Institute of Environmental Research Environmental Research Complex Hwangyeong-ro 42, Seo-gu, Incheon, 22689
	Eunjung Kim	National Institute of Environmental Research Environmental Research Complex Hwangyeong-ro 42, Seo-gu, Incheon, 22689
Suita (Japan)	Tomohiro Oda	Universities Space Research Association Global Modeling and Assimilation Office NASA Goddard Space Flight Center 8800 Greenbelt Road, Greenbelt, Maryland 20771
	Takashi Machimura	Osaka University Green Engineering Lab Division of Sustainable Energy and Environmental Engineering 2-1 Yamadaoka, Suita, Osaka 565-0871 Japan

## LIST OF CONTRIBUTORS (continued)

Station Country/Territory	Name	Address
Nagoya (Japan)	A. Matsunami	Research Center for Advanced Energy Conversion, Nagoya University Furo-cho, Chikusaku, Nagoya 464-8603, Japan
Mikawa-Ichinomiya (Japan)	Koji Ohno	Aichi Air Environment Division 1-2 Sannomaru-3chome, Naka-ku, Nagoya, Aichi 460-8501, Japan

### REGION III (South America)

El Tololo (Chile)	Martin Steinbacher	Swiss Federal Laboratories for Materials Science and Technology Ueberlandstrasse 129 CH-8600 Duebendorf Switzerland
	Gaston Torres	Dirección Meteorológica de Chile Av. Portales 3450, Estación Central - Santiago
Huancayo (Peru)	Mutsumi Ishitsuka	Observatorio de Huancayo, Instituto Geofisico del Peru Apartado 46, Huancayo, Peru
Arembepe (Brazil)	Luciana Vanni Gatti	Laboratory of Greenhouse Gases - LaGEE National Institute of Space Research - INPE Avenida dos Astronautas, 1758 - São José dos Campos - SP
Ushuaia (Argentina)	Maria Elena Barlasina	National Weather Service Dorrego 4019, (C1425GBE) Ciudad Autónoma de Buenos Aires, Argentina.
	Lino Condori	National Weather Service Station GAW Ushuaia - International Airport "Malvinas Argentinas" – Ushuaia Tierra del Fuego – Argentina
	Gerardo Carbajal Benítez	National Weather Service Dorrego 4019, (C1425GBE) Ciudad Autónoma de Buenos Aires, Argentina.

### REGION IV (North and Central America)

Churchill (Canada)	Shinji Morimoto	Tohoku University Aoba 6-3, Aramaki, Aoba-ku, Sendai 980-8578
Alert Churchill East Trout Lake Estevan Point Fraserdale Sable Island (Canada)	Lin Huang	Environment and Climate Change Canada Climate Research Division 4905 Dufferin Street, Toronto, Ontario CANADA M3H 5T4
	Doug Worthy	Environment and Climate Change Canada Climate Research Division 4905 Dufferin Street, Toronto, Ontario CANADA M3H 5T4

## LIST OF CONTRIBUTORS (continued)

Station Country/Territory	Name	Address
Candle Lake Chibougamau Egbert Lac La Biche (Alberta) (Canada)	Doug Worthy	Environment and Climate Change Canada Climate Research Division 4905 Dufferin Street, Toronto, Ontario CANADA M3H 5T4
<b>REGION V (South-West Pacific)</b>		
Cape Grim (Australia)	Alastair Williams	ANSTO, Locked Bag 2001 Kirrawee DC, NSW 2232 Australia
	Scott Chambers	ANSTO, Locked Bag 2001 Kirrawee DC, NSW 2232 Australia
Macquarie Island (Australia)	Paul Krummel	CSIRO Oceans and Atmosphere - Climate Science Centre 107-121 Station Street Aspendale Victoria, 3195 Australia
	Zoë Loh	CSIRO Oceans and Atmosphere - Climate Science Centre 107-121 Station Street Aspendale Victoria, 3195 Australia
	Ann Stavert	CSIRO Oceans and Atmosphere - Climate Science Centre 107-121 Station Street Aspendale Victoria, 3195 Australia
Cape Grim (Australia)	Paul Krummel	CSIRO Oceans and Atmosphere - Climate Science Centre 107-121 Station Street Aspendale Victoria, 3195 Australia
	Ray Langenfelds	CSIRO Oceans and Atmosphere - Climate Science Centre 107-121 Station Street Aspendale Victoria, 3195 Australia
	Zoë Loh	CSIRO Oceans and Atmosphere - Climate Science Centre 107-121 Station Street Aspendale Victoria, 3195 Australia
Lauder (New Zealand)	Sylvia Nichol	NIWA - Wellington Private Bag 14901, Kilbirnie, Wellington, 6241 301 Evans Bay Parade, Hataitai, Wellington 6021
	Gordon Brailsford	NIWA - Wellington Private Bag 14901, Kilbirnie, Wellington, 6241 301 Evans Bay Parade, Hataitai, Wellington 6021
Baring Head (New Zealand)	Jocelyn Turnbull	GNS Science
	Sylvia Nichol	NIWA - Wellington Private Bag 14901, Kilbirnie, Wellington, 6241 301 Evans Bay Parade, Hataitai, Wellington 6021

## LIST OF CONTRIBUTORS (continued)

Station Country/Territory	Name	Address
	Gordon Brailsford	NIWA - Wellington Private Bag 14901, Kilbirnie, Wellington, 6241 301 Evans Bay Parade, Hataitai, Wellington 6021
Danum Valley (Malaysia)	Ahmad Fairudz Jamaluddin	Malaysian Meteorological Department Jalan Sultan, 46667, Petaling Jaya, Selangor MALAYSIA
	Mohan Kumar Sammathuria	Malaysian Meteorological Department Jalan Sultan, 46667, Petaling Jaya, Selangor MALAYSIA
Bukit Kototabang (Indonesia)	Martin Steinbacher	Swiss Federal Laboratories for Materials Science and Technology Ueberlandstrasse 129 CH-8600 Duebendorf Switzerland
	Okaem, Tanti Tritama	Agency for Meteorology, Climatology and Geophysics Jl. Raya Bukittinggi-Medan Km. 17 Palupuh, District Agam, West Sumatera, Indonesia PO BOX 11 Bukittinggi 26100
	Nahas, Alberth Christian	Agency for Meteorology, Climatology and Geophysics Jl. Raya Bukittinggi-Medan Km. 17 Palupuh, District Agam, West Sumatera, Indonesia PO BOX 11 Bukittinggi 26100
	Reza Mahdi	Agency for Meteorology, Climatology and Geophysics Stasiun Pemantau Atmosfer Global Bukit Kototabang Jl Raya Bukittinggi-Medan Km 17 Palupuh 26100, Bukittinggi
	Arifin, Ikhsan Buyung	Agency for Meteorology, Climatology and Geophysics Stasiun Pemantau Atmosfer Global Bukit Kototabang Jl Raya Bukittinggi-Medan Km 17 Palupuh 26100, Bukittinggi

### REGION VI (Europe)

Diabla Gora / Puszcza Borecka (Poland)	Zdzislaw Przadka	Institute of Environmental Protection - NRI Kolektorska 4, 01-692 Warsaw, Poland
	Anna Degorska	Institute of Environmental Protection - NRI Kolektorska 4 01-692 Warsaw, Poland
	Krzysztof Skotak	Institute of Environmental Protection - NRI Kolektorska 4, 01-692 Warsaw, Poland
Monte Curcio (Italy)	Mariantonio Bencardino	CNR-Institute of Atmospheric Pollution Research c/o UNICAL-Polifunzionale 87036 Rende, Italy
BEO Moussala (Bulgaria)	Ivo Kalapov	Institute for Nuclear Research and Nuclear Energy Tsarigradsko shose Blvd. 1784 Sofia Bulgaria

## LIST OF CONTRIBUTORS (continued)

Station Country/Territory	Name	Address
Kloosterburen Kollumerwaard (Netherlands)	Ronald Spoor	National Institute of Public Health and the Environment PO Box 1 3720 BA Bilthoven the Netherlands
Ny Ålesund (Norway)	Taku Umezawa	National Institute for Environmental Studies 16-2 Onogawa, Tsukuba 305-8506, Japan
	Shinji Morimoto	Tohoku University Aoba 6-3, Aramaki, Aoba-ku, Sendai 980-8578
	Ryo Fujita	Oceanography and Geochemistry Research Department Meteorological Research Institute 1-1 Nagamine, Tsukuba, 305-0052, Japan
Brotjacklriegel Deuselbach Neuglobsow Waldhof-Langenbrügge Zingst (Germany)	Ludwig Ries	German Environment Agency Umweltbundesamt, Umweltforschungsstation Schneefernerhaus, Zugspitze 5, 82475 Zugspitze
Westerland Zugspitze-Schneefernerhaus (Germany)	Cedric Couret	German Environment Agency Umweltbundesamt, Umweltforschungsstation Schneefernerhaus, Zugspitze 5, 82475 Zugspitze
Schauinsland (Germany)	Frank Meinhardt	German Environment Agency Umweltbundesamt Messstation Schauinsland Schauinslandweg 2 79254 Oberried-Hofsgrund
Zugspitze-Gipfel (Germany)	Ludwig Ries	German Environment Agency Umweltbundesamt, Umweltforschungsstation Schneefernerhaus, Zugspitze 5, 82475 Zugspitze
	Cedric Couret	German Environment Agency Umweltbundesamt, Umweltforschungsstation Schneefernerhaus, Zugspitze 5, 82475 Zugspitze
Jungfraujoch (Switzerland)	Markus Leuenberger	University of Bern Physics Institute, Climate and Environmental Physics Sidlerstrasse 5, CH-3012 Bern
Tacolneston Tall Tower (United Kingdom of Great Britain and Northern Ireland)	Simon O'Doherty	Atmospheric Chemistry Research Group School of Chemistry University of Bristol Cantocks Close BS8 1TS Bristol United Kingdom
	Kieran Stanley	Atmospheric Chemistry Research Group School of Chemistry University of Bristol Cantocks Close BS8 1TS Bristol United Kingdom
	Daniel Say	Atmospheric Chemistry Research Group School of Chemistry University of Bristol Cantocks Close BS8 1TS Bristol United Kingdom

## LIST OF CONTRIBUTORS (continued)

Station Country/Territory	Name	Address
Ridge Hill (United Kingdom of Great Britain and Northern Ireland)	Simon O'Doherty	Atmospheric Chemistry Research Group School of Chemistry University of Bristol Cantocks Close BS8 1TS Bristol United Kingdom
	Daniel Say	Atmospheric Chemistry Research Group School of Chemistry University of Bristol Cantocks Close BS8 1TS Bristol United Kingdom
Heathfield (United Kingdom of Great Britain and Northern Ireland)	Caroline Dylag	National Physical Laboratory Hampton Road Teddington TW11 OLW
SONNBLICK Observatory (Austria)	Wolfgang Spangl	Federal Environment Agency Austria Spittelauer Lände 5 A-1090 Wien
	Iris Buxbaum	Federal Environment Agency Austria Spittelauer Lände 5 A-1090 Wien
	Andreas Wolf	Federal Environment Agency Austria Spittelauer Lände 5 A-1090 Wien
Ocean Station Charlie (United States of America)	Nina Paramonova	Voeikov Main Geophysical Observatory St. Petersburg, Karbyshev Street 7, Russian Federation, 194021
Teriberka (Russian Federation)	Nina Paramonova	Voeikov Main Geophysical Observatory St. Petersburg, Karbyshev Street 7, Russian Federation, 194021
	Viktor Ivakhov	Voeikov Main Geophysical Observatory St. Petersburg, Karbyshev Street 7, Russian Federation, 194021
Jungfraujoch (Switzerland)	Martin Steinbacher	Swiss Federal Laboratories for Materials Science and Technology Ueberlandstrasse 129 CH-8600 Dübendorf Switzerland
	Thomas Seitz	Swiss Federal Laboratories for Materials Science and Technology Überlandstrasse 129 CH-8600 Dübendorf Switzerland
Payerne Rigi (Switzerland)	Thomas Seitz	Swiss Federal Laboratories for Materials Science and Technology Überlandstrasse 129 CH-8600 Dübendorf Switzerland

## LIST OF CONTRIBUTORS (continued)

Station Country/Territory	Name	Address
Puy de Dôme (France)	Meyerfeld Yves	Laboratoire d'Aérologie 14 avenue Edouard Belin 31400 - TOULOUSE
	Pichon Jean-Marc	Laboratoire de Météorologie Physique LaMP 4 av. Blaise Pascal TSA 60026 CS 60026 63178 Aubière
Monte Cimone (Italy)	Stefano Amendola	Italian Air Force Mountain Centre Via Delle Ville, 40, 41029 Sestola (MO)
Pallas (Finland)	Juha Hatakka	Finnish Meteorological Institute Erik Palmenin aukio 1 FI-00560 Helsinki, Finland
Monte Cimone (Italy)	Igor Arduini	University of Urbino, Dep. of Pure and Applied Sciences (DISPEA) piazza Rinascimento 6, 61029 Urbino - Italy
Hegyhatsal K-Puszta (Hungary)	Laszlo Haszpra	Institute for Nuclear Research Bem tér 18/C H-4026 Debrecen, Hungary
Plateau Rosa (Italy)	Daniela Heltai	Ricerca sul Sistema Energetico - RSE S.p.A. via Rubattino 54, 20134 Milano, Italy
	Francesco Apadula	Ricerca sul Sistema Energetico - RSE S.p.A. via Rubattino 54, 20134 Milano, Italy
	Andrea Lanza	Ricerca sul Sistema Energetico - RSE S.p.A. via Rubattino 54, 20134 Milano, Italy
Giordan Lighthouse (Malta)	Martin Saliba	University of Malta Department of Geosciences Tal-Qroqq Msida, MSD 2080
	Marvic Grima	University of Malta Department of Geosciences Tal-Qroqq Msida, MSD 2080
	Raymond Ellul	University of Malta Department of Geosciences Tal-Qroqq Msida, MSD 2080
Kosetice Observatory (Czech Republic)	Adéla Holubová	Czech Hydrometeorological Institute Na sabatce 2050/17, 143 06 Praha 412-Komorany
Fundata (Romania)	Florin Nicodim	National Meteorological Administration Sos. Bucuresti-Ploiesti nr. 97, 71552 Bucharest, Romania

## LIST OF CONTRIBUTORS (continued)

Station Country/Territory	Name	Address
Zeppelin Mountain (Ny Ålesund) (Norway)	Hans-Christen  Birgitta Noone	Department of Applied Environmental Science (ITM) Stockholm University SE-10691 Stockholm  Department of Applied Environmental Science (ITM) Stockholm University SE-10691 Stockholm
Krvavec (Slovenia)	Marijana Murovec  Janja Turšič	Ministrstvo za okolje in prostor / Ministry of Environment and Spatial Planning Agencija RS za okolje / Slovenian Environment Agency Urad za stanje okolja / State of environment Office Sektor za kakovost zraka / Air Quality Division Vojkova 1b, 1001 Ljubljana, p.p  Ministrstvo za okolje in prostor / Ministry of Environment and Spatial Planning Agencija RS za okolje / Slovenian Environment Agency Urad za stanje okolja / State of environment Office Sektor za kakovost zraka / Air Quality Division Vojkova 1b, 1001 Ljubljana, p.p
	Mateja Gjerek	Ministrstvo za okolje in prostor / Ministry of Environment and Spatial Planning Agencija RS za okolje / Slovenian Environment Agency Urad za stanje okolja / State of environment Office Sektor za kakovost zraka / Air Quality Division Vojkova 1b, 1001 Ljubljana, p.p
Summit (Denmark)	Jacques Hueber  Detlev Helmig	INSTAAR, Univ. of Colorado 1560, 30th Street UCB 450 Boulder, CO 80309 U.S.A.  INSTAAR, Univ. of Colorado 1560, 30th Street UCB 450 Boulder, CO 80309 U.S.A.
Lampedusa (Italy)	Salvatore Chiavarini  Damiano Sferlazzo  Alcide di Sarra	ENEA-UTPRA Via Anguillarese, 301 00123 Rome, Italy  Italian National Agency for New Technologies, Energy and Sustainable Economic Development Laboratory for Observations and Measurements for Environment and Climate Station for Climate Observations Contrada Capo Grecale 92010 Lampedusa Italy  Italian National Agency for New Technologies, Energy and Sustainable Economic Development Laboratory for Observations and Measurements for Environment and Climate Via Anguillarese, 301 00123 Rome, Italy
	Salvatore Piacentino	Italian National Agency for New Technologies, Energy and Sustainable Economic Development Laboratory for Observations and Measurements for Environment and Climate Via Principe di Granatelli 24, 90139 Palermo, Italy

## LIST OF CONTRIBUTORS (continued)

Station Country/Territory	Name	Address
	Tatiana Di Iorio	Italian National Agency for New Technologies, Energy and Sustainable Economic Development Laboratory for Observations and Measurements for Environment and Climate Via Anguillarese 301, 00123 Rome, Italy
	Francesco Monteleone	Italian National Agency for New Technologies, Energy and Sustainable Economic Development Laboratory for Observations and Measurements for Environment and Climate Via Principe di Granatelli 24, 90139 Palermo, Italy
Madonie - Piano Battaglia (Italy)	Damiano Sferlazzo	Italian National Agency for New Technologies, Energy and Sustainable Economic Development Laboratory for Observations and Measurements for Environment and Climate Station for Climate Observations Contrada Capo Grecale 92010 Lampedusa Italy
	Alcide di Sarra	Italian National Agency for New Technologies, Energy and Sustainable Economic Development Laboratory for Observations and Measurements for Environment and Climate Via Anguillarese, 301 00123 Rome, Italy
	Salvatore Piacentino	Italian National Agency for New Technologies, Energy and Sustainable Economic Development Laboratory for Observations and Measurements for Environment and Climate Via Principe di Granatelli 24, 90139 Palermo, Italy
	Tatiana Di Iorio	Italian National Agency for New Technologies, Energy and Sustainable Economic Development Laboratory for Observations and Measurements for Environment and Climate Via Anguillarese 301, 00123 Rome, Italy
	Francesco Monteleone	Italian National Agency for New Technologies, Energy and Sustainable Economic Development Laboratory for Observations and Measurements for Environment and Climate Via Principe di Granatelli 24, 90139 Palermo, Italy
	Fabrizio Anello	Italian National Agency for New Technologies, Energy and Sustainable Economic Development Laboratory for Observations and Measurements for Environment and Climate Via Principe di Granatelli 24, 90139 Palermo, Italy
Lamezia Terme (Italy)	Daniel Gullì	National Research Council, Institute of Atmospheric Sciences and Climate Area Industriale Comp. 15, 88046 Lamezia Terme
	Claudia Calidonna	National Research Council, Institute of Atmospheric Sciences and Climate Area Industriale Comp. 15, 88046 Lamezia Terme

## LIST OF CONTRIBUTORS (continued)

Station Country/Territory	Name	Address
	Ivano Ammoscato	National Research Council, Institute of Atmospheric Sciences and Climate Area Industriale Comp. 15, 88046 Lamezia Terme
Lecce Environmental-Climate Observatory (Italy)	Adelaide Dinoi	National Research Council, Institute of Atmospheric Sciences and Climate Str. Prv. Lecce-Monteroni km 1.2 73100 Lecce
Capo Granitola (Italy)	Paolo Cristofanelli	ISAC-CNR, Vla Gobetti 101 - 40129 Bologna, Italy
	Ignazio Fontana	Istituto per lo studio degli impatti Antropici e Sostenibilità in ambiente marino via del Mare n. 3 - 91021 Torretta Granitola (TP) - Italy
	Giorgio Tranchida	Istituto per lo studio degli impatti Antropici e Sostenibilità in ambiente marino via del Mare n. 3 - 91021 Torretta Granitola (TP) - Italy
	Giovanni Giacalone	Istituto per lo studio degli impatti Antropici e Sostenibilità in ambiente marino via del Mare n. 3 - 91021 Torretta Granitola (TP) - Italy
Monte Cimone (Italy)	Jgor Arduini	University of Urbino, Dep. of Pure and Applied Sciences (DISPEA) piazza Rinascimento 6, 61029 Urbino - Italy
	Michela Maione	University of Urbino, Dep. of Pure and Applied Sciences (DISPEA) Istituto di Scienze Chimiche piazza Rinascimento 6, 61029 Urbino - Italy
	Paolo Cristofanelli	ISAC-CNR, Vla Gobetti 101 - 40129 Bologna, Italy
Finokalia (Greece)	Michel Ramonet	LSCE - CEA Saclay - Orme des Merisiers - 91191 Gif-sur-Yvette, France
Mace Head (Ireland)		
Begur (Spain)		
Ille Grande Pic du Midi Puy de Dôme (France)		
Pic du Midi (France)	Meyerfeld Yves	Laboratoire d'Aérologie 14 avenue Edouard Belin 31400 - TOULOUSE
	Gheusi Francois	Laboratoire d'Aérologie 14 avenue Edouard Belin 31400 Toulouse

## LIST OF CONTRIBUTORS (continued)

Station Country/Territory	Name	Address
Zugspitze-Schneefernerhaus (Germany)	Gabriele Frank	Deutscher Wetterdienst, German Meteorological Service Frankfurter Str. 135 63067 Offenbach Germany
Hohenpeissenberg (Germany)	Dagmar Kubistin	German Meteorological Service Albin-Schwaiger-Weg 10 D-82383 Hohenpeissenberg Germany
	Robert Holla	German Meteorological Service Albin-Schwaiger-Weg 10 D-82383 Hohenpeissenberg Germany
	Matthias Lindauer	German Meteorological Service Albin-Schwaiger-Weg 10 82383 Hohenpeissenberg
	Christian Plass-Dulmer	German Meteorological Service Albin-Schwaiger-Weg 10 D-82383 Hohenpeissenberg Germany
	Jennifer Müller-Williams	German Meteorological Service Albin-Schwaiger-Weg 10 D-82383 Hohenpeissenberg Germany
Gartow Karlsruhe Lindenberg Torfhaus (Germany)	Dagmar Kubistin	German Meteorological Service Albin-Schwaiger-Weg 10 D-82383 Hohenpeissenberg Germany
	Matthias Lindauer	German Meteorological Service Albin-Schwaiger-Weg 10 82383 Hohenpeissenberg
	Christian Plass-Dulmer	German Meteorological Service Albin-Schwaiger-Weg 10 D-82383 Hohenpeissenberg Germany
	Jennifer Müller-Williams	German Meteorological Service Albin-Schwaiger-Weg 10 D-82383 Hohenpeissenberg Germany
Wank Zugspitze-Gipfel (Germany)	Thomas Trickl	Fraunhofer-Institute for Atmospheric Environmental Research Kreuzeckbahnstr. 19 82467 Garmisch-Partenkirchen
Zeppelin Mountain (Ny Ålesund) (Norway)	Ove Hermansen	Norwegian Institute for Air Research P. O. Box 100 Instituttveien 18, N-2027 Kjeller, Norway
	Cathrine Lund Myrhe	Norwegian Institute for Air Research PO Box 100, 2027 Kjeller, NORWAY
	Martin Album Ytre-Eide	Norwegian Institute for Air Research PO Box 100, 2027 Kjeller, NORWAY
<b>ANTARCTICA</b>		
Syowa (Japan)	Shuji Aoki	Tohoku University Aoba 6-3, Aramaki, Aoba-ku, Sendai 980-8578

## LIST OF CONTRIBUTORS (continued)

Station Country/Territory	Name	Address
	Taku Umezawa	National Institute for Environmental Studies 16-2 Onogawa, Tsukuba 305-8506, Japan
	Shinji Morimoto	Tohoku University Aoba 6-3, Aramaki, Aoba-ku, Sendai 980-8578
	Daisuke Goto	National Institute of Polar Research 10-3 Midori-cho, Tachikawa, Tokyo 190-8518
	Ryo Fujita	Oceanography and Geochemistry Research Department Meteorological Research Institute 1-1 Nagamine, Tsukuba, 305-0052, Japan
Jubany (Argentina)	Horacio Rodriguez	Direccion Nacional del Antartico- Istituto Antartico Argentino, Buenos Aires, Argentina Dto. Ciencias de la Atmósfera Instituto Antártico Argentino DIRECCION NACIONAL DEL ANTARTICO Cerrito 1248 (1010) Capital Federal ARGENTINA
	Angelo Viola	National Research Council, Institute of Atmospheric Sciences and Climate via fosso del Cavaliere 100, Italy
King Sejong (Republic of Korea)	Haeyoung Lee	National Institute of Meteorological Sciences/Korea Meteorological Administration 33 Seohobuk-ro, Seogwipo, Jeju, 63568 Rep.of Korea
	Taejin Choi	Division of Polar Climate Research, KOPRI Get-Pearl Tower, 12 Gaetbeol-ro, Yeonsu-gu, Incheon, 406-840, Republic of Korea
Arrival Heights (New Zealand)	Sylvia Nichol	NIWA - Wellington Private Bag 14901, Kilbirnie, Wellington, 6241 301 Evans Bay Parade, Hataitai, Wellington 6021
	Gordon Brailsford	NIWA - Wellington Private Bag 14901, Kilbirnie, Wellington, 6241 301 Evans Bay Parade, Hataitai, Wellington 6021
Halley (United Kingdom of Great Britain and Northern Ireland)	Freya Squires	British Antarctic Survey High Cross, Madingley Road Cambridge, CB3 0ET
<b>MOBILE</b>		
CONTRAIL (Japan)	Hidekazu Matsueda	Meteorological Research Institute Nagamine 1-1, Tsukuba, Ibaraki 305-0052, Japan
	Toshinobu Machida	National Institute for Environmental Studies 16-2 Onogawa, Tsukuba 305-8506, Japan
	Yosuke Niwa	National Institute for Environmental Studies 16-2 Onogawa, Tsukuba 305-8506, Japan

## LIST OF CONTRIBUTORS (continued)

Station Country/Territory	Name	Address
Northern and western Pacific (Japan)	Shuji Aoki	Tohoku University Aoba 6-3, Aramaki, Aoba-ku, Sendai 980-8578
	Taku Umezawa	National Institute for Environmental Studies 16-2 Onogawa, Tsukuba 305-8506, Japan
	Kentaro ISHIJIMA	Meteorological Research Institute Department of Climate and Geochemistry Research 1-1 Nagamine, Tsukuba, Ibaraki 305-0052
	Shinji Morimoto	Tohoku University Aoba 6-3, Aramaki, Aoba-ku, Sendai 980-8578
	Ryo Fujita	Oceanography and Geochemistry Research Department Meteorological Research Institute 1-1 Nagamine, Tsukuba, 305-0052, Japan
Aircraft (off the coast of Sendai Plain) over Japan between Sendai and Fukuoka (Japan)	Shuji Aoki	Tohoku University Aoba 6-3, Aramaki, Aoba-ku, Sendai 980-8578
	Taku Umezawa	National Institute for Environmental Studies 16-2 Onogawa, Tsukuba 305-8506, Japan
	Shinji Morimoto	Tohoku University Aoba 6-3, Aramaki, Aoba-ku, Sendai 980-8578
Ship between Ishigaki Island and Hateruma Island (Japan)	Shuji Aoki	Tohoku University Aoba 6-3, Aramaki, Aoba-ku, Sendai 980-8578
	Shinji Morimoto	Tohoku University Aoba 6-3, Aramaki, Aoba-ku, Sendai 980-8578
CONTRAIL (Japan)	Shuji Aoki	Tohoku University Aoba 6-3, Aramaki, Aoba-ku, Sendai 980-8578
	Taku Umezawa	National Institute for Environmental Studies 16-2 Onogawa, Tsukuba 305-8506, Japan
Soyo Maru, R/V Wakataka-Maru (Japan)	Tsuneo Ono	Fisheries Research Agency Hokkaido National Fisheries Research Institute 116 Katsurakoi, Kushiro 085-0802, Japan
Mirai, R/V (Japan)	Akihiko Murata	Physical and Chemical Oceanography Research Group, Global Ocean Observation Research Center, Research Institute for Global Change (RIGC) Japan Agency for Marine-Earth Science and Technology (JAMSTEC), 2-15, Natsushima, Yokosuka, Kanagawa, Japan 237-0061
Mirai, R/V (Japan)	Hisayuki Yoshikawa-Inoue	Hokkaido University Laboratory of Marine and Atmospheric Geochemistry Graduate School of Environmental Earth

## LIST OF CONTRIBUTORS (continued)

Station Country/Territory	Name	Address
		Science N10W5, Kita-ku, Sapporo 060-0810, Japan
MRI Research, Wellington Maru, R/V (Japan)	Masao Ishii	Meteorological Research Institute Nagamine 1-1, Tsukuba, Ibaraki 305-0052, Japan
Aircraft (over Japan and surroundings) (Japan)	Kazuhiro Tsuboi	Meteorological Research Institute 1-1, Nagamine Tsukuba Ibaraki 305-0052
INSTAC MRI Research, Hakuho Maru, R/V MRI Research, Kaiyo Maru, R/V MRI Research, Natushima, R/V MRI Research, Ryofu Maru, R/V MRI Research, Ship observations (Japan)	Hidekazu Matsueda  Masao Ishii  Kazuhiro Tsuboi	Meteorological Research Institute Nagamine 1-1, Tsukuba, Ibaraki 305-0052, Japan  Meteorological Research Institute Nagamine 1-1, Tsukuba, Ibaraki 305-0052, Japan  Meteorological Research Institute 1-1, Nagamine Tsukuba Ibaraki 305-0052
Alligator liberty, M/V Keifu Maru, R/V Kofu Maru, R/V Ryofu Maru, R/V (Japan)	ENYO Kazutaka  KADONO Koji	Japan Meteorological Agency Atmosphere and Ocean Department Atmospheric Environment and Ocean Division 3-6-9 Toranomon, Minato City, Tokyo 105-8431  Japan Meteorological Agency Atmosphere and Ocean Department Atmospheric Environment and Ocean Division 3-6-9 Toranomon, Minato City, Tokyo 105-8431
Aircraft (Western North Pacific) (Japan)	SAITO Kazuyuki	Japan Meteorological Agency Atmosphere and Ocean Department Atmospheric Environment and Ocean Division 3-6-9 Toranomon, Minato City, Tokyo 105-8431
NOPACCS - Hakurei Maru - WEST COSMIC - Hakurei Maru No.2 - (Japan)	General Environmental Technos	The General Environmental Technos Co., Ltd. (Old:Kansai Environmental Engineering Center, Co., Ltd.) 1-3-5, Azuchi machi, Chuo-ku, Osaka 541-0052, Japan
Santarem (Brazil)	Luciana Vanni Gatti	Laboratory of Greenhouse Gases - LaGEE National Institute of Space Research - INPE Avenida dos Astronautas, 1758 - São José dos Campos - SP
Pacific Ocean (New Zealand)	Sylvia Nichol	NIWA - Wellington Private Bag 14901, Kilbirnie, Wellington, 6241 301 Evans Bay Parade, Hataitai, Wellington 6021

## **LIST OF CONTRIBUTORS (continued)**

Station Country/Territory	Name	Address
	Gordon Brailsford	NIWA - Wellington Private Bag 14901, Kilbirnie, Wellington, 6241 301 Evans Bay Parade, Hataitai, Wellington 6021
Aircraft: Orleans (France)	Michel Ramonet	LSCE - CEA Saclay - Orme des Merisiers - 91191 Gif-sur-Yvette, France

## LIST OF CONTRIBUTORS (continued)

Station Country/Territory	Name	Address
<b>NOAA /ESRL Flask Network</b>		
Ushuaia (Argentina)	Pieter Tans*	(*) R/GML1
Cape Grim (Australia)	Kirk Thoning* (CO <sub>2</sub> )	NOAA/ESRL 325 Broadway Boulder, CO 80305-3328
Ragged Point (Barbados)	Xin Lan* (CO <sub>2</sub> and CH <sub>4</sub> )	(**) Institute of Arctic and Alpine Research University of Colorado Campus Box 450 Boulder, CO 80309-0450 USA
Arembepe Natal (Brazil)	Ed Dlugokencky* (CO <sub>2</sub> , CH <sub>4</sub> , N <sub>2</sub> O and SF <sub>6</sub> )	
Alert Lac La Biche (Alberta) Mould Bay (Canada)	Colm Sweeney* (CO <sub>2</sub> , CH <sub>4</sub> , N <sub>2</sub> O, SF <sub>6</sub> and CO)	
Easter Island (Chile)	Sylvia Michel** James White** Bruce H Vaughn**	
Mt. Waliguan Shangdianzi (China)	Gabrielle Petron* (CO and H <sub>2</sub> )	
Hohenpeissenberg Ochsenkopf (Germany)	Scott Lehman** Jocelyn Turnbull ( <sup>14</sup> CO <sub>2</sub> )	
Summit (Denmark)		
Assekrem (Algeria)		
Izaña (Tenerife) (Spain)		
Pallas (Finland)		
Amsterdam Island Crozet (France)		
Ascension Island Bird Island (South Georgia) Halley St. David's Head Taconeston Tall Tower Tudor Hill (Bermuda) (United Kingdom of Great Britain and Northern Ireland)		
Hegyhatsal (Hungary)		

## LIST OF CONTRIBUTORS (continued)

Station Country/Territory	Name	Address
Bukit Kototabang (Indonesia)		
Mace Head (Ireland)		
Sede Boker (Israel)		
Storhofdi (Iceland)		
Lampedusa (Italy)		
Syowa (Japan)		
Mt. Kenya (Kenya)		
Christmas Island (Kiribati)		
Anmyeon-do Tae-ahn Peninsula (Republic of Korea)		
Plateau Assy Sary Taukum (Kazakhstan)		
Ulaan Uul (Mongolia)		
Dwejra Point (Malta)		
Kaashidhoo (Male Atoll) (Maldives)		
Mex High Altitude Global Climate Observation Center (Mexico)		
Gobabeb (Namibia)		
Ocean Station M Zeppelin Mountain (Ny Ålesund) (Norway)		
Baring Head Kaitorete Spit (New Zealand)		
Baltic Sea (Poland)		
Serreta (Terceira) (Portugal)		

## LIST OF CONTRIBUTORS (continued)

Station Country/Territory	Name	Address
Constanta (Black Sea) (Romania)		
Tiksi (Russian Federation)		
Mahé (Seychelles)		
Lulin (Taiwan, Province of China)		
Argyle (ME) Atlantic Ocean Barrow (AK) Cape Kumukahi (HI) Cape Meares (OR) Cold Bay (AK) Drake Passage Grifton - Georgia Station (NC) Guam (Mariana Island) Key Biscane (FL) Kitt Peak (AZ) La Jolla (CA) Mauna Loa (HI) McMurdo Moody (TX) Niwot Ridge - T-van (CO) Ocean Station Charlie Olympic Peninsula (WA) Pacific Ocean Pacific-Atlantic Ocean Palmer Station Park Falls (WI) Point Arena (CA) Samoa (Cape Matatula) Sand Island Shemya Island South China Sea South Pole Southern Great Plains E13 (OK) St. Croix Trinidad Head (CA) Wendover (UT) West Branch (Iowa) Western Pacific (United States of America)		
Cape Point (South Africa)		

### NOAA /ESRL HATS Network

Ushuaia (Argentina)	Debra J. Mondeel J. David Nance Stephen A. Montzka Bradley D. Hall Geoffrey S. Dutton	Halocarbons and Other Atmosphere Trace Species Group (HATS)/R/GML1 NOAA/ESRL 325 Broadway Boulder, CO 80305-3328
Cape Grim (Australia)		

## **LIST OF CONTRIBUTORS (continued)**

Station Country/Territory	Name	Address
Alert (Canada)		
Summit (Denmark)		
Mace Head (Ireland)		
Anmyeon-do (Republic of Korea)		
Barrow (AK) Cape Kumukahi (HI) Grifton - Georgia Station (NC) Harvard Forest (MA) Mauna Loa (HI) Niwot Ridge - T-van (CO) Palmer Station Park Falls (WI) Samoa (Cape Matatula) South Pole Trinidad Head (CA) (United States of America)		

## LIST OF CONTRIBUTORS (continued)

Station Country/Territory	Name	Address
<b>CSIRO Flask Network</b>		
Aircraft (over Bass Strait and Cape Grim)	Ann Stavert	Commonwealth Scientific and Industrial Research Organisation (CSIRO)
Cape Ferguson	Zoë Loh	CSIRO Oceans and Atmosphere - Climate Science Centre
Cape Grim	Ray Langenfelds	Private Bag 1, Aspendale, Vic, Australia 3195
Casey	Paul Krummel	
Gunn Point		
Macquarie Island		
Mawson		
(Australia)		
Alert		
Estevan Point		
(Canada)		
Lerwick		
(United Kingdom of Great Britain and Northern Ireland)		
Cape Rama		
(India)		
Mauna Loa (HI)		
South Pole		
(United States of America)		
<b>ALE/GAGE/AGAGE Network</b>		
Cape Grim (Australia)	Ray Wang Simon O'Doherty	Advanced Global Atmospheric Gases Experiment Massachusetts Institute of Technology, Center for Global Change Science
Ragged Point (Barbados)	Dickon Young Paul Krummel	Building 54-1312 Cambridge, MA 02139-2307
Jungfraujoch (Switzerland)	Ray F. Weiss Stefan Reimann Martin Vollmer Chris Lunder Michela Maione	
Adrigole Mace Head (Ireland)	Jgor Arduini	
Monte Cimone (Italy)		
Gosan (Republic of Korea)		
Zeppelin Mountain (Ny Ålesund) (Norway)		
Cape Meares (OR) Samoa (Cape Matatula) Trinidad Head (CA) (United States of America)		

## APPENDIX E LIST OF ABBREVIATIONS

### ORGANIZATIONS:

<b>AEMET</b>	State Meteorological Agency of Spain (Spain)
<b>AGAGE</b>	Advanced Global Atmospheric Gases Experiment Science Team
<b>AICH</b>	Aichi Air Environment Division (Japan)
<b>AIST</b>	National Institute of Advanced Industrial Science and Technology (Japan)
<b>AMERIFLUX</b>	AmeriFlux Network (USA)
<b>ANSTO</b>	Australian Nuclear Science and Technology Organisation (Australia)
<b>ARSO</b>	Slovenian Environment Agency (Slovenia)
<b>BAS</b>	British Antarctic Survey (United Kingdom)
<b>BLG</b>	Bowling Lab Group, Terrestrial Biogeochemistry, Department of Biology, University of Utah (USA)
<b>BMKG</b>	Agency for Meteorology, Climatology and Geophysics (Indonesia)
<b>CALTECH</b>	California Institute of Technology, Division of Geological and Planetary Science (USA)
<b>CHMI</b>	Czech Hydrometeorological Institute (Czech Republic)
<b>CMA</b>	China Meteorological Administration (China)
<b>CSIRO</b>	Commonwealth Scientific and Industrial Research Organisation (Australia)
<b>DMC</b>	Dirección Meteorológica de Chile (Chile)
<b>DWD</b>	German Meteorological Service (Germany)
<b>ECCC</b>	Environment and Climate Change Canada (Canada)
<b>ECN</b>	Energy Research Centre of the Netherlands (Netherlands)
<b>EMA</b>	Egyptian Meteorological Authority (Egypt)
<b>Empa</b>	Swiss Federal Laboratories for Materials Science and Technology (Switzerland)
<b>ENEA</b>	Italian National Agency for New Technologies, Energy and Sustainable Economic Development (Italy)
<b>FMI</b>	Finnish Meteorological Institute (Finland)
<b>FRA</b>	Fisheries Research Agency (Japan)
<b>GAGE</b>	Global Atmospheric Gases Experiment
<b>GAW</b>	Global Atmosphere Watch (WMO)
<b>GERC</b>	National Institute of Environmental Research (Republic of Korea)
<b>HATS</b>	Halocarbons and other Atmospheric Trace Species Group, NOAA/ESRL (USA)
<b>JKO</b>	Hong Kong Observatory (Hong Kong, China)
<b>HMS</b>	Hungarian Meteorological Service (Hungary)
<b>HU</b>	Hokkaido University (Japan)
<b>IAA</b>	Dirección Nacional del Antártico - Instituto Antartico Argentino, Buenos Aires, Argentina (Argentina)
<b>IAFMS</b>	Italian Air Force Mountain Centre (Italy)
<b>ICOS</b>	Integrated Carbon Observation System (European Union)
<b>IGP</b>	Instituto Geofísico del Perú (Peru)
<b>IIA</b>	CNR - Institute of Atmospheric Pollution Research (Italy)
<b>IMKIFU</b>	Fraunhofer - Institute for Atmospheric Environmental Research (Germany)
<b>INMH</b>	National Meteorological Administration (Romania)
<b>INPE</b>	National Institute in Space Research (Brazil)
<b>INRNE</b>	Institute for Nuclear Research and Nuclear Energy (Bulgaria)
<b>INSTAAR</b>	Institute of Arctic and Alpine Research, University of Colorado (USA)
<b>IOEP</b>	Institute of Environmental Protection - NRI (Poland)

<b>ISAC</b>	National Research Council, Institute of Atmospheric Sciences and Climate (Italy)
<b>ITM</b>	Department of Applied Environmental Science, Stockholm University (Sweden)
<b>JAMSTEC</b>	Japan Agency for Marine - Earth Science and Technology (Japan)
<b>JMA</b>	Japan Meteorological Agency (Japan)
<b>KIT</b>	Karlsruhe Institute of Technology (Germany)
<b>KMA</b>	Korea Meteorological Administration (Republic of Korea)
<b>KMD</b>	Kenya Meteorological Department (Kenya)
<b>KRISS</b>	Korea Research Institute of Standards and Science (Republic of Korea)
<b>KSNU</b>	Kyrgyz National University (Kyrgyzstan)
<b>KUP</b>	Physics Institute, Climate and Environmental Physics, University of Bern (Switzerland)
<b>Kyrgyzhydromet</b>	Agency on Hydrometeorology under Ministry of Emergency Situations of the Kyrgyz Republic (Kyrgyzstan)
<b>LA</b>	Laboratoire d'Aérologie (France)
<b>LAMP</b>	Laboratoire de Météorologie Physique (France)
<b>LSCE</b>	Laboratoire des Sciences du Climat et de l'Environnement (France)
<b>METRI</b>	National Institute of Meteorological Research, KMA (Republic of Korea)
<b>MGO</b>	Voeikov Main Geophysical Observatory (Russian Federation)
<b>MMD</b>	Malaysian Meteorological Department (Malaysia)
<b>MPI-BGC</b>	Max-Planck Institute (MPI) for Biogeochemistry in Jena (Germany)
<b>MRI</b>	Meteorological Research Institute (Japan)
<b>NAGOU</b>	Nagoya University (Japan)
<b>NCAR</b>	U.S. National Center For Atmospheric Research (USA)
<b>NEDO</b>	New Energy and Industrial Technology Development Organization (Japan)
<b>NEON</b>	National Ecological Observatory Network (USA)
<b>NIES</b>	National Institute for Environmental Studies (Japan)
<b>NILU</b>	Norwegian Institute for Air Research (Norway)
<b>NIST</b>	National Institute of Standards and Technology (USA)
<b>NIWA</b>	National Institute of Water & Atmospheric Research Ltd. (New Zealand)
<b>NOAA</b>	National Oceanic and Atmospheric Administration (USA)
<b>NOAA-CSD</b>	Chemical Sciences Division, NOAA (USA)
<b>NOAA/ESRL</b>	Earth System Research Laboratory, NOAA (USA)
<b>NPL</b>	National Physical Laboratory (United Kingdom)
<b>ONM</b>	Office National de la Météorologie (Algeria)
<b>OSAKAU</b>	Osaka University (Japan)
<b>PolyU</b>	The Hong Kong Polytechnic University (Hong Kong, China)
<b>PSU</b>	Penn State University (USA)
<b>RHUL</b>	Royal Holloway University London (United Kingdom)
<b>RIVM</b>	National Institute of Public Health and the Environment (Netherlands)
<b>RSE</b>	Ricerca sul Sistema Energetico - RSE S.p.A. (Italy)
<b>RUG</b>	University of Groningen (RUG), Centre for Isotope Research (CIO) (Netherlands)
<b>SAIPF</b>	Center for Environmental Science in Saitama (Japan)
<b>SAWS</b>	South African Weather Service (South Africa)
<b>SHIZU</b>	Shizuoka University (Japan)
<b>SIO</b>	Scripps Institution of Oceanography (USA)
<b>SMNA</b>	National Weather Service (Argentina)
<b>TU</b>	Tohoku University (Japan)
<b>UBAA</b>	Federal Environment Agency Austria (Austria)

<b>UBAG</b>	German Environment Agency (Germany)
<b>UBAG-SCHAU</b>	Umweltbundesamt, Station Schauinsland (Germany)
<b>UBAG/ZUG</b>	Umweltbundesamt, Zugspitze GAW Station (Germany)
<b>UEA</b>	University of East Anglia (United Kingdom)
<b>UHEI-IUP</b>	University of Heidelberg, Institut für Umweltphysik (Germany)
<b>UMLT</b>	University of Malta (Malta)
<b>UNIURB</b>	University of Urbino, Dep. of Pure and Applied Sciences (DISPEA) (Italy)
<b>UNIVBRIS</b>	Atmospheric Chemistry Research Group School of Chemistry University of Bristol (United Kingdom)
<b>UoE</b>	University of Exeter (United Kingdom)
<b>UYRK</b>	University of York (United Kingdom)
<b>VNMHA</b>	Viet Nam Meteorological and Hydrological Administration (Viet Nam)
<b>WCC-Empa</b>	World Calibration Centre (Empa)
<b>WDCGG</b>	World Data Centre for Greenhouse Gases (WMO)
<b>WMO</b>	World Meteorological Organization

#### ATMOSPHERIC SPECIES:

<b>Be</b>	beryllium
<b>CCl<sub>4</sub></b>	tetrachloromethane (carbon tetrachloride)
<b>C<sub>2</sub>Cl<sub>4</sub></b>	tetrachloroethene (tetrachloroethylene)
<b>CFC-11</b>	trichlorofluoromethane (chlorofluorocarbon-11, CCl <sub>3</sub> F)
<b>CFC-12</b>	dichlorodifluoromethane (chlorofluorocarbon-12, CCl <sub>2</sub> F <sub>2</sub> )
<b>CFC-113</b>	1,1,2-trichloro-1,2,2-trifluoroethane (chlorofluorocarbon-113, CCl <sub>2</sub> FCClF <sub>2</sub> )
<b>CFCs</b>	chlorofluorocarbons
<b>CH<sub>4</sub></b>	methane
<b>CHBr<sub>3</sub></b>	tribromomethane (bromoform)
<b>CH<sub>2</sub>Br<sub>2</sub></b>	dibromomethane (methylene bromide)
<b>CH<sub>3</sub>Br</b>	bromomethane (methyl bromide)
<b>CH<sub>3</sub>CCl<sub>3</sub></b>	1,1,1-trichloroethane (methyl chloroform)
<b>CH<sub>3</sub>D</b>	deuterated methane
<b>CH<sub>3</sub>I</b>	iodomethane (methyl iodide)
<b>CHCl<sub>3</sub></b>	trichloromethane (chloroform)
<b>CH<sub>2</sub>Cl<sub>2</sub></b>	dichloromethane (methylene chloride)
<b>CH<sub>3</sub>Cl</b>	chloromethane (methyl chloride)
<b>C<sub>2</sub>HCl<sub>3</sub></b>	trichloroethene (trichloroethylene)
<b>CO</b>	carbon monoxide
<b>CO<sub>2</sub></b>	carbon dioxide
<b>COS</b>	carbon oxide sulfide (carbonyl sulfide)
<b>H<sub>2</sub></b>	hydrogen
<b>Halon-1211</b>	bromochlorodifluoromethane (CBrClF <sub>2</sub> )
<b>Halon-1301</b>	bromotrifluoromethane (CBrF <sub>3</sub> )
<b>Halon-2402</b>	1,2-dibromo-1,1,2,2-tetrafluoroethane (CBrF <sub>2</sub> CBrF <sub>2</sub> )
<b>HCFC-141b</b>	1,1-dichloro-1-fluoroethane (hydrochlorofluorocarbon-141b, CH <sub>3</sub> CCl <sub>2</sub> F)
<b>HCFC-142b</b>	1-chloro-1,1-difluoroethane (hydrochlorofluorocarbon-142b, CH <sub>3</sub> CClF <sub>2</sub> )
<b>HCFC-22</b>	chlorodifluoromethane (hydrochlorofluorocarbon-22, CHClF <sub>2</sub> )
<b>HCFCs</b>	hydrochlorofluorocarbons
<b>HFC-134a</b>	1,1,1,2-tetrafluoroethane (hydrofluorocarbon-134a, CH <sub>2</sub> FCF <sub>3</sub> )
<b>HFC-152a</b>	1,1-difluoroethane (hydrofluorocarbon-152a, CHF <sub>2</sub> CH <sub>3</sub> )
<b>HFCs</b>	hydrofluorocarbons
<b>N<sub>2</sub>O</b>	nitrous oxide

<b>NF<sub>3</sub></b>	nitrogen trifluoride
<b>PFCs</b>	perfluorocarbons
<b>Rn</b>	radon
<b>SF<sub>6</sub></b>	sulfur hexafluoride
<b>SO<sub>2</sub>F<sub>2</sub></b>	sulfuryl fluoride

**UNITS:**

<b>ppm</b>	parts per million
<b>ppb</b>	parts per billion
<b>ppt</b>	parts per trillion

**Others:**

<b>TIC</b>	total inorganic carbon
<b>M/V</b>	merchant vessel
<b>R/V</b>	research vessel

## APPENDIX F LIST OF WMO/WDCGG PUBLICATIONS

### DATA REPORTING MANUAL:

WDCGG No. 1      January      1991

### WMO WDCGG DATA REPORT:

			(period of data accepted)				
WDCGG No. 2 Part A	October	1992	October	1990	~	August	1992
WDCGG No. 2 Part B	October	1992	October	1990	~	August	1992
WDCGG No. 3	October	1993	September	1992	~	March	1993
WDCGG No. 5	March	1994	April	1993	~	September	1993
WDCGG No. 6	September	1994	September	1993	~	March	1994
WDCGG No. 7	March	1995	April	1994	~	December	1994
WDCGG No. 9	September	1995	January	1995	~	June	1995
WDCGG No.10	March	1996	July	1995	~	December	1995
WDCGG No.11	September	1996	January	1996	~	June	1996
WDCGG No.12	March	1997	July	1996	~	November	1996
WDCGG No.14	September	1997	December	1996	~	June	1997
WDCGG No.16	March	1998	July	1997	~	December	1997
WDCGG No.17	September	1998	January	1998	~	June	1998
WDCGG No.18	March	1999	July	1998	~	December	1998
WDCGG No.20	September	1999	January	1999	~	June	1999
WDCGG No.21	March	2000	July	1999	~	December	1999
WDCGG No.23	September	2000	January	2000	~	June	2000
WDCGG No.25	March	2001	July	2000	~	December	2000

### WMO WDCGG DATA CATALOGUE:

WDCGG No. 4	December	1993
WDCGG No.13	March	1997
WDCGG No.19	March	1999
WDCGG No.24	March	2001

### WMO WDCGG DATA SUMMARY:

WDCGG No. 8	October	1995
WDCGG No.15	March	1998
WDCGG No.22	March	2000
WDCGG No.26	March	2002
WDCGG No.27	March	2003
WDCGG No.28	March	2004
WDCGG No.29	March	2005
WDCGG No.30	March	2006
WDCGG No.31	March	2007
WDCGG No.32	March	2008
WDCGG No.33	March	2009
WDCGG No.34	March	2010
WDCGG No.35	March	2011
WDCGG No.36	March	2012
WDCGG No.37	March	2013
WDCGG No.38	March	2014
WDCGG No.39	March	2015
WDCGG No.40	March	2016
WDCGG No.41	March	2017
WDCGG No.42	October	2018
WDCGG No.43	March	2020
WDCGG No.44	November	2020
WDCGG No.45	September	2021

**WMO WDCGG CD-ROM:**

CD-ROM No. 1	March	1995	October	1990	~	December	1994
CD-ROM No. 2	March	1996	October	1990	~	June	1995
CD-ROM No. 3	March	1997	October	1990	~	June	1996
CD-ROM No. 4	March	1998	October	1990	~	December	1997
CD-ROM No. 5	March	1999	October	1990	~	December	1998
CD-ROM No. 6	March	2000	October	1990	~	December	1999
CD-ROM No. 7	March	2001	October	1990	~	December	2000
CD-ROM No. 8	March	2002	October	1990	~	January	2002
CD-ROM No. 9	March	2003	October	1990	~	December	2002
CD-ROM No.10	March	2004	October	1990	~	December	2003
CD-ROM No.11	March	2005	October	1990	~	December	2004
CD-ROM No.12	March	2006	October	1990	~	December	2005
CD-ROM No.13	March	2007	October	1990	~	November	2006
CD-ROM No.14	March	2008	October	1990	~	November	2007

**WMO WDCGG DVD:**

DVD No. 1	March	2009	October	1990	~	November	2008
DVD No. 2	March	2010	October	1990	~	November	2009
DVD No. 3	March	2011	October	1990	~	November	2010
DVD No. 4	March	2012	October	1990	~	November	2011
DVD No. 5	March	2013	October	1990	~	November	2012
DVD No. 6	March	2014	October	1990	~	November	2013
DVD No. 7	March	2015	October	1990	~	November	2014
DVD No. 8	March	2016	October	1990	~	November	2015

(period of data accepted)

(period of data accepted)

# **REFERENCES**

## References

- Ballantyne, A. P., C. B. Alden, J. B. Miller, P. P. Tans, and J. W. C. White, Increase in observed net carbon dioxide uptake by land and oceans during the past 50 years, *Nature*, **488**, 70–72, <https://doi.org/10.1038/nature11299>, 2012.
- Basu, S., X. Lan, E. Dlugokencky, S. Michel, S. Schwietzke, J. B. Miller, L. Bruhwiler, Y. Oh, P. P. Tans, F. Apadula, L. V. Gatti, A. Jordan, J. Necki, M. Sasakawa, S. Morimoto, T. Di Iorio, H. Lee, J. Arduini, and G. Manca, Estimating Emissions of Methane Consistent with Atmospheric Measurements of Methane and  $\delta^{13}\text{C}$  of Methane, *Atmos. Chem. Phys. Discuss.* [preprint], <https://doi.org/10.5194/acp-2022-317>, in review, 2022.
- Chandra, N., P. K. Patra, J. S. H. Bisht, A. Ito, T. Umezawa, N. Saigusa, S. Morimoto, S. Aoki, G. Janssens-Maenhout, R. Fujita, M. Takigawa, S. Watanabe, N. Saitoh, and J. G. Canadell, Emissions from the Oil and Gas Sectors, Coal Mining and Ruminant Farming Drive Methane Growth over the Past Three Decades, *Journal of the Meteorological Society of Japan. Ser. II*, **99**, <https://doi.org/10.2151/jmsj.2021-015>, 2021.
- Cleveland, W. S., and S. J. Devlin, Locally weighted regression: an approach to regression analysis by local fitting, *J. Amer. Statist. Assn.*, **83**, 596–610, <https://doi.org/10.1080/01621459.1988.10478639>, 1988.
- Conway, T. J., P. P. Tans, L. S. Waterman, K. W. Thoning, D. R. Kitzis, K. A. Masarie, and N. Zhang, Evidence for interannual variability of the carbon cycle from the National Oceanic and Atmospheric Administration/Climate Monitoring and Diagnostics Laboratory global air sampling network, *J. Geophys. Res.*, **99**, 22831–22855, <https://doi.org/10.1029/94JD01951>, 1994.
- Crippa, M., E. Solazzo, G. Huang, D. Guizzardi, E. Koffi, M. Muntean, C. Schieberle, R. Friedrich, and G. Janssens-Maenhout, High resolution temporal profiles in the Emissions Database for Global Atmospheric Research, *Scientific Data*, **7**, 121, <https://doi.org/10.1038/s41597-020-0462-2>, 2020.
- Dlugokencky, E. J., B. P. Walter, K. A. Masarie, P. M. Lang, and E. S. Kasischke, Measurements of an anomalous global methane increase during 1998, *Geophys. Res. Lett.*, **28**, 499–502, <https://doi.org/10.1029/2000GL012119>, 2001.
- Dlugokencky, E. J., S. Houweling, L. Bruhwiler, K. A. Masarie, P. M. Lang, J. B. Miller, and P. P. Tans, Atmospheric methane levels off: Temporary pause or a new steady-state?, *Geophys. Res. Lett.*, **30**, 1992, <https://doi.org/10.1029/2003GL018126>, 2003.
- Dlugokencky, E. J., R. C. Myers, P. M. Lang, K. A. Masarie, A. M. Crotwell, K. W. Thoning, B. D. Hall, J. W. Elkins, and L. P. Steele, Conversion of NOAA atmospheric dry air  $\text{CH}_4$  mole fractions to a gravimetrically prepared standard scale, *J. Geophys. Res.*, **110**, D18306, <https://doi.org/10.1029/2005JD006035>, 2005.
- Duchon, C. E., Lanczos filtering in one and two dimensions, *J. Appl. Meteor.*, **18**, 1016–1022, [https://doi.org/10.1175/1520-0450\(1979\)018%3C1016:LFIOAT%3E2.0.CO;2](https://doi.org/10.1175/1520-0450(1979)018%3C1016:LFIOAT%3E2.0.CO;2), 1979.
- Engel, A. and M. Rigby (Lead Authors), J. B. Burkholder, R. P. Fernandez, L. Froidevaux, B. D. Hall, R. Hossaini, T. Saito, M. K. Vollmer, and B. Yao, Update on Ozone-Depleting Substances (ODSs) and Other Gases of Interest to the Montreal Protocol, Chapter 1 in *Scientific Assessment of Ozone Depletion: 2018, Global Ozone Research and Monitoring Project - Report No. 58*, World Meteorological Organization, Geneva, Switzerland, 2018.
- Friedlingstein, P., M. W. Jones, M. O'Sullivan, R. M. Andrew, D. C. E. Bakker, J. Hauck, C. Le Quéré, G. P. Peters, W. Peters, J. Pongratz, S. Sitch, J. G. Canadell, P. Ciais, R. B. Jackson, S. R. Alin, P. Anthoni, N. R. Bates, M. Becker, N. Bellouin, L. Bopp, T. T. T. Chau, F. Chevallier, L. P. Chini, M. Cronin, K. I. Currie, B. Decharme, L. Djedjougouang, X. Dou, W. Evans, R. A. Feely, L. Feng, T. Gasser, D. Gilfillan, T. Gkritzalis, G. Grassi, L. Gregor, N. Gruber, Ö. Gürses, I. Harris, R. A. Houghton, G. C. Hurtt, Y. Iida, T. Ilyina, I. T. Luijkx, A. K. Jain, S. D. Jones, E. Kato, D. Kennedy, K. Klein Goldewijk, J. Knauer, J. I. Korsbakken, A. Kötzinger, P. Landschützer, S. K. Lauvset, N. Lefèvre, S. Lienert, J. Liu, G. Marland, P. C. McGuire, J. R. Melton, D. R. Munro, J. E. M. S. Nabel, S. Nakaoka, Y. Niwa, T. Ono, D. Pierrot, B. Poulter, G. Rehder, L. Resplandy, E. Robertson, C. Rödenbeck, T. M. Rosan, J. Schwinger, C. Schwingshackl, R. Séférian, A. J. Sutton, C. Sweeney, T. Tanhua, P. P. Tans, H. Tian, B. Tilbrook, F. Tubiello, G. van der Werf, N. Vuichard, C. Wada, R. Wanninkhof, A. Watson, D. Willis, A. J. Wiltshire, W. Yuan, C. Yue, X. Yue, S. Zaehle, and J. Zeng, Global Carbon Budget 2021, *Earth Syst. Sci. Data*, <https://doi.org/10.5194/essd-2021-386>, 2021.
- Fujita, R., S. Morimoto, T. Umezawa, K. Ishijima, P. K. Patra, D. E. J. Worthy, D. Goto, S. Aoki, and T. Nakazawa, Temporal Variations of the Mole Fraction, Carbon, and Hydrogen Isotope Ratios of Atmospheric Methane in the Hudson Bay Lowlands, Canada, *J. Geophys. Res.*, **123**, 4695–4711, <https://doi.org/10.1002/2017JD027972>, 2018.
- Haan, D., and D. Raynaud, Ice core record of CO variations during the last two millennia: atmospheric implications and chemical interactions within the Greenland ice, *Tellus*, **50B**, 253–262, <https://doi.org/10.3402/tellusb.v50i3.16101>, 1998.

- Hall, B. D. (ed.), J. W. Elkins, J. H. Butler, S. A. Montzka, T. M. Thompson, L. Del Negro, G. S. Dutton, D. F. Hurst, D. B. King, E. S. Kline, L. Lock, D. MacTaggart, D. Mondeel, F. L. Moore, J. D. Nance, E. A. Ray, and P. A. Romashkin, Halocarbons and Other Atmospheric Trace Species, Section 5 in Climate Monitoring and Diagnostics Laboratory Summary Report No. 25, 1998–1999, R. S. Schnell, D. B. King, and R. M. Rosson (eds.), NOAA-CMDL, Boulder, CO., USA, 2001.
- Hall, B. D., G. S. Dutton, and J. W. Elkins, The NOAA nitrous oxide standard scale for atmospheric observations, *J. Geophys. Res.*, **112**, D09305, <https://doi.org/10.1029/2006JD007954>, 2007.
- Hall, B. D., G. S. Dutton, D. J. Mondeel, J. D. Nance, M. Rigby, J. H. Butler, F. L. Moore, D. F. Hurst, and J. W. Elkins, Improving measurements of SF<sub>6</sub> for the study of atmospheric transport and emissions, *Atmospheric Measurement Techniques*, **4**, 2441–2451, <https://doi.org/10.5194/amt-4-2441-2011>, 2011.
- Hall, B. D., A. M. Crotwell, D. R. Kitzis, T. Mefford, B. R. Miller, M. F. Schibig, and P. P. Tans, Revision of the World Meteorological Organization Global Atmosphere Watch (WMO/GAW) CO<sub>2</sub> calibration scale, *Atmos. Meas. Tech.*, **14**, 3015–3032, <https://doi.org/10.5194/amt-14-3015-2021>, 2021.
- Höglund-Isaksson, L., A. Gómez-Sanabria, Z. Klimont, P. Rafaj, and W. Schöpp, Technical potentials and costs for reducing global anthropogenic methane emissions in the 2050 timeframe – results from the GAINS model, *Environmental Research Communications*, **2**, 025004, <https://doi.org/10.1088/2515-7620/ab7457>, 2020.
- IPCC, Climate Change 2021: The Physical Science Basis. Contribution of Working Group I to the Sixth Assessment Report of the Intergovernmental Panel on Climate Change [Masson-Delmotte, V., P. Zhai, A. Pirani, S. L. Connors, C. Pean, S. Berger, N. Caud, Y. Chen, L. Goldfarb, M. I. Gomis, M. Huang, K. Leitzell, E. Lonnoy, J. B. R. Matthews, T. K. Maycock, T. Waterfield, O. Yelekci, R. Yu, and B. Zhou (eds.)]. Cambridge University Press, 2021. In Press.
- Jackson, R. B., M. Saunois, P. Bousquet, J. G. Canadell, B. Poulter, A. R. Stavert, P. Bergamaschi, Y. Niwa, A. Segers, and A. Tsuruta, Increasing anthropogenic methane emissions arise equally from agricultural and fossil fuel sources, *Environmental Research Letters*, **15**, 071002, <https://doi.org/10.1088/1748-9326/ab9ed2>, 2020.
- Ji, Q., M. A. Altabet, H. W. Bange, M. I. Graco, X. Ma, D. L. Arévalo-Martínez, and D. S. Grundle, Investigating the effect of El Niño on nitrous oxide distribution in the eastern tropical South Pacific, *Biogeosciences*, **16**, 2079–2093, <https://doi.org/10.5194/bg-16-2079-2019>, 2019.
- Lan, X., P. Tans, C. Sweeney, A. Andrews, E. Dlugokencky, S. Schwietzke, J. Kofler, K. McKain, K. Thoning, M. Crotwell, S. Montzka, B. R. Miller, and S. C. Biraud, Long-Term Measurements Show Little Evidence for Large Increases in Total U.S. Methane Emissions Over the Past Decade, *Geophysical Research Letters*, **46**, 4991–4999, <https://doi.org/10.1029/2018GL081731>, 2019.
- Lee, H., S. Kim, H. Yoo, H. Choe, S.-O. Han, S.-B. Ryoo, B. Hall, G. Forster, Y. K. Camille, F. Meinhardt, I. Levin, L. Ries, C. Couret, M. Guillevic, S. A. Wyss, D. Rzesanke, A. Jordan, R. Moss, J. Lee, and J. Yu, The report of the result on SF<sub>6</sub> Inter-Comparison Experiment, 2016 – 2017, World Calibration Centre for SF<sub>6</sub>, National Institute of Meteorological Sciences, Korea Meteorological Administration, available at: <http://www.nims.go.kr/wcc/pdf/4.Intercomparison%20report.pdf>, 2017.
- Montzka S. A., G. S. Dutton, P. Yu, E. Ray, R. W. Portmann, J. S. Daniel, L. Kuijpers, B. D. Hall, D. Mondeel, C. Siso, J. D. Nance, M. Rigby, A. J. Manning, L. Hu, F. Moore, B. R. Miller, and J. W. Elkins, An unexpected and persistent increase in global emissions of ozone-depleting CFC-11, *Nature*, **557**, 413–417, <https://doi.org/10.1038/s41586-018-0106-2>, 2018.
- Montzka, S. A., G. S. Dutton, R. W. Portmann, M. P. Chipperfield, S. Davis, W. Feng, A. J. Manning, E. Ray, M. Rigby, B. D. Hall, C. Siso, J. D. Nance, P. B. Krummel, J. Mühlle, D. Young, S. O'Doherty, P. K. Salameh, C. M. Harth, R. G. Prinn, R. F. Weiss, J. W. Elkins, H. Walter-Terrinoni, and C. Theodoridi, A decline in global CFC-11 emissions during 2018–2019, *Nature*, **590**, 428–432, <https://doi.org/10.1038/s41586-021-03260-5>, 2021.
- Nisbet, E. G., E. J. Dlugokencky, M. R. Manning, D. Lowry, R. E. Fisher, J. L. France, S. E. Michel, J. B. Miller, J. W. C. White, B. Vaughn, P. Bousquet, J. A. Pyle, N. J. Warwick, M. Cain, R. Brownlow, G. Zazzeri, M. Lanoiselé, A. C. Manning, E. Gloor, D. E. J. Worthy, E.-G. Brunke, C. Labuschagne, E. W. Wolff, and A. L. Ganesan, Rising atmospheric methane: 2007–2014 growth and isotopic shift, *Global Biogeochemical Cycles*, **30**, 1356–1370, <https://doi.org/10.1002/2016GB005406>, 2016.
- Novelli, P. C., K. A. Masarie, and P. M. Lang, Distributions and recent changes of carbon monoxide in the lower troposphere, *J. Geophys. Res.*, **103**, 19015–19033, <https://doi.org/10.1029/98JD01366>, 1998.
- Novelli, P. C., K. A. Masarie, P. M. Lang, B. D. Hall, R. C. Myers, and J. W. Elkins, Reanalysis of tropospheric CO trends: Effects of the 1997–1998 wildfires, *J. Geophys. Res.*, **108**, 4464, <https://doi.org/10.1029/2002JD003031>, 2003.
- Oh, Y., Q. Zhuang, L. R. Welp, L. Liu, X. Lan, S. Basu, E. J. Dlugokencky, L. Bruhwiler, J. B. Miller, S. E. Michel, S. Schwietzke, P. Tans, P. Ciais, J. P. Chanton, Improved global wetland carbon isotopic signatures

- support post-2006 microbial methane emission increase, *Commun. Earth Environ.*, **3**, 159, <https://doi.org/10.1038/s43247-022-00488-5>, 2022.
- Patra, P. K., T. Saeki, E. J. Dlugokencky, K. Ishijima, T. Umezawa, A. Ito, S. Aoki, S. Morimoto, E. A. Kort, A. Crotwell, K. Ravi Kumar, and T. Nakazawa, Regional methane emission estimation based on observed atmospheric concentrations (2002–2012), *Journal of the Meteorological Society of Japan. Ser. II*, **94**, 91–113, <https://doi.org/10.2151/jmsj.2016-006>, 2016.
- Prinn, R. G., R. F. Weiss, P. J. Fraser, P. G. Simmonds, D. M. Cunnold, F. N. Alyea, S. O'Doherty, P. Salameh, B. R. Miller, J. Huang, R. H. J. Wang, D. E. Hartley, C. Harth, L. P. Steele, G. Sturrock, P. M. Midgley, A. McCulloch, A history of chemically and radiatively important gases in air deduced from ALE/GAGE/AGAGE, *Journal of Geophysical Research*, **105**, 17751–17792, <https://doi.org/10.1029/2000JD900141>, 2000.
- Prinn, R. G., R. F. Weiss, J. Arduini, T. Arnold, H. L. DeWitt, P. J. Fraser, A. L. Ganeshan, J. Gasore, C. M. Harth, O. Hermansen, J. Kim, P. B. Krummel, S. Li, Z. M. Loh, C. R. Lunder, M. Maione, A. J. Manning, B. R. Miller, B. Mitrevski, J. Mühle, S. O'Doherty, S. Park, S. Reimann, M. Rigby, T. Saito, P. K. Salameh, R. Schmidt, P. G. Simmonds, L. P. Steele, M. K. Vollmer, R. H. Wang, B. Yao, Y. Yokouchi, D. Young, and L. Zhou, History of chemically and radiatively important atmospheric gases from the Advanced Global Atmospheric Gases Experiment (AGAGE), *Earth Syst. Sci. Data*, **10**, 985–1018, <https://doi.org/10.5194/essd-10-985-2018>, 2018.
- Rice, A. L., C. L. Butenhoff, D. G. Team, F. H. Röger, M. A. K. Khalil, and R. A. Rasmussen, Atmospheric methane isotopic record favors fossil sources flat in 1980s and 1990s with recent increase, *Proceedings of the National Academy of Sciences*, **113**, 10791–10796, <https://doi.org/10.1073/pnas.1522923113>, 2016.
- Saunois, M., A. R. Stavert, B. Poulter, P. Bousquet, J. G. Canadell, R. B. Jackson, P. A. Raymond, E. J. Dlugokencky, S. Houweling, P. K. Patra, P. Ciais, V. K. Arora, D. Bastviken, P. Bergamaschi, D. R. Blake, G. Brailsford, L. Bruhwiler, K. M. Carlson, M. Carroll, S. Castaldi, N. Chandra, C. Crevoisier, P. M. Crill, K. Covey, C. L. Curry, G. Etiope, C. Frankenberg, N. Gedney, M. I. Hegglin, L. Höglund-Isaksson, G. Hugelius, M. Ishizawa, A. Ito, G. Janssens-Maenhout, K. M. Jensen, F. Joos, T. Kleinen, P. B. Krummel, R. L. Langenfelds, G. G. Laruelle, L. Liu, T. Machida, S. Maksyutov, K. C. McDonald, J. McNorton, P. A. Miller, J. R. Melton, I. Morino, J. Müller, F. Murguia-Flores, V. Naik, Y. Niwa, S. Noce, S. O'Doherty, R. J. Parker, C. Peng, S. Peng, G. P. Peters, C. Prigent, R. Prinn, M. Ramonet, P. Regnier, W. J. Riley, J. A. Rosentreter, Arjo Segers, Isobel J. Simpson, H. Shi, S. J. Smith, L. P. Steele, B. F. Thornton, H. Tian, Y. Tohjima, F. N. Tubiello, A. Tsuruta, N. Viovy, A. Voulgarakis, T. S. Weber, M. van Weele, G. R. van der Werf, R. F. Weiss, D. Worthy, D. Wunch, Y. Yin, Y. Yoshida, W. Zhang, Z. Zhang, Y. Zhao, B. Zheng, Q. Zhu, Q. Zhu, and Q. Zhuang, The Global Methane Budget 2000–2017, *Earth Syst. Sci. Data*, **12**, 1561–1623, <https://doi.org/10.5194/essd-12-1561-2020>, 2020.
- Schafer, H., S. E. Mikaloff Fletcher, C. Veidt, K. R. Lassey, G. W. Brailsford, T. M. Bromley, E. J. Dlugokencky, S. E. Michel, J. B. Miller, I. Levin, D. C. Lowe, R. J. Martin, B. H. Vaughn, and J. W. C. White, A 21st-century shift from fossil-fuel to biogenic methane emissions indicated by  $^{13}\text{CH}_4$ , *Science*, **352**, 80–84, <https://doi.org/10.1126/science.aad2705>, 2016.
- Schwietzke, S., O. A. Sherwood, L. M. P. Bruhwiler, J. B. Miller, G. Etiope, E. J. Dlugokencky, S. E. Michel, V. A. Arling, B. H. Vaughn, J. W. C. White, and P. P. Tans, Upward revision of global fossil fuel methane emissions based on isotope database, *Nature*, **538**, 88–91, <https://doi.org/10.1038/nature19797>, 2016.
- Simpson, I.J., M. P. Sulbaek Andersen, S. Meinardi, L. Bruhwiler, N. J. Blake, D. Helmig, F. S. Rowland, and D. R. Blake, Long-term decline of global atmospheric ethane concentrations and implications for methane, *Nature*, **488**, 490–494, <https://doi.org/10.1038/nature11342>, 2012.
- Solomon, S., J. Alcamo and A. R. Ravishankara, Unfinished business after five decades of ozone-layer science and policy, *Nature Communications*, **11**, 4272, <https://doi.org/10.1038/s41467-020-18052-0>, 2020.
- Thompson, R. L., E. G. Nisbet, I. Pisso, A. Stohl, D. Blake, E. J. Dlugokencky, D. Helmig, and J. W. C. White, Variability in Atmospheric Methane From Fossil Fuel and Microbial Sources Over the Last Three Decades, *Geophysical Research Letters*, **45**, 11,499–11,508, <https://doi.org/10.1029/2018GL078127>, 2018.
- Thompson, R. L., L. Lassaletta, P. K. Patra, C. Wilson, K. C. Wells, A. Gressent, E. N. Koffi, M. P. Chipperfield, W. Winiwarter, E. A. Davidson, H. Tian, and J. G. Canadell, Acceleration of global  $\text{N}_2\text{O}$  emissions seen from two decades of atmospheric inversion, *Nat. Clim. Chang.*, **9**, 993–998, <https://doi.org/10.1038/s41558-019-0613-7>, 2019.
- Tian, H., R. Xu, J. G. Canadell, R. L. Thompson, W. Winiwarter, P. Suntharalingam, E. A. Davidson, P. Ciais, R. B. Jackson, G. Janssens-Maenhout, M. J. Prather, P. Regnier, N. Pan, S. Pan, G. P. Peters, H. Shi, F. N. Tubiello, S. Zaehle, F. Zhou, A. Arneth, G. Battaglia, S. Berthet, L. Bopp, A. F. Bouwman, E. T. Buitenhuis, J. Chang, M. P. Chipperfield, S. R. S. Dangal, E. Dlugokencky, J. W. Elkins, B. D. Eyre, B. Fu, B. Hall, A. Ito, F. Joos, P. B. Krummel, A. Landolfi, G. G. Laruelle, R. Lauerwald, W. Li, S. Lienert, T. Maavara, M. MacLeod, D. B. Millet, S. Olin, P. K. Patra, R. G. Prinn, P. A. Raymond, D. J. Ruiz, G. R. van der Werf, N. Vuichard, J. Wang, R. F. Weiss, K. C. Wells, C. Wilson, J. Yang, and Y. Yao, A

- comprehensive quantification of global nitrous oxide sources and sinks, *Nature*, **586**, 248–256, <https://doi.org/10.1038/s41586-020-2780-0>, 2020.
- Weiss, R. F., C. D. Keeling, and H. Craig, The determination of tropospheric nitrous oxide, *J. Geophys. Res. -Oceans*, **86**, 7197–7202, <https://doi.org/10.1029/JC086iC08p07197>, 1981.
- WMO, Technical Report of Global Analysis Method for Major Greenhouse Gases by the World Data Center for Greenhouse Gases, GAW Report No. 184, WMO TD No. 1473, 2009.
- WMO, WMO Global Atmosphere Watch (GAW) Implementation Plan: 2016-2023, GAW Report No.228, 2017.
- WMO, 19th WMO/IAEA Meeting on Carbon Dioxide, Other Greenhouse Gases and Related Measurement Techniques (GGMT-2017), GAW Report No.242, 2018.
- WMO, 20th WMO/IAEA Meeting on Carbon Dioxide, Other Greenhouse Gases and Related Measurement Techniques (GGMT-2019), GAW Report No.255, 2020.
- WMO, WMO Greenhouse Gas Bulletin No.17, 2021a.
- WMO, Report on the Unexpected Emissions of CFC-11, WMO-No.1268, 2021b.
- Worden, J. R., A. A. Bloom, S. Pandey, Z. Jiang, H. M. Worden, T. W. Walker, S. Houweling, and T. Röckmann, Reduced biomass burning emissions reconcile conflicting estimates of the post-2006 atmospheric methane budget, *Nature Communications*, **8**, 2227, <https://doi.org/10.1038/s41467-017-02246-0>, 2017.
- Worthy, D. E. J., I. Levin, N. B. A. Trivett, A. J. Kuhlmann, J. F. Hopper, and M. K. Ernst, Seven years of continuous methane observations at a remote boreal site in Ontario, Canada, *J. Geophys. Res.*, **103**, 15995–16007, <https://doi.org/10.1029/98JD00925>, 1998.
- Yang S., B. X. Chang, M. J. Warner, T. S. Weber, A. M. Bourbonnais, A. E. Santoro, A. Kock, R. E. Sonnerup, J. L. Bullister, S. T. Wilson, and D. Bianchi, Global reconstruction reduces the uncertainty of oceanic nitrous oxide emissions and reveals a vigorous seasonal cycle, *Proceedings of the National Academy of Sciences*, **117(22)**, 11954–11960, <https://doi.org/10.1073/pnas.1921914117>, 2020.
- Zhao, C. L., P. P. Tans, and K. W. Thoning, A high precision manometric system for absolute calibrations of CO<sub>2</sub> in dry air, *J. Geophys. Res.*, **102**, 5885–5894, <https://doi.org/10.1029/96JD03764>, 1997.